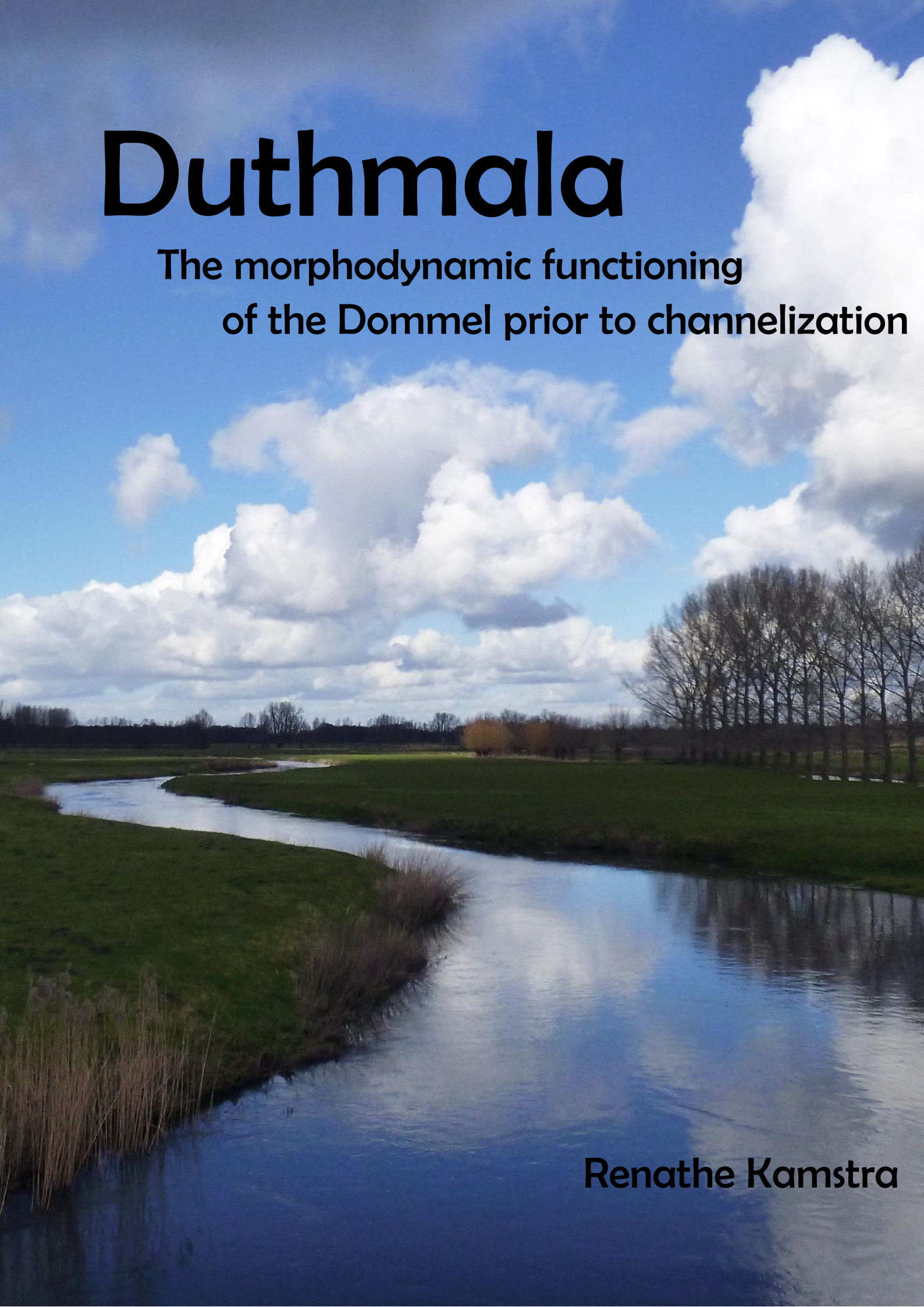

Duthmala

The morphodynamic functioning of the Dommel prior to channelization

Renathe Kamstra

In 704 the Dommel is mentioned for the first time as Duthmala (Nouwen, 1982).

Wageningen University

Department of Environmental Sciences

Master Thesis

Duthmala

The morphodynamic functioning of the Dommel prior to channelization, southern Netherlands

Author

Renathe Kamstra

Master Programme

Earth & Environment:

Soil Geography & Earth Surface Dynamics

Supervisors/Examinors

Drs. J. H. J. Candel

Dr. B. Makaske

Prof. Dr. J. Wallinga

U leidt het water van de bronnen door beken,
Tussen de bergen beweegt het zich voort
Het drenkt alles wat leeft in het veld,
De wilde ezels lessen er hun dorst.
Daarboven wonen de vogels van de hemel,
Uit het dichte groen klinkt hun gezang.

Hoe talrijk zijn Uw werken Heer.
Alles hebt U met wijsheid gemaakt,
Vol van uw schepselen is de aarde.

Voor de Ene wil ik zingen zolang ik leef,
Een lied voor mijn God zolang ik besta.
Moge mijn lofzang de Heer behagen,
Zoals ik mijn vreugde vind in Hem.

Psalm 104

Acknowledgements

From the first moment I read about the topic of this thesis I was very enthusiastic about it. I didn't need time to convince myself to apply for this project, since it contained all the topics I am most interested in. I like the interface between geography and fluvial dynamics, especially in combination with landscape history and this project combines all of them. I am very happy that I had the opportunity to work on this study. Looking back at the process I can conclude that I have learned a lot from it, I have gained deeper insight in the process of doing research, I have improved my English writing skills and I have learned how to receive and process feedback, lessons that I wouldn't want to have missed. However I could not have done my research without the help of many people. I would like to thank Jasper for his enthusiastic support and guidance during the process and his large contribution to the fieldwork. I would like to thank Niels for being my thesis buddy. I could not have accomplished the fieldwork without him and I really appreciate it that he was always there to help me and to discuss the results we found. I would like to thank Dr. B. Makaske and Prof. Dr. J. Wallinga for their involvement in the project and their guidance, valuable feedback and examination. Furthermore I would like to thank Alice and Erna for assisting me during the OSL laboratory work and data analysis. Together with Miranda, they made my 'dark' OSL period very bright. I would like to thank Christian, Piet, Oeds, Claudia and Ruben for their assistance during fieldwork. I would like to thank family van Hamond for their willingness to care for our equipment during the field work period. I would like to thank Mieke for arranging the formal business. I would like to thank the SGL group for the availability of field work equipment, the nice work place and the pleasant working ambiance. I would like to thank Wilfred, Stefan, Ieke, Viktoria and Maryse for their reviewing and feedback. And last but no least I want to thank Donnah for her reminders that life is not all about thesis and of course I could not neglect the unconditional support of my housemates Marlieke, Christiaan, Johanna, Ieke, Lijsje, Matthijs Tjeerd and Esther, and the support of my family and friends.

I hope you will enjoy this research as much as I did and still do.

Renathe Kamstra,

Wageningen,

2018

Abstract

A lot of research has been done on the morphodynamics of rivers and streams, but their planform evolution is still not completely understood. Especially detailed knowledge about the morphodynamic functioning of small to medium sized lowland streams is lacking. Lowland streams are low-energetic systems that can be found in the lowland areas of Western Europe. They are characterised by a channel gradient smaller than 1 m/km, a channel width smaller than 25 m and a stream power of less than 10 W/m^2. Lowland streams are often classified as laterally stable systems although, at historical maps dated prior to channelization, they generally show a highly sinuous planform.

In this research the morphodynamic functioning of lowland stream the Dommel prior to channelization was investigated by using Ground Penetrating Radar (GPR), coring and Optically Stimulated Luminescence (OSL) dating. In the study area, located south of St. Oedenrode in the Netherlands, remnants of four meanders are preserved. GPR was applied to determine whether and in which direction these bends migrated in the past. The coring data provided insight in the lithology and lithogenesis of the floodplain. OSL dating was applied to reconstruct how fast and in which period the meanders evolved. The planform evolution of the Dommel at this location could be reconstructed by combining these data.

In the inner bend area of all four meander remnants inclined surfaces appear at the GPR images. Despite their steep angle, the inclined surfaces were interpreted as lateral accretion surfaces. The occurrence of lateral accretion surfaces, indicated active migration of the bends. Lithological profiles confirm the fluvial origin of the floodplain, since the major part of the floodplain was characterized by a fining upward sequence. It seemed that the depth of the former bends and the steepness of the banks were similar to the channel of the current Dommel, indicating that the Dommel was originally characterized by a relatively deep channel and a small width/depth ratio. There were some indications for floodplain aggradation in the area, which might be related to land use changes or the introduction of water mills. However it is unsure whether this might have induced or fostered lateral stability of the channel. The present-day stream power and sediment load of the Dommel suggests that the stream currently has the potential for lateral migration, however its power is close to the threshold between a laterally stable and a meandering system and active migration might thus be a very slow process.

OSL dating of two of the former meanders might indicate the occurrence of distinct periods of increased migration rates. These periods (3000 to 2000 years ago and 1000 to 160 years ago) coincide with climate deterioration and are also known of important changes in land use. Both, climate and land use changes might have triggered a phase of active migration. The development of peat in the area might indicate a period of less flooding. However there is more research required to confirm the existence of separate periods of increased migration rates, since merely two former meanders were dated.

Considering the planform evolution of the Dommel it seemed that resistance-bearing layers were important determining factors. Floodplain deposits with a high resistance, might have prevented the stream from migration. At the other hand the occurrence of seepage flow could have weakened channels and fostered erosion. The combination of floodplain resistance, sharp bends and reworked organic deposits might indicate that counterpoint bar development and the process of flow separation played an important role in the planform evolution of the Dommel. The heterogeneity in the floodplain of the Dommel in combination with the processes of counter point bar development and flow separation might have resulted in the complex sinuous planform of the Dommel.

Table of contents

1. Introduction

This chapter introduces the challenge captured by this research. It provides an illustration of the history and background of the subject leading to the problem statement and the purpose of this research. The chapter ends with a description of the context of this research.

1.1 Background

Rivers and streams are one of the most important factors that shape the landscape and scientists throughout history have been inspired by their meander dynamics (Eekhout *et al.,* 2013). Although there has been a lot of research on the morphodynamics of rivers and streams, their development is still not completely understood (Blanckaert, 2011), especially detailed knowledge about the morphodynamic functioning of small to medium sized lowland stream systems is lacking (Moor *et al.,* 2006). Large river systems, as the Rhine and Meuse in the Netherlands, have been thoroughly studied (e.g. Berendsen & Stouthamer, 2001; Stouthamer & Middelkoop, 2003; Makaske & Weerts, 2005), whereas only a few studies have investigated the fluvial and morphological dynamics of lowland streams (e.g. Moor *et al.,* 2006; Eekhout, 2014; Candel *et al.,* 2017). Lowland streams can be found in the lowland areas of Western Europe (Verdonschot & Nijboer, 2002). They are characterised by a channel gradient smaller than 1 m/km, a channel width smaller than 25 m (Van der Molen *et al.,* 2012; Eekhout, 2014) and a stream power of less than 10 W/m^2 (Nanson & Croke, 1992).

In the Netherlands currently only about 4% of the lowland streams has a near-natural geomorphology (Eekhout, 2014; Verdonschot & Nijboer, 2002). Many lowland streams lost their natural physical properties as a consequence of large-scale channelization projects in the 19th and 20th century. Large irregular meanders were cut off and channels were straightened and made more continuous in width and depth. This affected the hydrological conditions in catchments due to the strong discharge function (Brookes & Gregory, 1983; Kroes & Hupp, 2010; Eekhout & Hoitink, 2015). The discharges were managed and the variety in habitats disappeared, which led to a decrease in fish and invertebrate communities (Iversen *et al.*, 1993). Channelization also affected the ecosystems further away from the stream by a lowering of groundwater tables and a decrease in water storage (Verdonschot & Nijboer, 2002; Makaske & Maas, 2015).

One of the solutions to this lowland stream deterioration is stream restoration; the restoration of the sinuous planform of rivers and streams, which is often based on historical maps (Verdonschot & Nijboer, 2002; Makaske & Maas, 2015). Stream restoration should lead to decreased peak flows, increased base flows and a rise in groundwater tables (Makaske & Maas, 2015). Due to restored variations in stream velocity and depth, it will also lead to increasing habitat diversion (Iversen *et al.,* 1993). Furthermore, sinuous streams improve the landscape values and the increase in stream length buffers the discharge (Eekhout & Hoitink, 2015). This buffering is favourable for future water management which should anticipate on more extreme weather as a result of climate change. A buffered discharge decreases the vulnerability of the catchment to periods of extreme rainfall or drought (Makaske & Maas, 2015).

In the last few decades stream restoration is regularly applied in the Netherlands. According to the last stream restoration evaluation conducted by Alterra (Didderen *et al.,* 2009), a total of 489 planned projects were counted in 2008, of which 287 projects were already finished. Most restoration projects (84%) were finished during 1993 – 2008. However in practice the accomplishment of a successful project seems to be quite complex and many stream restoration projects fail (Candel *et al.,* 2017). One of the reasons mentioned by Didderen *et al.* (2009) is that stream restoration projects often have a too specific focus on merely one physical, chemical or biological aspect instead of approaching the system as a whole.

1.2 Problem statement

In restoration projects it is often aimed to construct a near-natural geomorphology and to advance free morphological behaviour (Eekhout *et al.,* 2013). To achieve this, detailed knowledge about the natural morphodynamic functioning of the system is required, however many restoration projects are conducted with minimal scientific context (Wohl *et al.*, 2005). It is regularly assumed that the sinuous shape drawn on historical maps represents the natural planform of lowland streams (Eekhout *et al.,* 2013) developed through meandering. However it is unknown whether lowland streams were able to function in a natural way prior to channelization (Makaske & Maas, 2015; Makaske *et al.,* 2016). There is scarcely information about the (natural) morphodynamic functioning of lowland streams in the past, since there are no structural measurements available prior to channelization and consecutive, reliable maps are missing. It is therefore unknown when and how the sinuous planforms evolved (Candel *et al.,* 2017).

The planform evolution of lowland streams strongly depend on their history (Hoffman, 2008). The morphodynamic functioning of lowland streams is determined by a complex interaction of natural factors, as climate, stream flow dynamics and floodplain characteristics, and artificial factors, as land use changes and hydraulic engineering (Grabrowski *et al.,* 2014; Lespez *et al.,* 2015). There are several theories that discuss important processes that lead to the development of the sinuous planforms of lowland streams. Some studies argue that the sinuous pattern has a natural origin, for instance the shape is (1) inherited from past fluvial regimes and actually laterally stable (e.g. Brown & Keough, 1992; Brown *et al.,* 1994), (2) caused by meandering which is restricted by heterogeneity in floodplain resistance, due to peat growth (Candel *et al.,* 2017), local seepage flow (Van Balen *et al.,* 2008; Eekhout *et al.,* 2013) or cohesive sediments (Kleinhans *et al.,* 2009) probably in combination with typical stream flow dynamics called 'flow separation' (Kleinhans *et al.,* 2009; Blanckaert, 2010; Blanckaert, 2011). Other studies found evidence that the shape has an artificial cause, for instance (1) land use changes starting around the Bronze Age (e.g Tipping *et al.,* 2008; Broothaerts *et al.,* 2014; Lespez *et al.,* 2015), (2) hydraulic engineering, such as the introduction of water mills (Walter and Merritts, 2008) or (3) they are constructed for agricultural purposes and lack a natural origin (Baaijens *et al.,* 2011).

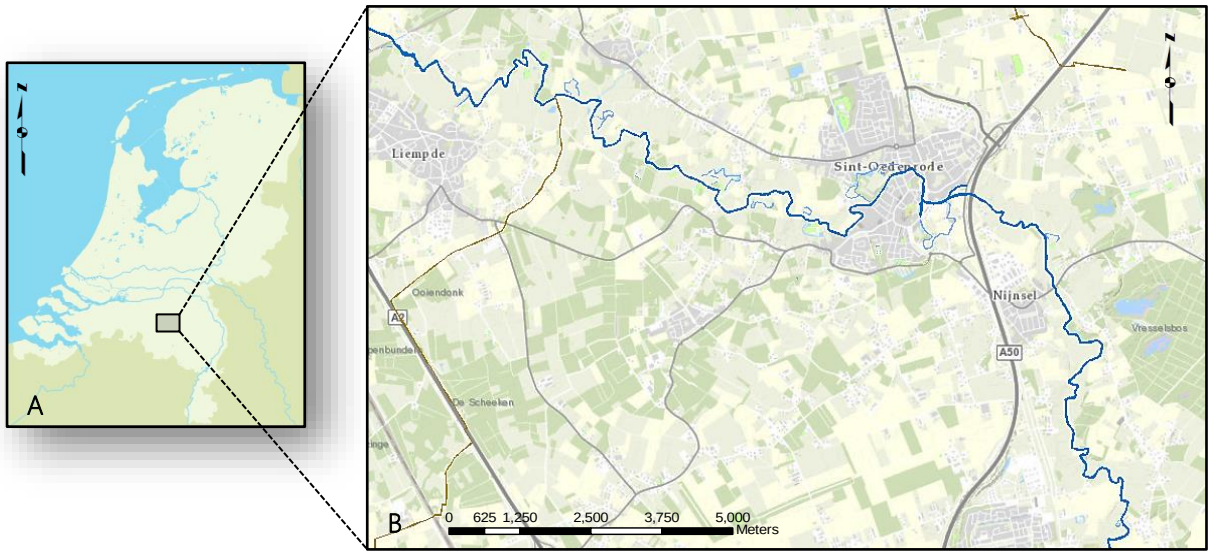

Figure 1 A: Location of the catchment of the Dommel in the Netherlands. B: Part of the Dommel that clearly shows the sinuous planform. The channelized parts could be recognised by the remnants of the former bends that still remain in the landscape. Retrieved from: A: www.ovplaza.nl; B: GeoDesk, Wageningen

Since lowland streams are slow-responding systems (Candel *et al.*, 2017) understanding the planform evolution is only possible when the long-term fluvial dynamics are taken into account (Hoffmann, 2008; Grabrowski *et al*, 2014)). A paleo geographic reconstruction as described in Grabrowski *et al.* (2014) will provide insight in past fluvial regimes and morphodynamic functioning of lowland streams: the combination of various methods as ground radar, coring and OSL-dating sequences will provide information on planform evolution. Furthermore pollen analyses, historical maps and archaeological research can be used to reconstruct past trends in climate and human influence, which will offer a broader understanding of the development of the area and increase insight in the past morphodynamic functioning of lowland streams.

In this research, such a paleo geographic reconstruction will be applied to lowland stream the Dommel, located in the south of the Netherlands (Figure 1). This is one of the lowland streams that still has a highly sinuous pattern, although the stream is normalized at several locations. The Dommel is a convenient lowland stream to study the natural morphodynamic functioning of lowland streams as many old bends still remain in the landscape, representing the situation before channelization.

1.3 Objective and research questions

The objective of this research is to investigate the morphodynamic functioning of the Dommel prior to channelization by a paleo geographic reconstruction. In order to achieve this the following research questions were formalized:

What was the morphodynamic functioning of the Dommel before channelization?

- How did the Dommel develop and gain its sinuous pattern?
- How fast did the bends form and could the forming of the bends be related to specific periods?
- How could the morphodynamic functioning before channelization be related to the current morphodynamic functioning of the Dommel and what does this mean for stream restoration projects?

1.4 Context of this research

This study is part of a combined study about the morphodynamic functioning of the Dommel during the Holocene. This study will provide information on the developments in the Middle and Late Holocene, the study of Niels Kijm will provide more information on the developments in the late Pleistocene and early Holocene. The study area is chosen so that remnants of more recent fluvial systems as well as very old systems are present, providing information about the long-term history of morphodynamic functioning of the system. The same field data will be used for analysis. Together both studies fit into the PhD project of Jasper Candel about morphodynamic functioning of lowland streams which is commissioned by the RiverCare STW project.

2. Theory

This chapter provides an overview of the theoretical background important for this research. It will introduce the important processes determining river morphodynamic functioning in general. Subsequently the geomorphology of meandering rivers will be described in more detail. Furthermore, the influence of climate and human intervention on planform evolution will be explained. Human intervention encompasses the land use changes and hydraulic engineering, which are discussed separately.

2.1 Morphodynamic functioning of rivers

In this study morphodynamic functioning refers to the planform evolution of rivers and streams. Important factors in planform evolution are stream power and floodplain characteristics (Makaske *et al.,* 2016). Stream power is the hydraulic component that combines the (bank-full) discharge, the valley gradient and the channel morphology (e.g. size and shape of the cross-section) to describe the erosional power of the river (Makaske & Maas, 2015). Floodplain characteristics are related to the lithogenesis of the floodplain and determine the bank stability and the sediment calibre (amount and size of the bed load). Variations in these characteristics are associated with various degrees of erosion and sedimentation resulting in a continuum of different channel patterns and planform geometries (Robert, 2003).

Channel patterns can roughly be divided in three groups based on their morphodynamic functioning (Makaske & Maas, 2015): braided systems, meandering systems and straight or laterally stable systems (Figure 2).

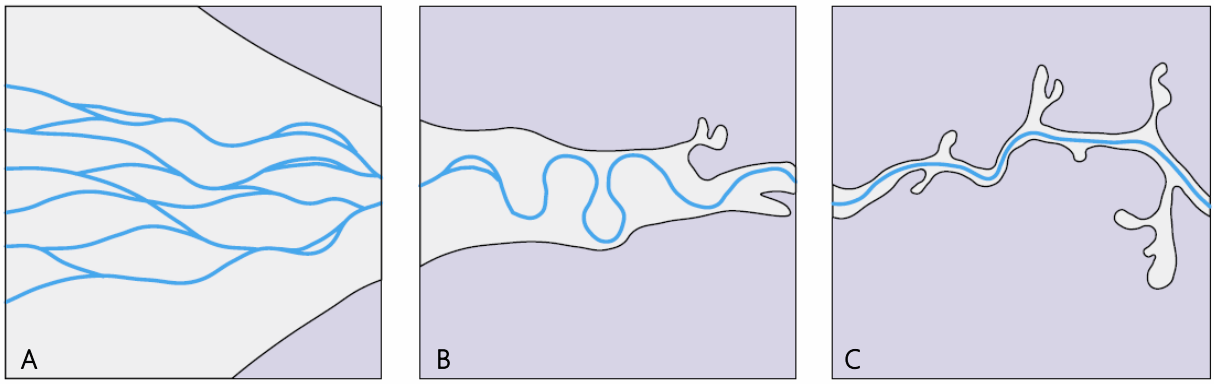

Figure 2 An overview of the different types of river systems. **A**: A braided river system. **B**: A meandering river system. **C:** A straight river system. Retrieved from Makaske & Maas, 2015.

Braided channels are associated with a high stream power and are the most energetic and dynamic river systems (Figure 2A). These rivers are characterized by several shallow channels separated by low bars and some higher areas (Miall, 1977). The channels have a low sinuosity, a high width-depth relation (it can exceed 300) and a coarse (median grain size > 2 mm) bed load is common (Miall, 1977). Meandering rivers are characterized by one sinuous channel that shows lateral migration (Figure 2B). They often have a moderate to low stream power and usually a more fine-textured bed load (median grain size < 2 mm) compared to braided rivers. Straight rivers have one channel that barely show lateral movement (Figure 2C). Such laterally stable systems often occur downstream, where the floodplain has a small gradient resulting in a low stream power and a deep channel, confining lateral migration. Lateral stability can also be caused by a relatively high bank resistance, due to vegetation cover or cohesive sediments (Makaske *et al.,* 2016).

When a river has enough power to transport the bed load and erode the banks, lateral migration can occur (Nanson & Croke, 1992; Makaske & Maas, 2015). To determine whether a system has the potential for lateral movement, the river can be plotted in a stability diagram (Figure 3). This diagram is based on data of rivers that are close to their natural state. These rivers are in morphological equilibrium, which means that the sediment input equals the sediment output (Makaske *et al.,* 2016). Although the diagram is based on the data of rivers, it is assumed that it is also applicable to smaller (low land) streams (Makaske *et al.,* 2016).

In the stability diagram the potential specific stream power (based on the bank-full discharge, $Q_{2.3}$) is plotted against the median grain size of the bed load (D_{50}). The potential specific stream power (ω_{pv} [W/m^2]) is calculated by:

$$\omega_{pv} = \rho\, g\, Q_{2.3}\, S_v / W_r \qquad [\ 2.1\ ]$$

In which:

ρ	= water density	[kg/m^3]
g	= gravity constant	[m/s^2]
$Q_{2.3}$	= bank-full discharge	[m^3/s]
S_v	= gradient of the valley	[-]
W_r	= width of a reference channel	[m]

Morphodynamic functioning of rivers is something continuous, however high discharges are the most important in determining the river planform and geometry. This is because during peak floods most sediment transport took place and in case of overbank flow, deposition on the floodplain will occur (Meade, 1982). The bank-full discharge $Q_{2.3}$ is used to caculate the potential specific stream power.

W_r is a theoretical channel-width, independend of the river type. This independency is important because the potential specific stream power depends on the surface area of the channels, which is different for the river types. Braided river channels are shallow which lead to a small surface area; while meandering and stable rivers have deep channels resulting in a relatively high surface area.

For a coarse bedload (D_{50} > 2 mm) W_r is defined as:

$$W_r = 3.0\ \sqrt{Q_{2.3}} \qquad [\ 2.2\ ]$$

For a sandy bedload (D_{50} < 2 mm) defined as:

$$W_r = 4.7\ \sqrt{Q_{2.3}} \qquad [\ 2.3\ ]$$

In the stability diagram four types of rivers are distinguished. Firstly the strongly braided channels, secondly the braided or meandering channels characterized by scrolls and chutes, followed by meandering channels with scrolls and finally the laterally stable channels. In this research the last two groups are the most important. The borders of the different groups should be interpreted as a lower limit (Kleinhans & Van den Berg, 2011); which means that a river that plots in the area 'meandering with scrolls' has too less energy to become 'braided or meandering with scrolls and chutes' however it could be 'laterally stable'. In that case the stream power of the sinuous river is too low for lateral migration, considering the current $Q_{2.3}$ – value, and the sinuous planform of the river is inherited from past fluvial regimes. A meandering river can become laterally stable as a consequence of a decrease in stream power or a change in sediment load.

In the last centuries in North-Western Europe most rivers are regulated by control structures as weirs and dams (Brown & Keough, 1992; Marren *et al.,* 2014), which strongly reduced free morphological behavior of rivers and resulted in lateral immobile channels that still have a sinuous planform. Since meandering in low-energetic systems can be a very slow process (Makaske *et al.,* 2016), it is not always easy to see the difference between laterally stable and meandering systems. To determine whether a river is meandering or laterally stable, it is important to consider the long-term development of the river.

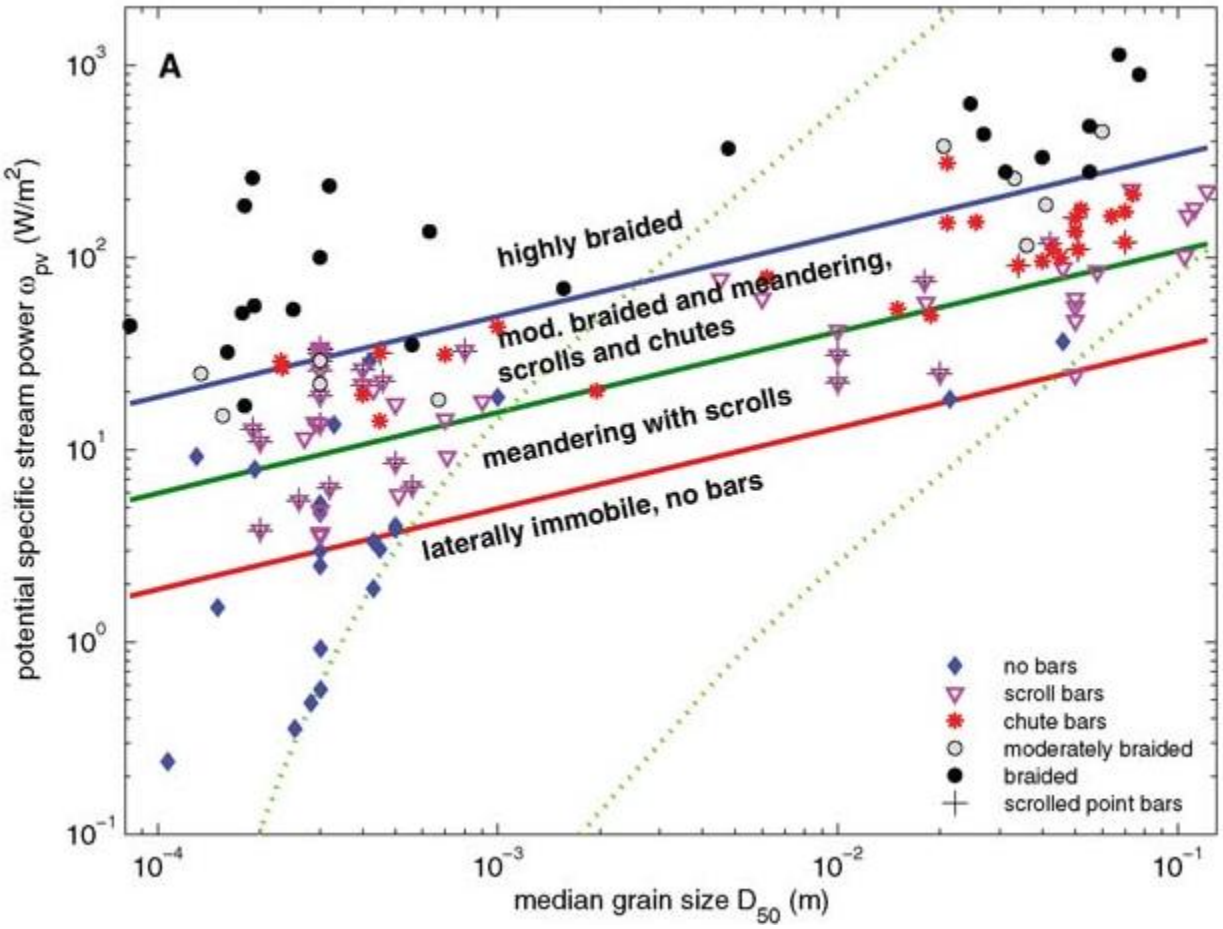

Figure 3 The stability diagram that represents the patterns of alluvial rivers in equilibrium. The data is subdivided by bar pattern. The y-axis indicates the potential specific stream power, calculated by: $\omega_{pv} = \rho\, g\, Q_{2.3}\, S_v / W_r$; the x-axis represents the median grain size of the bed load (D_{50}). Both axis are on a log-scale. Top-down the following river types are distinguished: highly braided, moderately braided or meandering with scrolls and chutes, meandering with scrolls and laterally stable or immobile; no bars. Retrieved from: Kleinhans & Van den Berg (2011).

2.2 Geomorphology of meandering rivers

Meandering rivers form by far the greater part of the rivers across the globe (Leoppold, 1994). They are characterized by a sinuous planform that migrates sideward and downstream (Berendsen, 2004). In a meandering channel, the stream velocity is the largest near the outside of a bend, which causes erosion of the outside bank. At the inside bend the stream velocity is the lowest, resulting in sedimentation. The line that indicates the highest stream velocity is called the thalweg. In the bends, the streambed has an asymmetrical cross-section, characterized by a steep outside bank and a shallow inside bank (Makaske & Maas, 2015). The deepest parts of the streambed, the pools, are located in the bends (Robert, 2003).

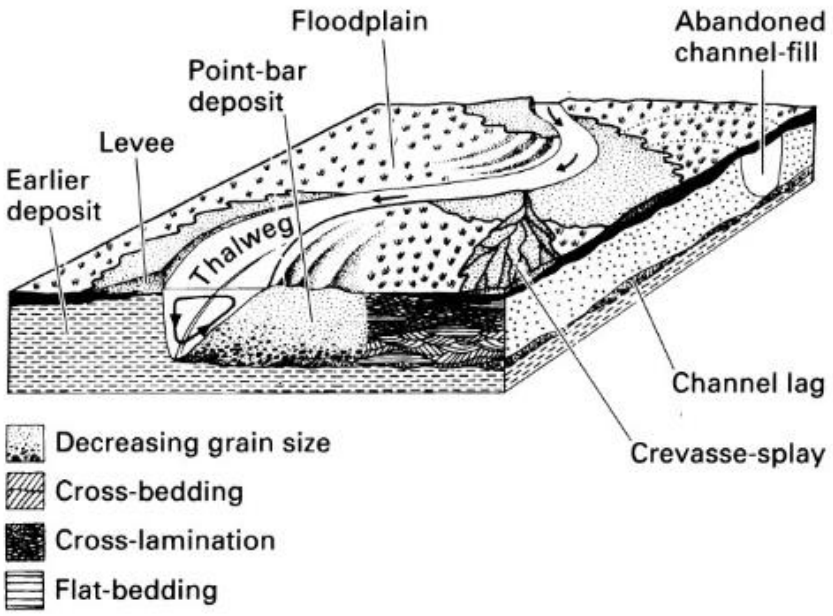

Figure 4 An overview of the important morphological structures and deposits characterizing the floodplain of a meandering river. Retrieved from: http://strata.uga.edu/4500/fluvial/fluvial.html; original: Allen (1964)

The floodplain or the channel belt of meandering rivers encompasses the area that will be flooded at very high discharges. In the floodplain a sequence of morphological structures will develop (Figure 4). The floodplain formation is controlled by the interplay of lateral and vertical accretion (Wolman & Leopold, 1953; Marren *et al.,* 2014). The deposits of meandering rivers consist of fining upward cycles (Miall, 1977). When the discharge is high and the water level exceeds the banks, vertical accretion of the floodplain will take place (Allen, 1964). The coarsest material will be deposited close to the channel resulting in the development of levees and the finer particles, such as loam or clay, will be deposited distant from the channel forming the backswamps. The coarsest grains of the fining upward sequences remark the channel lag (Allen, 1964). A crevasse-splay is formed as flood-waters break out of the main channel, their deposits are relatively coarse comparable to levee deposits (Allen, 1964).

The processes of erosion and sedimentation result in lateral migration of the channel and point bar development. The deposition of point bars occur along inclined surfaces and the deposits are called lateral accretion surfaces or inclined heterolithic strata (IHS). Point bars can be observed in the field as ridge and swales topography in the inner bend area. This morphology is typical for migrating channels (Miall, 1977). Besides lateral migration, the planform of a river can, also be changed by a meander cut-off. When a river has a relatively high stream power a meander chute cut-off can occur (Eekhout & Hoitink, 2015). A new channel will form in at the inner bend floodplain area, parallel to the original meander bend (Figure 5A). Rivers with a lower stream power will rather change their stream path by a meander neck cut-off, which is the result of evolving bends that a one point meet each other (Figure 5B).

After a meander cut-off the abandoned channel changes into an oxbow lake. Over time this oxbow lake will be filled with fine-textured deposits originating from flooding events and also peat can develop (Allen, 1964). Chute cut-offs often occur more gradually (Eekhout & Hoitink, 2015). Therefore these channels will mainly be filled with the bed load sediment of the river, which is relatively coarse grained (Allen, 1964).

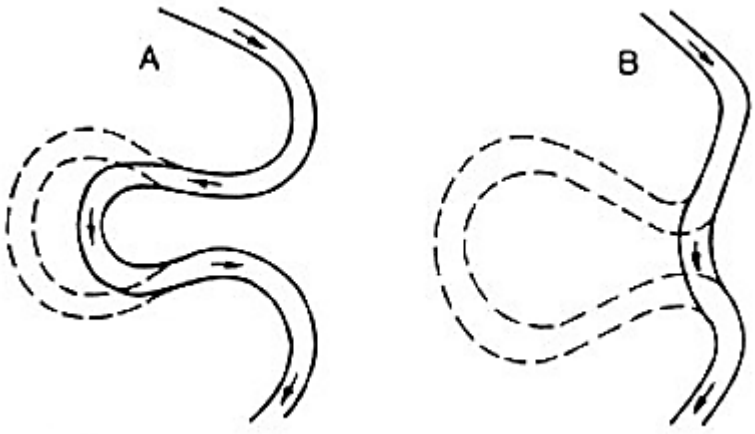

Figure 5 Types of a meander cut-off. **A:** A meander chute cut-off. **B:** A meander neck cut-off. Retrieved from: http://strata.uga.edu/4500/fluvial/fluvial.html

The occurrence of high resistant bodies in the floodplain, such as an oxbow lake fill, can result in counter point bar development (Smith *et al.*, 2009). Counter point bars develop when the river flow is forced to make a sharp bend because it meets a body of highly resistant sediment, which results in separation of the flow and the development of a reverse eddy, upstream of the obstacle (Smtih *et al.,* 2009). The meander migrates downvalley against the resistant body and developing scroll bars change from point bars to counterpoint bars which merge towards the resistant sediment body (Figure 6). Counter point bar development is opposite to point bar development. Counter point bars are characterized by fine-textured sediment and also small layers, up to 10 cm, containing organic matter can occur (Smith *et al.,* 2009). They can be recognised in the field by a concave scroll bar morphology. The dip direction of the lateral accretion surfaces of the scroll bars is always towards the river.

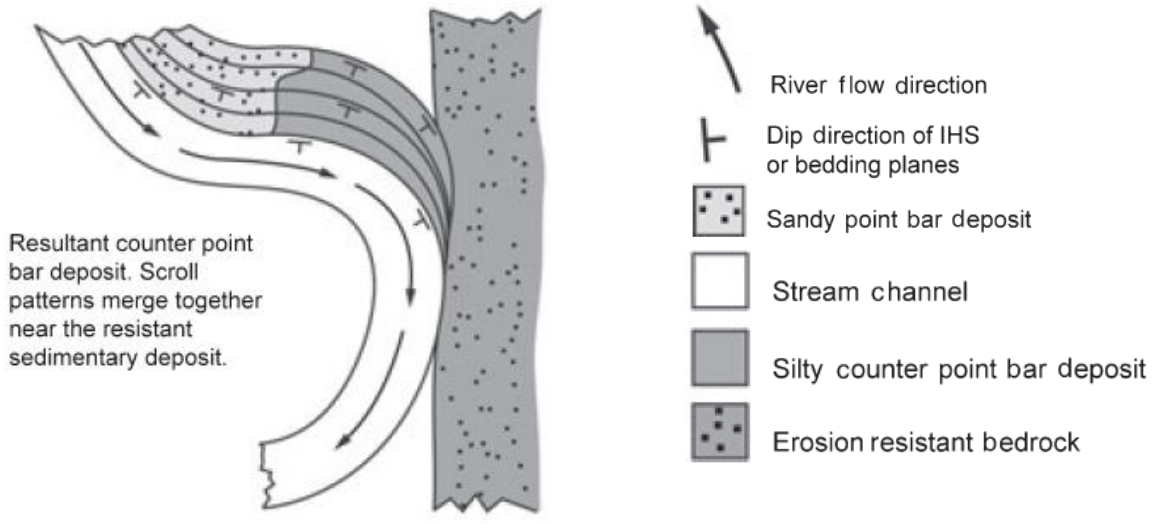

Figure 6 A schematic diagram that represents scroll patterns of point bar deposits and counter point bar deposits that are preserved in meandering river systems. Retrieved from: Smith *et al.,* (2009).

2.3 External controls on planform evolution

2.3.1 Climate and land use

Important determining factors in planform evolution of rivers and streams are bank stability, discharge and sediment supply. These factors strongly depend on external controls as climate and human intervention on land use. The interaction between the external controls and river morphodynamics is very complex as many factors are involved, which also interact with each other. In this section some general observations are discussed.

Climate encompasses the long term averages of temperature and rainfall and is therefore an important determining factor for growth conditions, the type of vegetation, discharge, sediment transport and sedimentation and erosion rates (Berendsen, 2004). Variations in climate, especially when associated with extreme events resulting in high peak discharges, are strongly related to fluvial activity (Starkel *et al.,* 2007). Periods remarked by transitions in climate often coincidence with changes in fluvial morphology. Cold-to-warm climate transitions are related to major incision phases and changes in river style (e.g. Mol *et al.*, 2000; Antoine *et al.*, 2003) often followed by aggradational phases (Kostic & Aigner, 2007). Also the transition from warm to cold led to increased fluvial activity (Notebaert & Verstraeten, 2010), due to an increase in flooding and channel instability (Lamb, 1977; Van Geel *et al.,* 1996; Brown 1998; Brown, 2002). The causes of climatological variations are varied and complex. Solar variability, volcanic activity, and ocean-atmosphere interactions all represent plausible forcing mechanisms (Malcolm & Diaz, 1994; Dergachev *et al.,* 2004; McDonald & Sangster, 2017).

Since the Bronze Age (3000 BC) human influence on the landscape steadily increased (Tipping *et al.,* 2008; Broothaerts *et al.,* 2014; Lespez *et al.,* 2015). When human influence on land use increases, the influence of climate relatively decreases or can even become invisible (Zolitschka *et al.,* 2003). This is because the effect of climate, in, for example, sediment accumulation in the floodplains, is much less pronounced than the influence of land use changes (Notebaert & Verstraeten, 2010). Human intervention almost always leads to changes in erosion and sedimentation rates (Berendsen, 2004; Merritts *et al.,* 2011). Intensification of deforestation and agriculture, enhances floodplain aggradation by the increasing sediment supply and the suspended load (Walter & Merritts, 2008).

Sediment transport is very important in establishing the morphological style of a river (Robert, 2003). Changes in water-to-sediment ratio could result in the change of fluvial style (Huisink, 2000; Mol *et al.*, 2000; Antoine *et al.*, 2003). The most dramatic short-term changes in river morphology are effected by abrupt changes in sediment supply (Robert, 2003). Variations in sediment supply to streams can be caused abruptly by for example major landslides or more gradually by a change in run-off from the land caused by climate change of human impact on land use (Robert, 2003). Land use changes affect both the run-off and the erosion by changes in vegetation cover.

Vegetation cover is an important factor in river morphodynamics as it determines bank and soil stability (Huisink, 2000; Makaske *et al,* 2016) and influences the rate of sediment supply (Kostic & Aigner, 2007). Reduced vegetation cover, may account for higher suspension rates (Kostic & Aigner, 2007). On the other hand an increase in density of riparian trees is associated with a decrease in erosion rates (Pizzuto & O'Neal, 2009) and thus a lowering of the suspended load. When the suspended load in low-energetic systems increases, this lead to an increase in overbank sedimentation, aggradation of the floodplain and siltation of secondary channels (Brown, 2002; Marren *et al.,* 2014). In the context of floodplain impacts, reductions in suspended load are less important, except where they enhance rates of bank erosion and migration (Marren *et al.,* 2014). Changes in vegetation can also affect the system more indirect by changes in

evapotranspiration (Huisink, 2000; Berendsen, 2004) or by buffering the run-off and thereby lowering the peak discharge.

Besides vegetation, bank stability is determined by the lithology of the floodplain. Floodplains consisting of peat or fine textured cohesive sediments as loam or clay, have a high resistance and are hard to erode, especially for rivers and streams with a low stream power. The local occurrence of peat, loam or clay in floodplains, can originate from abandoned channels or over bank deposits (Brown & Keough, 1992; Smith *et al.*, 2009). These morphological structures enhance floodplain heterogeneity and could result in complex channel planforms.

Of all discharges, the peak discharges are the most important in determining the river planform and geometry. Since during peak floods most sediment transport took place and in case of overbank flow, floodplain aggradation will occur (Meade, 1982). Variation in discharge will impact the flows within the channel that account for bank erosion and meander migration rates (Marren *et al.,* 2014). Variation in discharge can be caused by changes in climate resulting in increased or decreased wetness or extreme events. Discharge can also vary as vegetation cover reduces or increases, as it accounts for the direct run-off, resulting in higher or lower peak discharges. At a constant valley slope, a decrease in water discharge generally results in a reduction of stream power (Kostic & Aigner, 2007). A reduced flow velocity could result in a decrease in erosion and meander migration rates, which will over time be accompanied by narrowing of the channel and vegetation establishment; the growth of vegetation will lead to more stable banks and therefore the occurrence of meander cut-offs will be reduced (Marren *et al.,* 2014).

2.3.2 Hydraulic engineering

Considering the major artificial channel works from Medieval times (Brown & Keough, 1997), the influence of hydraulic engineering on planform evolution, may not be neglected. According to Barends *et al.*, (2004) humans have tried to get rid of the water since the Iron Age, by constructing weirs and dams. In general the construction of a dam lead to a reduction in frequency and magnitude of high discharges and low discharges, resulting in a reduction of meander migration rates and over bank flows (Marren *et al.,* 2014). The most common and important dams in history were the mill dams. Probably in the early Middle Ages the first watermills were build (Stuurman *et al.*, 1997), however there are no remnants or documents left that remind of mills at that time. Watermills had a wide applicability, they were used to grind grain, full wool, produce textiles and paper, cut wood, stamp and melt ores, pound metals and squeeze oil and juice from seeds and fruits (Van Halder, 2010; Merritts *et al.,* 2011). In valleys with a low gradient the water flows towards the bottom side of the row, this mill type is called an 'onderslag watermolen'. Water mills needed a constant discharge. To achieve this often a small channel was dug that led the water of the stream to a milldam, where the mill row was constructed. Upstream of the milldam slackwater ponds developed.

A milldam caused a rise in base level and a decrease in stream flow velocity, which was noticeable several kilometres upstream, especially in floodplains with a low valley gradient. A reduced flow velocity resulted in a decrease in erosion and meander migration rates, which was accompanied by narrowing of the channel and vegetation establishment; the growth of vegetation led to more stable banks and therefore the occurrence of meander cut-offs was reduced (Marren *et al.,* 2014). The widespread construction of milldams created a series of slackwater ponds, which gradually changed into sediment-filled reservoirs (Walter & Merritts, 2008), since dams are efficient sediment traps (Marren *et al.,* 2014). This floodplain aggradation was enhanced by the increasing sediment supply due to intensification of deforestation and agriculture (Walter & Merritts, 2008). Figure 7 provides an overview of the effects of flow regulation on floodplain topography and sedimentology. In the past 100 years many water mills have been expired and the mill dams have been breached (Walter & Merritts, 2008). Dam breaching resulted in channel incision into the milldam reservoir sediments and it also led to increased erosion of the steep stream banks (Walter & Merritts, 2008; Pizzuto & O'Neal, 2009). The relatively high and flat areas around channels are described as being the former surfaces

of mill ponds (Merritts *et al.,* 2011) instead of floodplains formed by a combination of lateral migrating channels and over bank deposits consisting of silt and clays (Wolman & Leopold, 1953). The incision of streams after dam breaching could be an explanation for the deep channels and steep banks (Walter & Merritts, 2008), which are often found in lowland streams.

Floodplain aggradation in lowland stream catchments can also be the result of the widely application of the natural meadow-inundation system (Baaijens *et al.,* 2011). In the Netherlands regular flooding was common in until the first half of the 19th century (Heezik, 2007; Baaijens *et al.,* 2011). These flooding events were very useful, because the nutrient-rich water functioned as natural fertilizer for the meadows, increasing the hay production (Baaijens *et al.*, 2011). In addition to that the temperature of seepage water is approximately 10 °C to 12 °C on average and flooding could therefore avoid frozen fields in winter, which was also in favour of the hay production. The application of this inundation system worked well will the practice of milling, as both require relatively high base levels. Over years the practice of inundation led to aggradation of the floodplains.

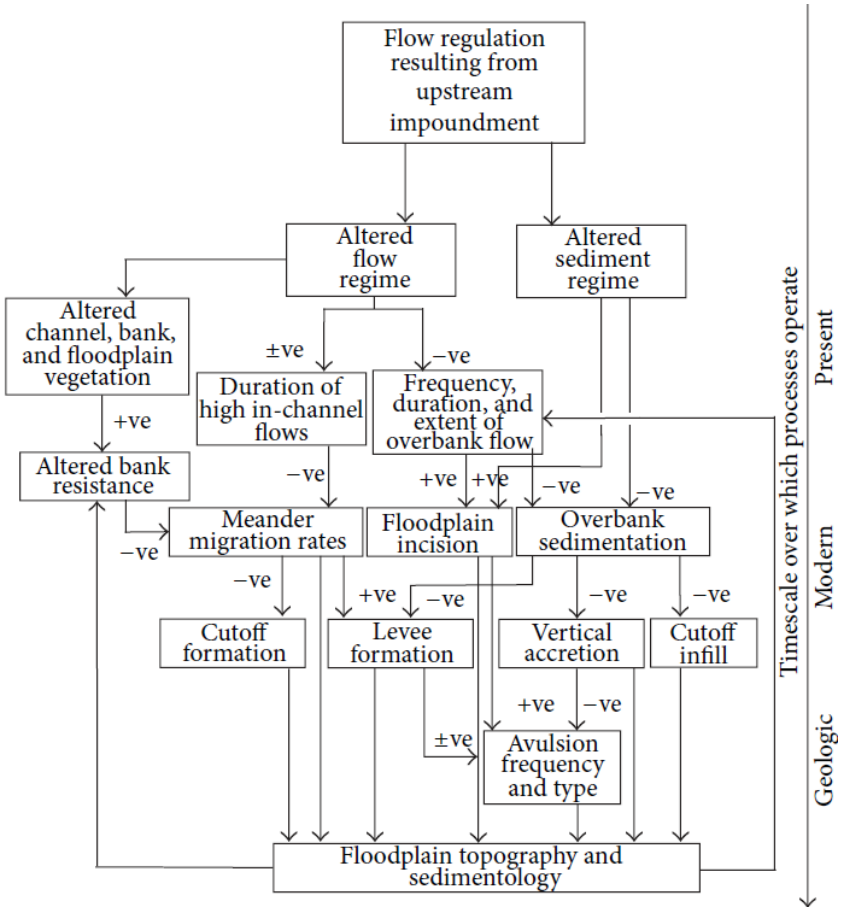

Figure 7 A conceptual model of the effects of dams on floodplain geomorphology. Timescales over which processes operate are arranged vertically through the model. 'Present' encompasses decades, 'Modern' encompasses centuries and 'Geologic' points to the longer timescale. The +ve and –ve symbols indicate whether the changes induced by damming typically result in an increase or decrease in the rates of a particular process. Retrieved from: Grove *et al.,* (2012).

The meadow-inundation system lost its functionality in 1850 when industrialized fertilizer was introduced (Barends *et al.*, 2010; Baaijens *et al.*, 2011). The need of the natural fertilizer gradually disappeared and drainage became much more important (Eekhout, 2014). The growing industrialisation led to the introduction of heavy machinery that enabled more efficient farming but required well-drained fields. The regular flooding became more and more vexatious, especially in winter (Heezik, 2007; Baaijens *et al.*, 2011). In the second half of the 19th century, this resulted in the establishment of Water Boards that aimed to improve the water management of catchments (Heezik, 2007). In favour of fast discharge and well-drained fields, large normalization projects had been constructed and in the period of 1850 to 1965 this led to channelization of many rivers and streams (Heezik, 2007; Buskens *et al.*, 2011).

3. Study area

This chapter introduces the study area and provides information on the origin and hydrology of the Dommel. Furthermore the geomorphology of the environment and the study area itself is described. The chapter ends with an illustration of the history of land use and hydraulic engineering in the surrounding area.

3.1 The Dommel

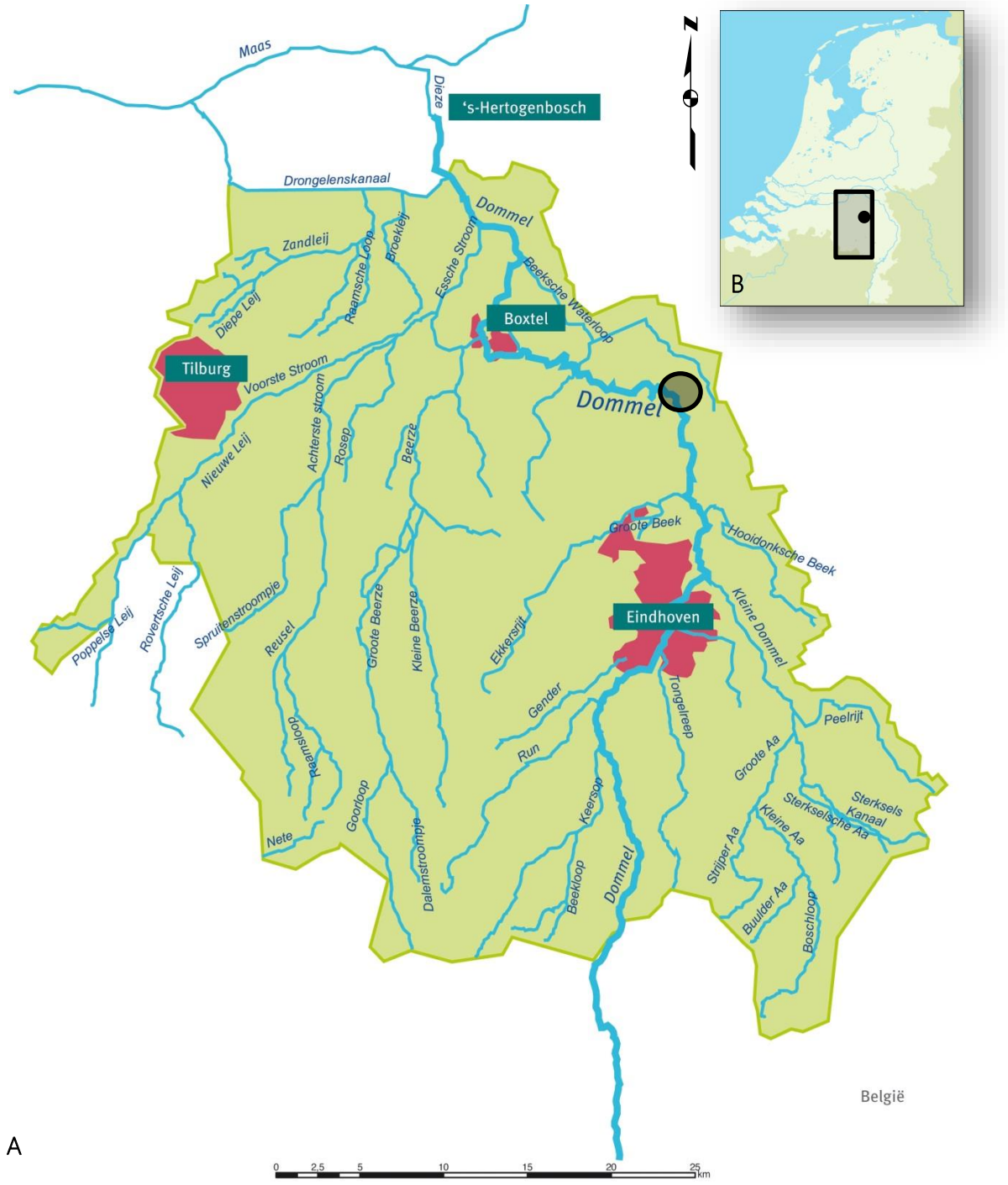

Figure 8 An overview of the Dutch part of the catchment area of the Dommel (**A**) and its location in the Netherlands (**B**). The black circle indicates the study area of this research. **A:** Retrieved from https://www.dommel.nl/algemeen/bestuur-en-organisatie/werkgebied/werkgebied.html. **B**: Retrieved from: www.ovplaza.nl, edited.

The Dommel is a lowland stream in the southern part of the Netherlands (Figure 8). It finds its origin in the 'Donderslagse Heide' at the Kempens Plateau in the northern Belgium, just across the Dutch border (Buskens *et al.*, 2011) from which 85 km are located in the Netherlands. The surface area of the catchment in the Netherlands is 153.500 ha. The Dommel is a stream mainly fed by rainwater, with a small groundwater contribution. Groundwater contribution is most important in the upstream part of the catchment, in the middle and downstream part the discharge is more related to precipitation (M. Berg, personal communication, January 10, 2018). In Eindhoven a water purification system treats all the water coming from the sewage system of the upstream catchment and this water discharges into the Dommel (M. Berg, personal communication, January 10, 2018). The catchment area has a long-term annual precipitation of 775 to 825 mm, measured over the period 1981 – 2010 (KNMI, unknown). The Dommel is a low-energetic stream that has a total elevation difference of 35 m, which results in an average longitudinal slope of 0.24 m/km. The longitudinal slope at the study area is 0.00032, measured over a distance of 11 km. The channel width varies between 12 and 20 m, however at some locations, in the curves, it reaches a width of 30 m. The current depth of the stream is approximately 6 m + NAP which corresponds with 4 to 4.5 m below the surface, depending on the height of the banks. A stream width of 20 m, leads to an unusual small width/depth ratio (~5). The average stream velocity is between 0.5 and 1 m/s (Waterschap de Dommel). The average discharge of the Dommel is 14 m^3/s and the bank-full discharge ($Q_{2.3}$) is 22.3 m^3/s (Waterschap de Dommel, 2016). The latter is retrieved from hourly discharge measurements over the last six years executed by waterschap de Dommel. The measuring device was located slightly upstream of the study area.

3.2 Geomorphology of the floodplain

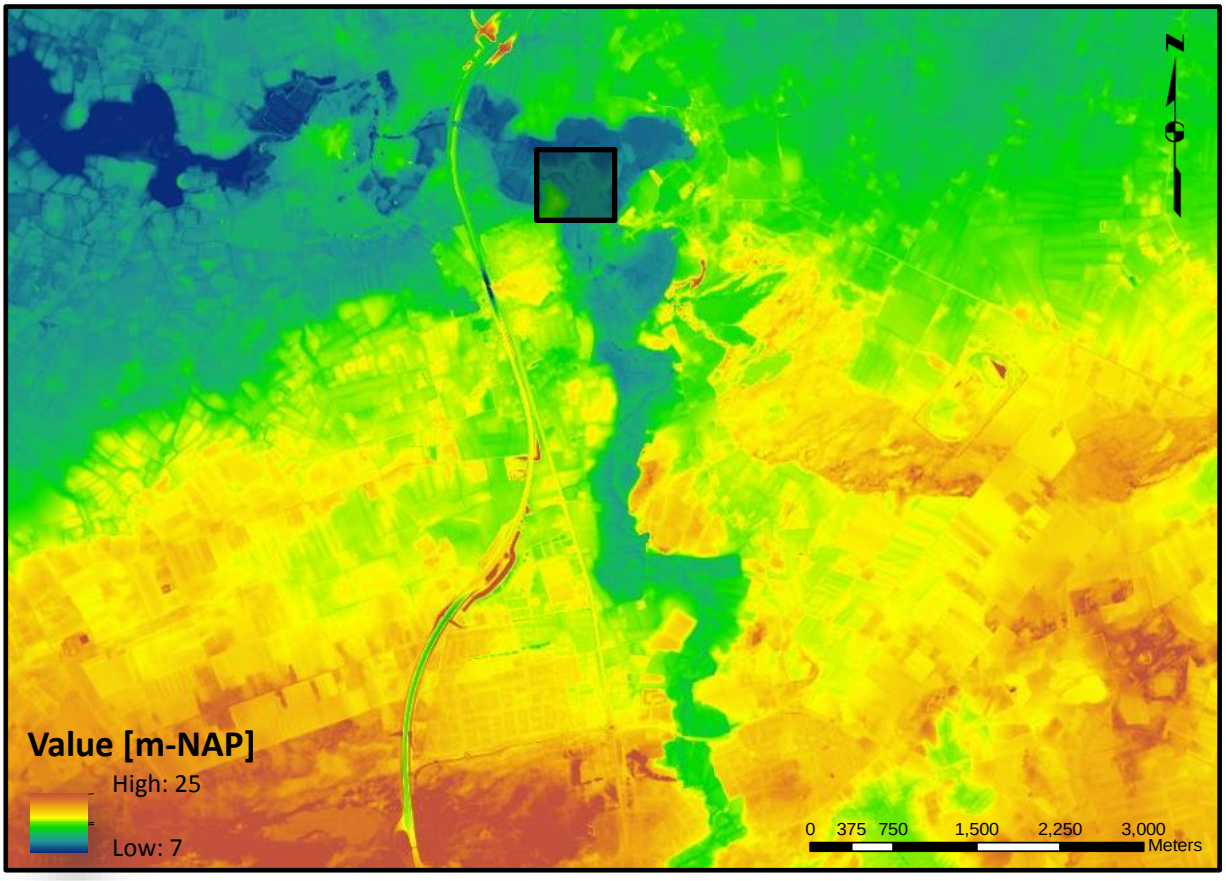

Figure 9 Digital Elevation Map of the landscape surrounding the study area, which is indicated by the black square. Retrieved from: GeoDesk Wageningen.

The floodplain of the Dommel is located in a cover sand setting. The landscape around the study area can roughly be divided in a high (red/yellow) and a lower (green/blue) part (Figure 9). The high part mainly consists of cover and drift sand deposits. Originally most of the villages were built in this area (Barends *et al.,* 2010). The floodplain of the Dommel, in blue, remarks the lowest part of the area. The width of the floodplain varies from 200 to 1000 m. As a consequence of seepage the floodplain is relatively wet and in the lowest parts peat can be found (Figure 10). The floodplain is therefore mainly extensively used as grassland.

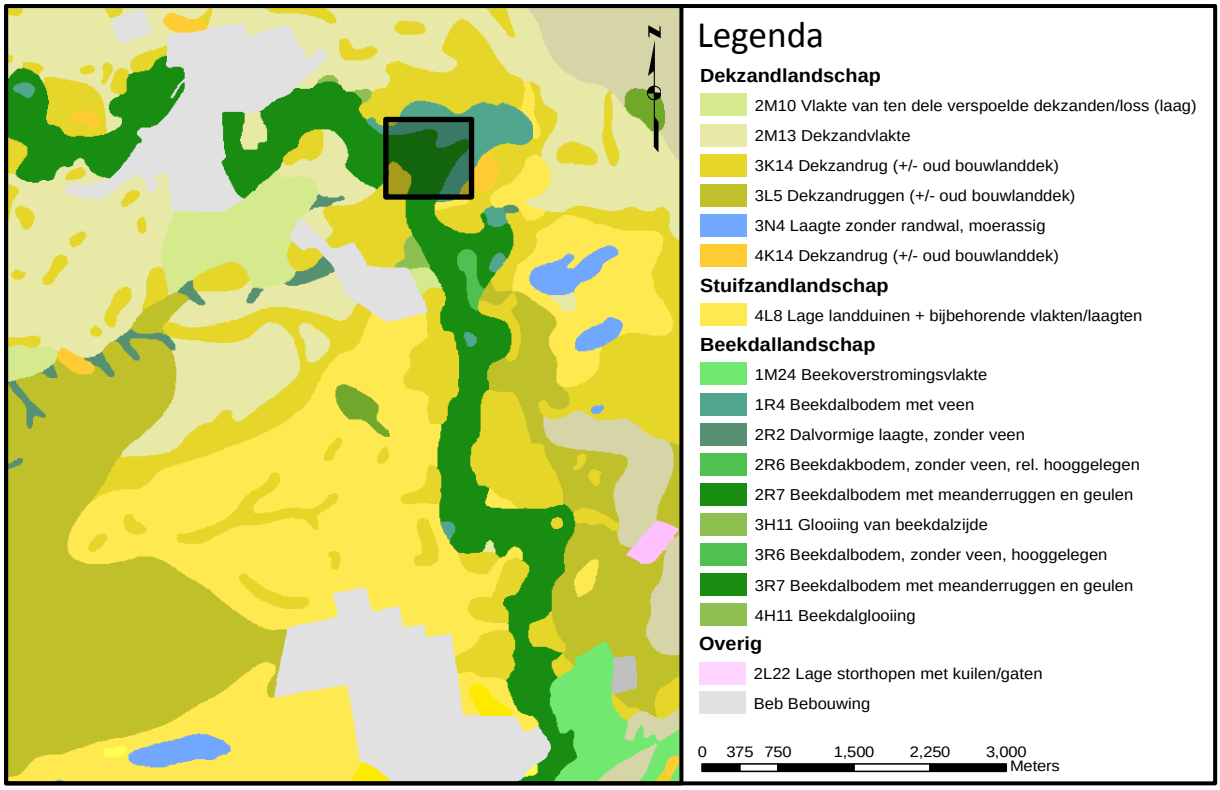

Figure 10 Dutch Geomorphological Map of the study area. The black square indicates the study area. Main groups of the legend: Coversand landscape, Driftsand landscape, Lowlandstream floodplain landscape and Other (containing artficial units). Source: Geodesk, Wageningen.

The geomorphological map (Figure 10) represents the types of deposits that occur in the area. It becomes clear that the largest part of the environment of the Dommel consists of sandy deposits. Four groups of deposits are distinguished in the legend of the map. The first two groups contains the cover and drift sand deposits. These are coloured yellow or light green. The blue unit indicates low, wet marsh areas. The third group contains the lowland stream floodplain deposits. The green colour, which indicates the major part of the floodplain, refers to floodplain deposits without peat development. The pale green colour, also occurring in the study area, indicates floodplain deposits that contain peat development. The fourth group contains artificial units as urban development.

At several locations the floodplain is disproportionally wide compared to the width of the Dommel. A close up view of the most extreme location (1000 vs 20 m) is represented in Figure 11 At the right border of the (old) large floodplain a (younger) smaller fluvial system has been developed. There is no other location along the stream valley of the Dommel were both old and more recent deposits are so well preserved next to each other, which makes this a unique and very interesting location.

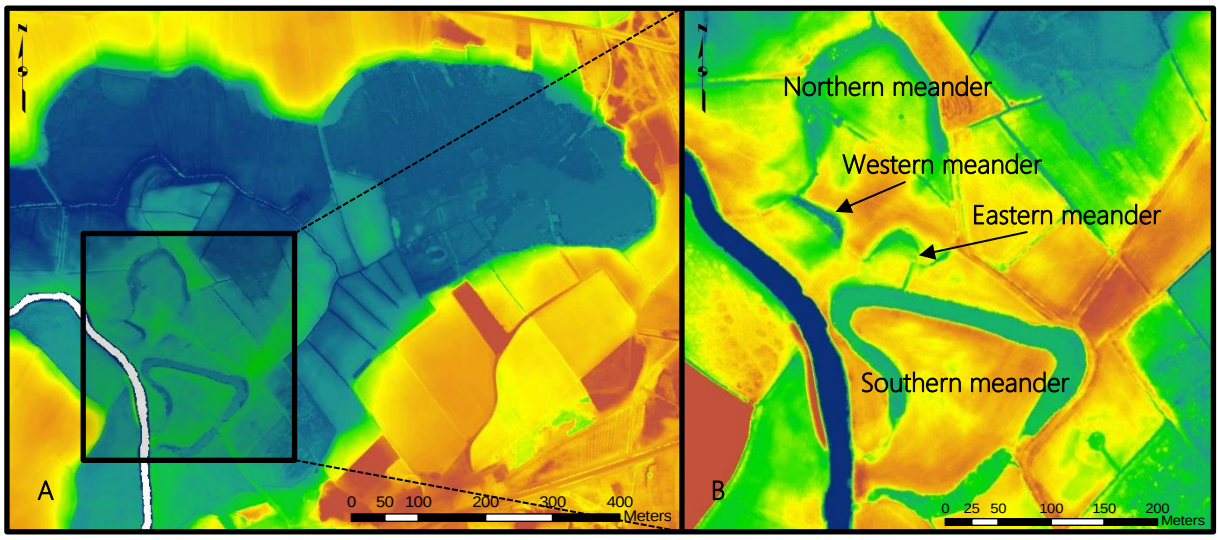

Figure 11 Digital elevation map of the large floodplain and the study area in detail. **A**: A close up view of the location where the stream valley of the Dommel is widest. An elevation value of 8 to 20 m-NAP is used. The black square indicates the study area. **B**: The study area in detail including two large and two smaller former meanders. An elevation value of: 9.5 to 11 m-NAP is applied to visualize small differences in height. Retrieved from: GeoDesk, Wageningen

This study will focus on the younger part of the floodplain (Figure 11B). In this part four small paleo meanders can be distinguished. Henceforth these bends will be called northern, (little) eastern, southern and (little) western meander. The area is owned by the State Forestry and is extensively used for grazing. The landscape is characterized by small fields, bordered by ditches and trees. In the northern part also wetlands occur and west of the area a swamp forest developed (Figure 12). The area is called the Moerkuilen, which refers to the lake located west in the area, which is the result of small-scale peat excavation. The excavation of peat in this area probably started in the Middle Ages and continued until the mid-20th century (Brock, ~1825). Considering the small extent of the excavation, the peat was probably only used by the neighbouring farmers.

Figure 12 Aerial photograph of the study area taken in 2013. **A:** Extensively used grassland. **B:** Wetlands. **C:** Swamp forest. **D:** The Moerkuilen. **E:** Remnants of an old inundation system: a pond and ditches at short distance parallel to each other. Retrieved from: GeoDesk, Wageningen

3.3 History of the area

At the end of the Late Glacial the temperature increased and the sea level rose (Berendsen, 2004). This led to a rise of the groundwater levels. The open landscape of the floodplain of the Dommel gradually changed into a more forested landscape dominated by pine and birch trees in the Post Glacial (Leeuwarden & Janssen, 1986). Towards the Atlantic (8000 to 5000 years ago) the pine tree vegetation gradually changed into a deciduous forest. This causes a precipitation surplus, because pine trees evaporate more water compared to deciduous forest (700 mm/yr vs 400 mm/yr) (Berendsen, 2004). In the low-lying areas of the floodplain of the Dommel this led to peat growth (Leeuwarden & Janssen, 1986; Berendsen, 2004).

Figure 13 The historical Dommel and one of the planned channelization works at St. Oedenrode. **A:** Topografisch Militaire Kaart (TMK; i.e. Topographical Military Map), sheet 51, dating form 1850. This is the oldest historical map that represents waterbodies topographically correct. This map shows the irregular rectangular planform of the Dommel prior to channelization. The rectangle indicates the area of B. **B:** A drawing of the planned channelization in the Dommel at St. Oedenrode. One large irregular bend and two smaller bends were planned to be cut off and this is indeed accomplished. The icon of the watermill represents the location of the Borchmolen (1312 to 1945) at St Oedenrode. For the location of St. Oedenrode in the Netherlands see Figure 1. Retrieved from: **A**: GeoDesk, Wageningen; **B**: BHIC, 1st series, 7-6001-466-8 –St.Oedenrode.

In the Neolithic period (5000 to 2000 BC) the first settlements start to develop in the sandy areas in the Netherlands, starting in the loss areas of Southern Limburg (Heesters & Prinssen, 1984; Barends *et al.*, 2010; Notebaert & Verstraeten, 2010). The presence of human occupation around 2300 BC in the neighbourhood of the study area is confirmed by archaeological and paleo botanical research (Beekx, 1970; Janssen, 1972; Heesters & Prinssen, 1984). In the sand dunes that run parallel to the Dommel numerous artefacts dating from the Neolithic period, the Bronze Age (2000 to 800 BC) and the Iron Ages (800 to 12 BC) were found (Beekx, 1970; Heesters & Prinssen, 1984). Especially numerous artefacts were found in the neighbourhood of the Moerkuilen (Janssen, 1972). The occurrence of Calluna (Heather) and Pteridium (Eagle fern) indicates the Iron Age occupation phase (Janssen, 1972). In the early Iron Age a new ploughing method was introduced, which enables tilling of the heavier clay soils (Clark, 1952), this method was probably also used in the floodplain of the Dommel (Janssen, 1972). The so called 'Celtic fields', which were discovered at several locations in the south of the Netherlands are also remnants of the Iron Age (Arnoldussen, 2013). These are small square parcels surrounded by small embankments (Spek *et al.*, 2013). The appearance of rye in the

Moerkuilen 2000 years ago indicates the Roman occupation phase (Janssen, 1972), which is characterized by further deforestation followed by intensification of agricultural practices (Renes, 1988; Notebaert & Verstraeten, 2010).

Prior to the Middle Ages the major part the southern Netherlands was too wet for permanent settlement however this changed around 1000 AD (De Bont, 1993). At that time large-scale exploitation of the uplands started, indicated by the expansion of rye and buckwheat (Janssen, 1972). Farmers began to combine agriculture with cattle breeding and started to use the oxcart for ploughing and started to produce milk and wool (Barends *et al.*, 2010). In this period the heathlands expanded and drift sands started to occur because of overexploitation of the poor sandy soils (Janssen, 1972; Barends *et al.*, 2010). The occurrence of drift sands continued until the Late Middle Ages (De Bont, 1993). The typical micro relief of drift sand dunes is still recognisable in the landscape (Figure 12).

In the Middle Ages (500 to 1500 AD) several watermills were constructed at the Dommel. The first reporting of a watermill in North-Brabant dates from 965 AD (Van Halder, 2010)[1]. In the centuries following, the construction of many other water mills is reported. Downstream of the Moerkuilen there was a watermill called the Borch Mill (Figure 13), which was built in 1312 (Van Halder, 2010). Although this watermill was 2 km away from the study area, the rise in base level and the decrease in stream velocity should have been noticeable, due to the small valley gradient. Four kilometres upstream of the Moerkuilen there was another watermill, called the Mill of Wolfswinkel. This mill was active from 1381 to 1947, the exact year of construction of the mill is unsure (Van Halder, 2010). Both mills were removed in the 20th century. For more details on the watermills of the Dommel see Appendix I.

At the end of the Middle Ages the floodplains of the Dommel were extensively used as haylands (Janssen, 1972; De Bont, 1993). To increase the yield the farmers made use of a semi-natural inundation system in which the regularly flooding of the Dommel acted as a natural fertilizer for the fields. Because of this fertile water it was possible to harvest hay three times a year (Baaijens *et al.*, 2011). For optimal water use a pattern of parallel ditches was dug with a small distance to each other. The water inundated the fields during winter, when the water reached its highest levels. This inundation system disappeared with the introduction of artificial fertilizer in the 19th century (Eekhout, 2014). The remnants of the patterns of ditches can still be found in the landscape (Figure 11 & 12).

Figure 14 An overview of the changes in the study area over the last 150 years. **A**: The digital elevation map of the study area. The remnants of both former meanders are visible. An elevation value between 9.5 to 11 m-NAP is used. **B**: Topografisch Militaire Kaart, 1850 (TMK). The southern meander is still part of the Dommel, the northern meander is visible in the ditches. **C**: Bonnebladen 1920. The southern meander is visible but uncoupled of the Dommel. The northern meander is visible in the ditches. Retrieved from: GeoDesk, Wageningen

[1] The mill was called the Kaarschotse watermill of Rijnsbergen and is mentioned in official documents of the St. Baafsabbey in Gent.

In the 19th and 20th century large-scale channelization projects were constructed (Figure 13). In that period also one of the meanders in the study area (southern meander) is cut-off (Figure 14). The southern meander was still connected to the Dommel in 1850 (Figure 14B), however in 1920 the meander was cut-off and a straight channel was constructed (Figure 14C). In the field it can be observed that the eastern bank of the new channel is reinforced by an embankment. The cut-offf meander still remains in the landscape, however the small channel at the east side of the new Dommel disappeared (Figure 14A).

4. Research Methodology

This chapter describes the research methodology as applied in this study. The chapter starts with an explanation of the application of Ground Penetrating Radar (GPR) and is continued by a description of the collection and analysis of coring data. Subsequently Optically Stimulated Luminescence (OSL) dating and its application in this research are explained and finally it is described how the data will be integrated.

4.1 Ground Penetrating Radar

Ground Penetrating Radar (GPR) is a fast, non-destructive geophysical technique which provides insight in the shallow subsurface (Bersezio *et al.*, 2007; Rey *et al.,* 2013). This technique makes use of high frequency (100 MHz to 1 GHz) electromagnetic energy to detect contrasts in dielectric properties of the subsoil to a maximum depth of 50 m (Neal, 2004). The required frequency of the device depends on the aim of the research. A high frequency results in a larger penetration depth but a lower resolution (Neal, 2004; Rey *et al.,* 2013). GPR is increasingly applied to reconstruct past depositional environments[2] and it is powerful in combination with coring (Candel*, et al.*, 2016).

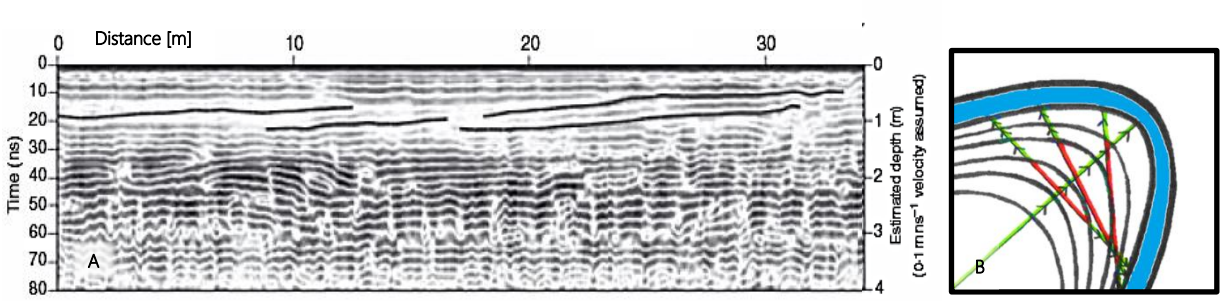

Figure 15 The occurrence of lateral accretion surfaces in the subsoil. **A:** Inclined lines on a GPR image, which are interpreted as lateral accretion surfaces. **B:** A sketch of the top view of a meander bend, the black lines indicate the lateral accretion surfaces and the arrows indicate the direction of migration. Further explanation is in the text. Retrieved from: **A**: Kostic & Aigner, (2007); **B**: Own drawing.

A two dimensional profile of the subsoil is obtained, which in particularly provides insight in changes in lithological composition and the residual water content (Asprion & Aigner, 1997). In the unsaturated zone, the residual water content is mainly determined by grain-size and sorting, as it depends on the size and geometry of the pore space (Kostic & Aigner, 2007). Since grain-size and sorting could be recognised, this technique is able to visualize point bar development and lateral accretion surfaces. This is very important for this research, as lateral accretion surfaces could indicate whether and where a stream had been migrated. When the stream had migrated, lateral accretion surfaces appear as inclined lines at the radar images (e.g. Bersezio *et al.,* 2007; Kostic & Aigner, 2007; Rey *et al.,* 2013). However the occurrence of lateral accretion surfaces on the radar images also depends on the direction of the radar transect (Figure 15). When the radar transect is parallel to the direction of migration, the lateral accretion surfaces will appear (Figure 15B: green lines). At a radar transect more or less perpendicular to the direction of migration the inclined surfaces will not appear, since they are in line with this transect (Figure 15B: red lines).

There are more difficulties in interpreting GPR images. Below the phreatic surface the images often show attenuation of the signal (e.g. Bersezio *et al.,* 2007; Rey *et al.,* 2013). The floodplain of the Dommel has a shallow ground water table (1 to 2 m below surface), which could thus complicate the interpretation of the images.

[2] For an overview see: Neal, 2004

Furthermore parabolic structures could appear, when obstacles, for example wood particles or bricks, are present. In that case the radar will receive the signal of the obstacle before, during and after passage, resulting in a parabolic structure at the GPR image (Figure 16).

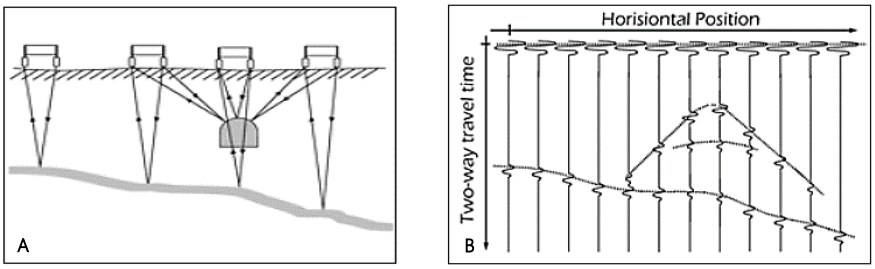

Figure 16 Explanation of the appearance of parabolic structures on GPR images. **A:** The emitted signal reflect the obstacle before, during and after passing, the grey line (i.e. texture difference) also reflects the signal. **B:** The resulting structures that appear on the GPR image: a parabolic structure representing the obstacle and an inclined line representing change in texture. Retrieved from: https://www.eoas.ubc.ca/courses/eosc350/content/methods/gpr-06.htm.

In this study, five GPR transect lines were acquired, covering the northern, western and southern meander (Figure 17). The transects are more or less in the expected direction of migration of the bends. These transects were mainly used to complement the coring data[3]. For a detailed overview of the appearance of lateral accretion surfaces in this area, the data of 31 GPR transects is used, which are obtained from Candel *et al.,* (2018).

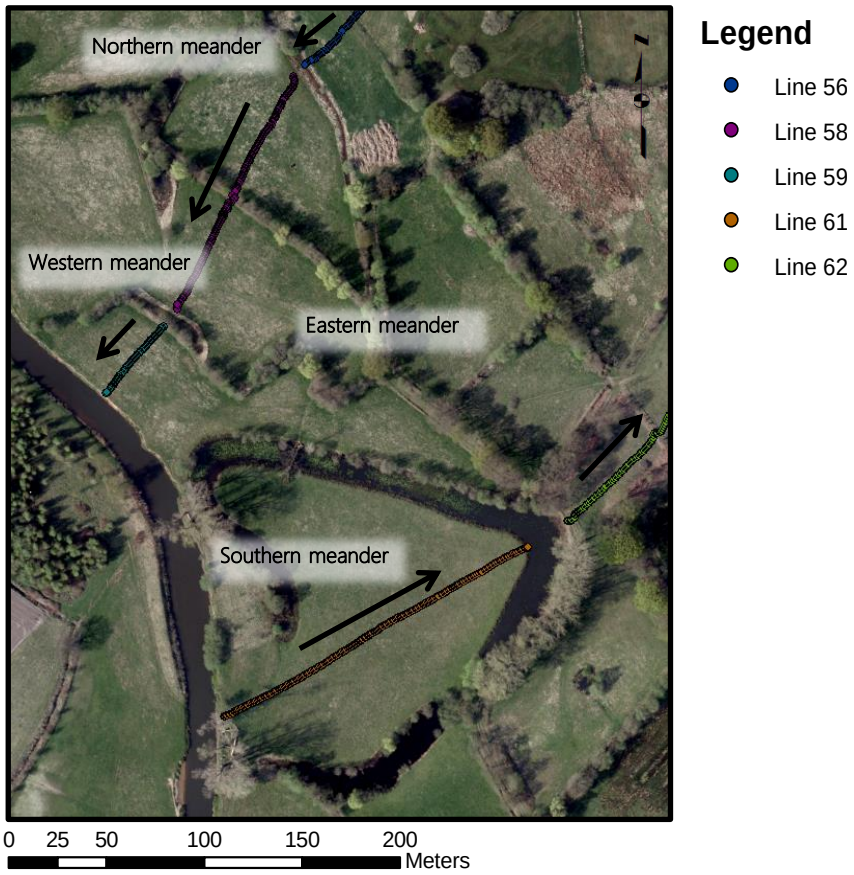

Figure 17 The locations of the GPR transects that cover the Eastern, Northern and Southern meander. The arrows indicate the direction of the measurements. Background: Aerial photograph of 2010, retrieved from: GeoDesk, Wageningen

[3] See section 4.2 Coring

The measurements were all conducted with a pulse EKKO PRO using a SmartTow configuration (Figure 18). The equipment consisted of a device that is moved across the surface of the terrain, emitting very short temporal pulses every 10 cm. The dielectric properties of the subsoil reflect the waves which were recorded. The distance was measured by an odometer and a GPS device was used to trace the location of each measurement. A frequency of 250 MHz is used, as a small penetration depth (maximum reach: 8 m) is sufficient and this frequency provides relatively high-resolution images. This frequency is often applied to shallow fluvial deposits (e.g. Bersezio *et al.,* 2007; Kostic & Aigner, 2007; Rey *et al.,* 2013).

Figure 18 The pulse EKKO pro GPR measurement device as used in this research. **A:** Measurement device that record and display the signal. **B:** GPS device. **C:** Transmitter (250 MHz). **D:** Receiver. **E:** Odometer: measuring distance. Source: own pictures.

4.2 Coring

To obtain detailed information of the lithology of the floodplain, two types of coring instruments were used. The first type is the Edelman auger with extension pieces, which is convenient for boring the sandy and clayey soil above the groundwater table. In very peaty areas a gouch is used (Oele *et al.,* 1983). The second type is the Van der Staay suction-corer, whose working principle is explained in Figure 19. This suction-corer is used for coring below the groundwater table down to a maximum depth of 4.8 m.

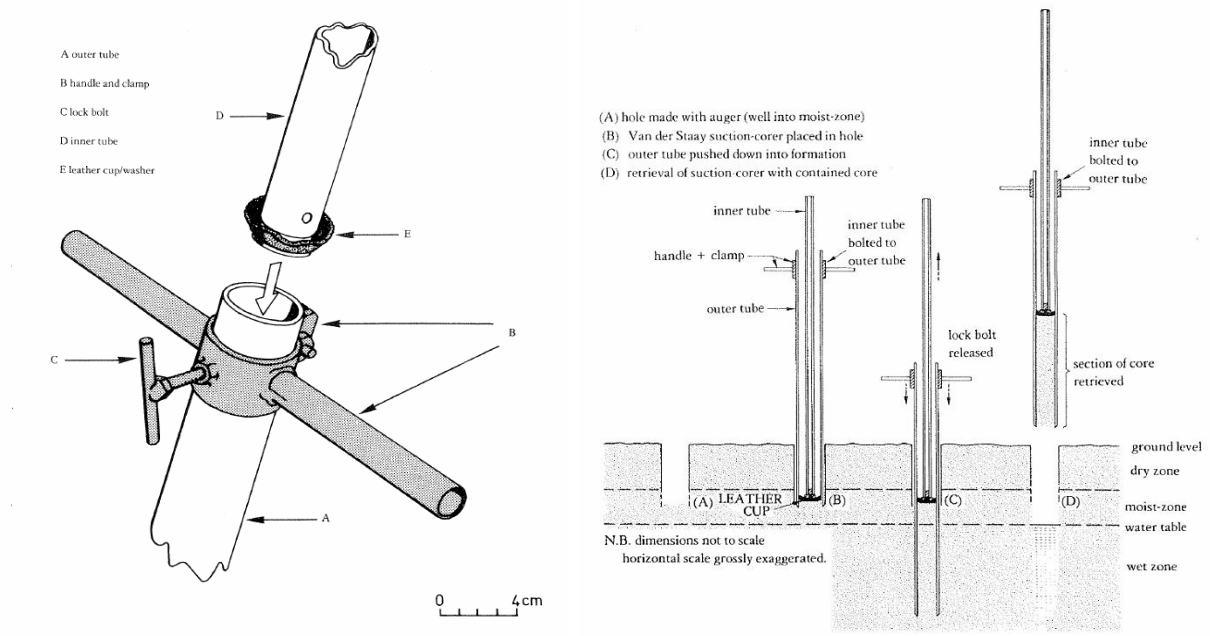

Figure 19 The working principle of the Van der Staay suction-corer. Retrieved from: Van de Meene *et al.,* (1979)

The location of the drill observation points (Figure 20) was determined, based on AHN and the GPR profiles. For every observation point the method as described in Berendsen & Stouthamer, (2001) was used. The exact location of the observations was determined by GPS and the height was calculated using GIS. For every 10 cm the following information was described at an 'Augering Description Form':

- The dominant texture
- The type and amount of organic matter and plant remnants
- Roughly the colour(s)
- If present: oxidation and reduction mottles
- If present: small layers (mm to cm) with a different texture within the 10 cm interval
- Additional information (minerals, charcoal, chalk, etc.)

Five different types of peat were distinguished: (1) Peat: Dark (soft) plant remnants; roots, leaves and wood; this type contained almost no sand or clay and was dark brown or black coloured. (2) Clayey peat: A combination of peat and clay which contained more peat than clay: often dark coloured (3) Peaty clay: A combination of peat and clay which contained more clay than peat, it was lighter of colour and contained some decomposed organic matter. (4) Sandy peat: Peat with a certain amount of sand; lighter of colour, grains can clearly be distinguished. (5) Peaty sand: Sand with a certain amount of peat; light of colour, contains some decomposed organic matter.

The type of sand was estimated using a sand ruler that could distinguish six different classes: extremely fine sand (90 to 150 μm), very fine sand (150 to 210 μm), fine sand (210 to 250 μm), medium sand (250 to 420 μm), coarse sand (420 to 600 μm) and gravel (> 600 μm). The remaining texture classes (e.g. loamy sand, sandy loam, silt loam, clay loam and sandy clay) were determined by comparison with other textures. Their distinction was mainly based on colour and loam/clay content.

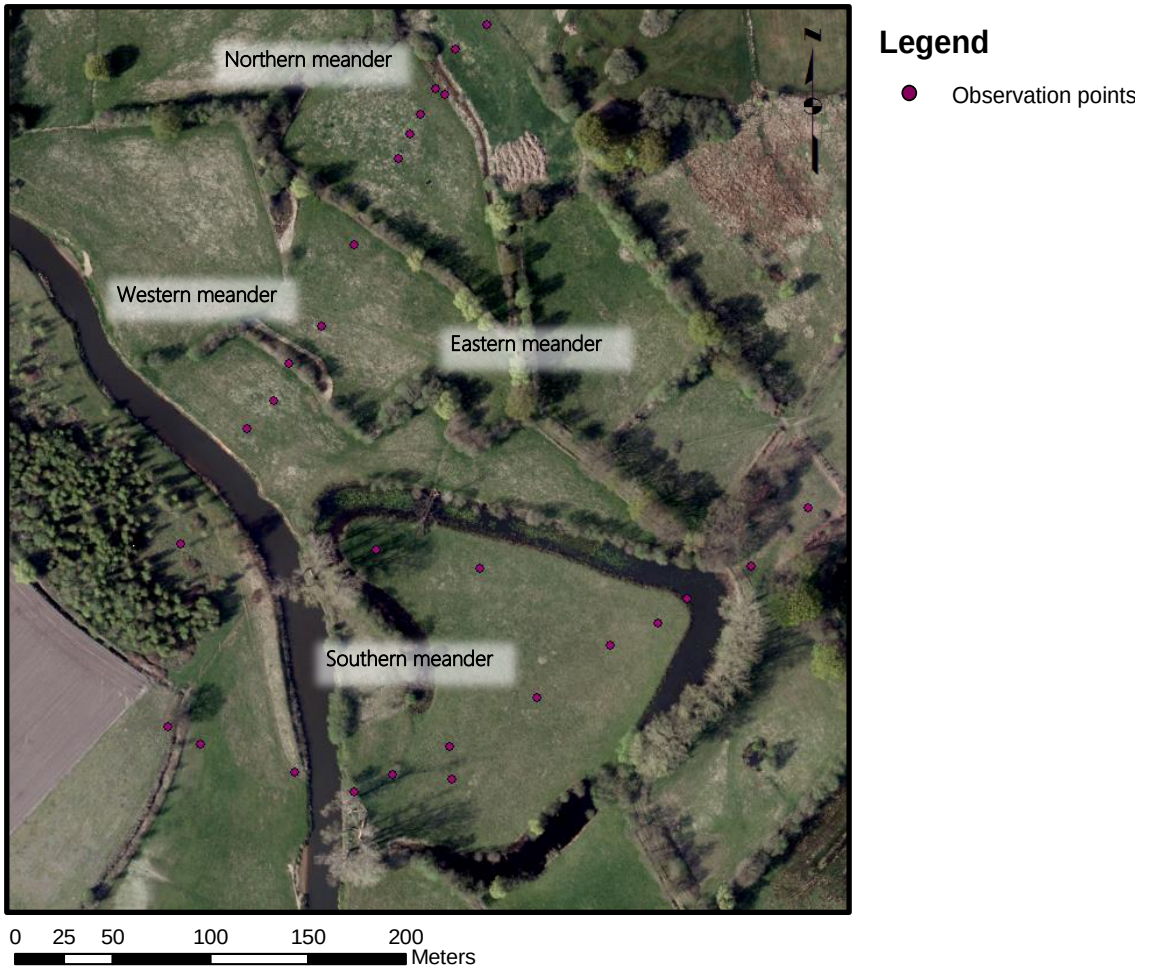

Figure 20 The locations of the observation points in the study area. Background: Arial photo of 2010, retrieved from: GeoDesk, Wageningen

The collected data is loaded in the soil profile description program LLG, which creates a spatial database of all the coring data over distance. From this database a lithological cross-section is reconstructed, by correlation of the different texture layers. Subsequently, several lithogenetical units were distinguished based on the lithological profile and additional features found during the coring (e.g. the presence of organic matter and plant remnants, colour differences and layering). The AHN and GPR images complemented the coring data as they provided information on morphological structures, such as abandoned channels. The integration of this information, including the OSL dates, resulted in a lithogenetical profile.

4.3 Optically Stimulated Luminescence Dating

4.3.1 General application

Optically Stimulated Luminescence (OSL) dating is a rapidly developing dating technique which is widely applied in Late Quarternary sediments (Aitken, 1998). The calculated luminescence age of deposits refer to the last exposure of the minerals to daylight, and this exposure time is implicitly assumed to be sufficient to remove any pre-existing signal (Duller, 2004). OSL dating offers the possibility to investigate geomorphological processes and their dynamics using high resolution chronologies (Rodnight *et al.*, 2005; Madsen & Murray, 2009). One of the advantages of OSL dating compared to ^{14}C dating is that it has a wide range of applicability; ages in the range of 10 yr to 1 Ma could be obtained (Preusser *et al.*, 2008; Cunningham & Wallinga, 2012), while the maximum age that can be determined with ^{14}C dating is approximately 35 ka (Wallinga, 2002). Furthermore, OSL dating is applicable to aeolian (e.g. Jia, *et al.,* 2015; Hesse, 2016; Carr, *et al.,* 2016) and fluvial deposits (e.g. Braillard & Guelat, 2008; Cunningham & Wallinga, 2012; Gao *et al.,* 2016) that frequently show a lack of in-situ organic material, which is required for application of ^{14}C dating. When organic matter is present in fluvial deposits it is mostly reworked (Fiałkiewicz-Kozieł *et al.*, 2015), while the sand grain fraction used for OSL is almost always present.

OSL dating is based on the release of energy that is captured as charge in defects of the crystal lattice of quartz and feldspar minerals. The energy or charge can accumulate when grains are exposed to natural ionising radiation from the environment. This natural radiation is composed of three components: cosmic radiation from space, external radiation from neighbouring grains and internal radiation from within the grain (Preusser *et al.*, 2008). The charge trapped at defects of the crystal lattice is stable for a long period and can accumulate as long as the grains are buried (Wallinga, 2002). This energy is released when the grains are exposed to light (e.g. during transport by wind or water) or heat by showing a small light (luminescence) signal. The intensity of this luminescence signal is related to the age of the deposit. The luminescence age is calculated by:

$$\textit{Luminescence age [yr] = Paleo dose [Gy] / Dose rate [Gy yr}^{-1}\textit{]} \qquad [\,1\,]$$

In which the paleo dose represents a value retrieved by laboratory experiments and the dose rate (DR) represents the background radiation signal which led to accumulation of charge of the natural signal. To calculate the paleo dose a sample will be exposed to light which results in the so-called 'natural luminescence signal' and lead to bleaching of the sample. Subsequently, the sample will be exposed to a Strontium/Yttrium Bèta source which again leads to accumulation of charge, which however occur much faster than that would happen in nature due to the high radiation of the Bèta source. Then the sample will be exposed to light again which results in a 'test dose luminescence signal' and again bleaches the sample. Several test dose signals will be obtained by differing the exposure time of the sample to the Bèta source. Older samples need a longer exposure time to obtain a 'test dose signal' that approaches the 'natural signal' and therefore more test dose measurements are required. When the test dose signal exceeds the natural signal the measurement series is accomplished. The natural luminescence signal will then be compared with the series of test dose signals resulting in a paleo dose value. This value provides, in combination with the natural ionising radiation (e.g dose rate), information on the last exposure to daylight and therefore the time that the sediment is buried.

For a good estimation of the burial time it is essential that the grains are well bleached before they were buried. Full bleaching cost some tens of seconds of bright sunlight (Cunningham, 2011). During aeolian transport the grains are almost always well-bleached before deposition, however fluvial transport is more turbulent and these deposits therefore generally contain a high contribution of poorly bleached grains. In studies dealing with fluvial deposits extra attention must be paid to the degree of bleaching of the grains

(Preusser *et al.*, 2008; Wallinga, 2002). When the exposure time to light was too short for complete bleaching, the minerals could still contain charge trapped in defects of the crystal lattice. After a certain burial time the charge captured in the minerals consist of old, not completely zeroed charge and new accumulated charge, resulting in a brighter luminescence signal and an overestimation of the age. When a sample consists of a mixture of poor and well bleached grains, this results in a wide range of ages. The sub-samples that represent younger ages are assumed to be a better approach of the real age of a sample.

4.3.2 Sampling

In this research OSL dating is applied to investigate the planform evolution of lowland stream the Dommel. Ten samples were taken for OSL dating, covering the northern and the southern meander (Figure 21). The sample locations are chosen so that they are parallel to the assumed direction of migration. The northern meander shows a curvature that can be expected in a natural situation, characterized by erosion of the outside bank and deposition on the inside bank. This made it plausible to assume a direction of migration perpendicular to the curvature. In contrast, at the southern meander it is not directly visible in which direction the stream migrated due to the quite irregular shape.

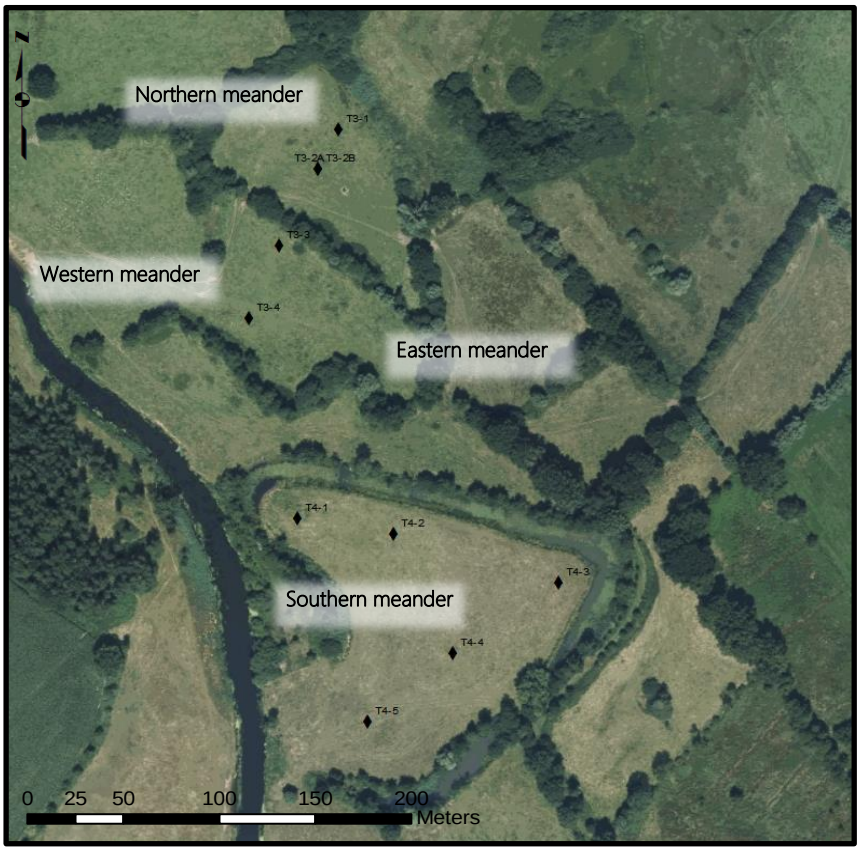

Legend

♦ OSL sample locations

Name	NCL-code 21160~	Depth [cm]
T3-1	69	250-280
T3-2A	70	220-250
T3-2B	71	380-410
T3-3	72	255-280
T3-4	73	270-295
T4-1	74	270-300
T4-2	75	210-240
T4-3	76	260-290
T4-4	77	225-250
T4-5	78	230-260

Figure 21 The OSL sample locations including the depths of the samples. Note that sample T3-2A and T3-2B were from the same core at different depths. The depths are measured form the surface. Background: Aerial photo of 2014, retrieved from GeoDesk Wageningen.

In Figure 22 a theoretical explanation for the building phases of the latter is given assuming a straight stream at the start of the development. In the second stage a small sinuous shape started to develop, directed to the south. In the third stage a larger curve developed in south-eastern direction. The fourth stage is characterized by migration to the north-west. The fifth stage shows the abandoned meander as it is now.

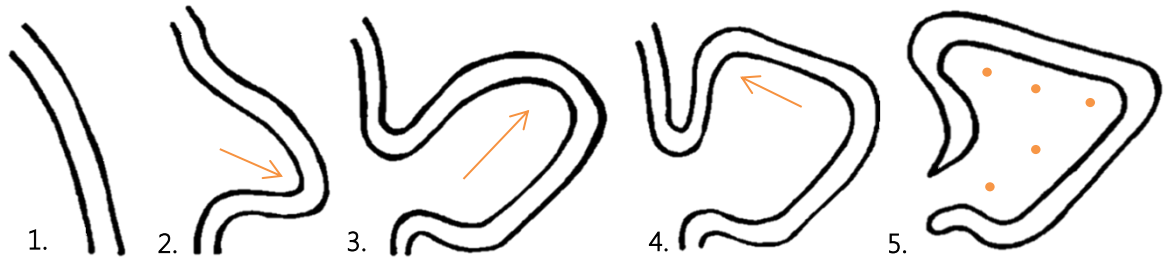

Figure 22 A theoretical reconstruction of the lateral migration of the Southern meander. **1**. Assuming a straight stream at the start of development. **2**. Lateral migration eastward, slightly directed downward. **3**. Lateral migration to the south east. **4**. Lateral migration to the northwest and sharpening of the bends. **5**. The abandoned meander as it is now and the sampling points following from the assumed development of the bend. Source: own drawing.

The samples were taken using the Van der Staay suction corer, with a loose pvc tube at the end for collecting the OSL sample (Figure 23A). The depth of the samples was determined based on the coring data, to make sure that the samples were at the depth of the fluvial deposits and below the groundwater table. Nine samples were taken at approximately the same depth, varying between 210 to 290 m below surface. In the northern meander two samples (T3-2a & T3-2B) were taken from the same core at different depths. The deep sample was taken to identify the age of the coarser material, which was found at 4 m below surface. This change of texture probably indicates an older deposit, therefore this sample is expected to be the oldest.

From historical maps[4] it is known that the southern meander was still part of the Dommel in 1850, whereas the northern meander was merely partly recognisable in the pattern of ditches. The northern meander should thus have been developed earlier. The expected sequence of ages from old to young is therefore: T3 – 2B, (deep sample of the northern meander) T3 – 4, T3 – 3, T3 – 2A, T3 – 1, (northern meander) T4 - 5, T4 – 4, T4 – 3, T4 – 2, T4 – 1 (southern meander). In NCL codes the sequence is expected to follow this order: 71 – 73 – 72 – 70 – 69 – 74 – 75 – 76 – 77 – 78.

[4] See section 3.3 History of the area

4.3.3 Measurements

General explanation

In fluvial deposits poorly bleached grains are common and it is therefore very important to have a good indication of the degree of bleaching as the accuracy of the final age estimation largely depends on this (Reimann *et al.*, 2014). The method as applied in this research consists of two measurement series; first a measurement series that provided an indication of the degree of bleaching and secondly a more precise measurement series that lead to the final age estimation. In the following sections the measurement series will be explained in more detail. The samples were prepared and measured in the Netherlands Centre of Luminescence dating (NCL), located in Wageningen. The measurements were conducted by Risø TL/OSL readers (Bøtter-Jensen *et al.*, 2000, 2003) fitted with a Strontium/Yttrium Bèta source.

Figure 23 The practical application of OSL dating. **A**: The samples were collected in tubes closed by plastic lids. **B**: After separating, sieving and chemical treatment, the sediment was ready to be measured. The picture shows the prepared wheels with the aliquots containing grains, that were put in the machine. The picture is taken after the measurements.

First measurement series

To prepare the samples for the measurements they were sieved to get the 212 to 250 µm grain fraction. Subsequently the samples were treated with 10% HCL to remove calcium carbonates and with 10% H_2O_2 to remove organic matter. After this chemical treatments the sample still contained quartz and feldspar minerals and heavy minerals, if present. For every sample five aliquots with a large mask size (5 mm ≈ 300 grains) were prepared. This mask size is chosen because the samples are expected to be quite young (< 4000 years) and might therefore show only a small signal coming from a few grains. Using a smaller mask size would probably lead to a lack of luminescence signal. The disadvantage of a large mask size is that the equivalent dose signals represent an average value. This leads to uncertainty in age estimation, as high and low values will be averaged out. However in the first measurements series this was acceptable, as an indication of the age and the degree of bleaching is sufficient.

For the first measurement series the method as described in Reimann *et al.*, (2015) was applied. This method has several advantages compared to a complete OSL measurement. Firstly, the application is much faster, as only a few sub-samples of a minimally treated sample are used. In addition to that, this method offers the possibility to study the degree of bleaching prior to the full OSL measurement, so that the best samples can be selected for further analysis (Reimann *et al.,* 2015). With the adopted method the degree of bleaching was studied through comparison of quartz and feldspar signals, as quartz and feldspar minerals bleach at different rates (Murray *et al.,* 2012).

In this study a single-aliquot regenerative-dose (SAR) protocol was used as described in Murray & Wintle, (2000) to measure multiple luminescence signals with different bleaching characteristics. Table 1 shows the modified SAR protocol step by step.

Table 1 Multiple signal single-aliquot regenerative-dose (MS-SAR) measurement protocol for the first measurement series.

Step	Action	Light	Temperature (°C)	Time (s)
1	Bèta regenerative dose or Natural*	-	-	*See comment
2	Preheat	-	250	10
3	Measuring feldspar signal	IR LED's	50	60
4	Measuring feldspar signal	IR LED's	150	60
5	Measuring feldspar signal	IR LED's	225	60
6	Measuring quartz signal	Blue LED's	125	20
7	Exposure to Beta source (Beta test dose)	-	-	50
8	Cut heat	-	250	10
9	Measuring feldspar signal	IR LED's	50	60
10	Measuring feldspar signal	IR LED's	150	60
11	Measuring feldspar signal	IR LED's	225	60
12	Measuring quartz signal	Blue LED's	125	20
13	Measuring quartz signal	Blue LED's	125	40
14	Repeating step 1 to 13			

* For step 1 different time intervals are used to measure the natural luminescence signal and the equivalent doses. For all the aliquots consecutive 0, 50, 100, 200, 0, 50 are used. Some aliquots receive an extra test dose for 100 or 150 seconds.

The quartz and feldspar minerals were measured by using infrared (IR) LED's (~875 nm) and blue LED's (~470 nm). The feldspar signal was measured in three steps at 50°C, 150°C and 225°C (i.e. IR50, IR150 and IR225). The luminescence signal obtained at higher temperatures is related to traps at the crystal lattice, that need more energy to bleach (Murray *et al.,* 2012). The feldspar signal was measured first, because the traps in the feldspar minerals will already empty using IR stimulation, which is possible without disturbing the quartz signal (Murray *et al.,* 2012; Reimann *et al.,* 2015). Preheating of the aliquots is needed to empty thermally unstable traps (Wallinga, 2002) however this would cause noise in the results.

First the natural signal was measured, which is the luminescence signal of the sample without exposure to the Bèta source. Subsequently the full cycle was repeated using different time intervals of the Bèta test dose (i.e. 50, 100, 200, 0 (for recuperation), 50 (for recycling) seconds). Step 7 to 11 are included to correct for potential sensitivity changes of the grains during the measurement. Step 13 is meant to completely reset the sample.

Second measurement series

In the second measurement series a better estimation of the quartz age was pursued. In young samples the feldspar signal can fade and the quartz signal, which has a better bleaching, therefore gives a more accurate indication of the equivalent dose. The already prepared samples were chemically treated with 10% HF, 40% HF and washed with 10% HCL, removing the feldspar minerals and etching the quartz grains. Based on the brightness of the luminescence signal of the samples in the first measurement series, it was now decided to use a smaller mask size, which reduces the effect of averaging. For every sample eight aliquots with a mask size of 3 mm (≈ 100 grains) were used for the measurements (Figure 23B). Table 2 shows step by step the modified single-aliquot regenerative-dose (SAR) protocol to measure multiple luminescence signals.

Table 2 Multiple signal single-aliquot regenerative-dose (MS-SAR) measurement protocol for the second measurement series

Step	Action	Light	Temperature (°C)	Time (s)
1	Bèta regenerative dose or Natural*	-	125	*See Comment
2	Preheat	-	180	10
3**	Measuring feldspar signal	IR LED's	30	40
4	Measuring quarz signal	Blue LED's	125	20
5	Bèta test dose	-	125	20
6	Cutheat	-	180	0
7	Measuring quarz signal	Blue LED's	125	20
8	Measuring quarz signal	Blue LED's	125	200
9	Repeating step 1 - 8			

* For step 1 different time intervals are used to measure the natural luminescence signal and the equivalent doses. For all the aliquots first the natural signal is measured and consecutive a regenerative dose of 40, 0, 40 and 40 s. are applied. Some aliquots receive an extra test dose for 200 seconds.

** Step 3 is only applied in the last measurement which had a Beta test dose of 40 seconds in step 1.

The steps were again first applied to the undisturbed sample which gives the natural luminescence signal (i.e. a Bèta regenerative dose of 0 s.). Subsequently the steps were repeated using different time intervals of the regenerative dose (i.e. 40, 0, 40, 40). Step 5 to 7 are included for correction of the potentially change in sensitivity of the grains to radiation during the measurement. Step 8 is meant to completely reset the OSL signal. Repetition of the measurements for zero and forty seconds of exposure to Bèta radiation in step 1 are included for calibration. Step 3 is only applied in the last measurement which had a regenerative dose of 40 seconds in step 1. This measurement is included to check if there are maybe still feldspar minerals present which could disturb the luminescence signal.

Determination of the Dose Rate

The dose rate (DR) is not determined for all the samples as the deposits in the area likely have the same origin (i.e. reworked cover sand) and therefore contain comparable values for internal and external ionising radiation. Of both, the northern and southern meander one sample is chosen for DR determination, based on homogeneity (e.g. no organic matter or loamy layers present) and available amount of material. The DR values were obtained using high-resolution gamma-ray spectroscopy. For both samples the ionised radiation of ^{40}K, $^{210, 212, 214}$Pb, $^{212, 214}$Bi, ^{228}Ac and ^{234}Th was measured. For good comparison between the samples the weighted average was calculated, from which the effective dose rate of every sample was determined by using sample-specific information on depth, water content and organic matter content. The grainsize is assumed to be the same for all samples. The water content and organic matter content differ per sample and this influences the natural ionising radiation. They are taken into account as they were different for every sample. For the water content an error of 25% is assumed and for the organic matter content an error of 10% is assumed. The depth is included for determination of the cosmic dose rate. The final age of the samples was determined by combining the paleo dose and the effective dose rate value[5].

[5] See formula 4.1

4.3.4 Analysis

Risø TL/OSL software (Duller, 2016) was used for analysis of the raw data. Figure 24 represents the integration limits of the feldspar and quartz measurements. Following Cunningham & Wallinga (2010) a three-component model of OSL decay was used to determine the integration limits of the quartz measurements.

Figure 24 Settings of the Risø TL/OSL software; the integration limits used for the equivalent dose calculation. Quartz refers to the quartz measurements of both the first and second measurement series.

In the first measurement series a maximum test dose error of 15% was used for the feldspar measurements. For the quartz measurements a maximum test dose error of 10% already led to acceptance of all the aliquots. The data of the second measurement series is accepted using a maximum test dose error of 15%.

Further calculations for both measurement series were executed in Excel (e.g. final dose, error estimation, standard deviation). To calculate one representative paleo dose value for every sample a Minimum Age Model was applied (Galbraith *et al.,* 1999; Cunningham & Wallinga, 2012) using MatLab. This model assigned a higher weight to the lower values, assuming that the lowest ages are the most representative. In the model an overdispersion of 0.15 $^{+}/_{-}$ 0.05 is assumed. This model was only applied to the data of the second measurement series.

4.4 Integration of data

The integration of the collected data resulted in a paleo geographic reconstruction of the planform evolution of the four meanders in the study area. The GPR images were used to reconstruct the direction of lateral migration and the occurrence of paleo channels. The lithological and lithogenetical profiles complement these profiles by providing a detailed overview of the texture, structure and depth of the system. Whereas the OSL dates provide information about the sequence and time span of the planform evolution. The combination of this data resulted in a step-by-step reconstruction of the planform evolution of the lowland stream in the study area. This paleo-geographic reconstruction represents a possible explanation for the planform evolution of the Dommel at this location.

5. Results

In this chapter the results of this study are presented. Firstly, the patterns visible on the GPR images will be explained. This is followed by a description of the lithological and lithogenetical cross-sections of the northern and southern meander including the explanation of the lithogenetical units. Subsequently the results of the first and second OSL measurement series are examined. And finally all the data is combined in a paleo-geographic reconstruction.

5.1 GPR Images

The Ground Penetrating Radar transects provided information on the deposits of the subsoil. At first two transects were obtained visualizing the subsoil of the northern and southern meander[6]. Roughly three dominant patterns could be recognised: inclined surfaces, parabolic structures and straight lines. Within the northern meander inclined surfaces appear, which can be interpreted as lateral accretion surfaces. In the southern meander these surfaces were hardly visible due to hyperbolic structures. To increase the insight of the development of the meanders and to confirm the occurrence of lateral accretion surfaces in the floodplain, additional radar transects were executed in the area (Candel *et al.,* 2018). These transects were taken in different directions covering a large area inside and outside the bends, including the eastern and western meander (Figure 25).

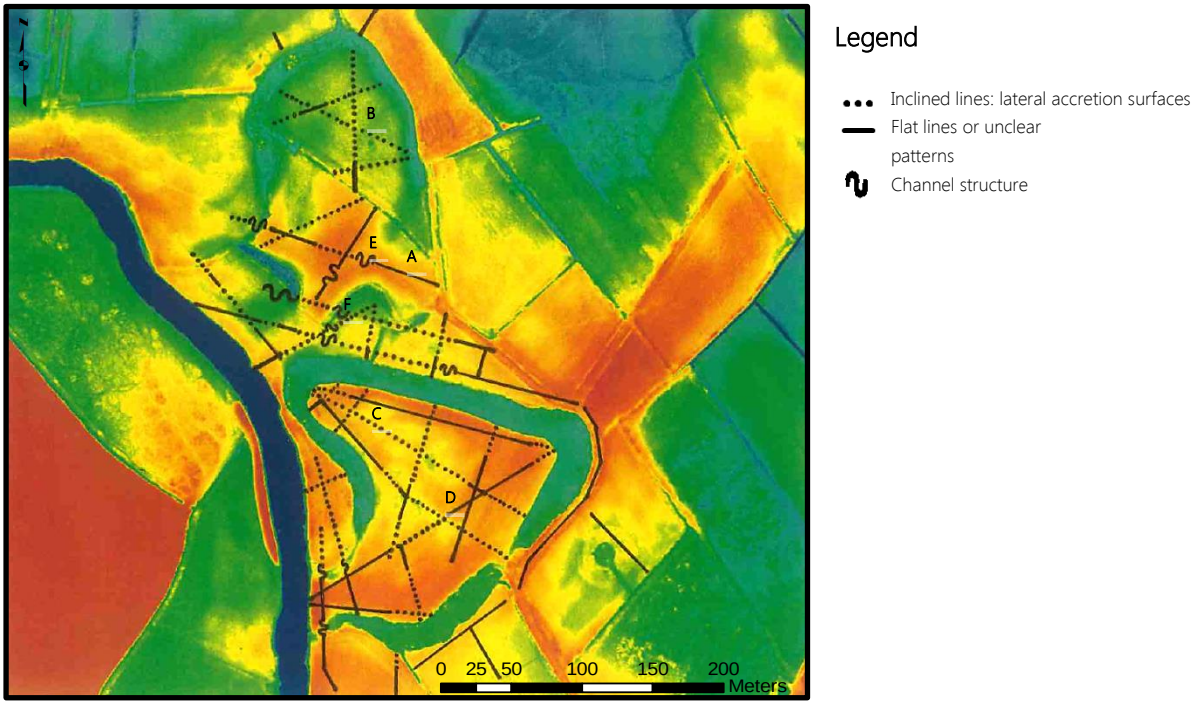

Figure 25 An overview of the additional radar transects where the shape of the lines represent the occurrence of lateral accretion surfaces, gully structures and straight lines or unclear (parabolic) structures, based on the interpretation of the GPR images. The letters A to F indicate the locations of the images of Figure 26 to 31. Background: DEM with an elevation value of: 9.5 to 11 m-NAP. Retrieved from: GeoDesk, Wageningen.

A pattern of straight lines might indicate the absence of lateral migration (Figure 26). This pattern often appeared outside de bends (Figure 25). This is in accordance with the general development of meanders, since the migration of channels is usually directed towards the outer bank resulting in lateral accretion surfaces at the inner and not at the outer bank. An exception is the development of counterpoint bars, which results in lateral accretion surfaces at the outer bank (Smith *et al.,* 2009).

Straight lines can also appear when the transect is not in the direction of lateral migration but more or less parallel to the channel[6]. Straight lines appear for example along the inner bank of the most straight side of the southern meander (Figure 25). However the transects in the southern meander that were perpendicular to the channel show lateral accretion surfaces (Figure 25).

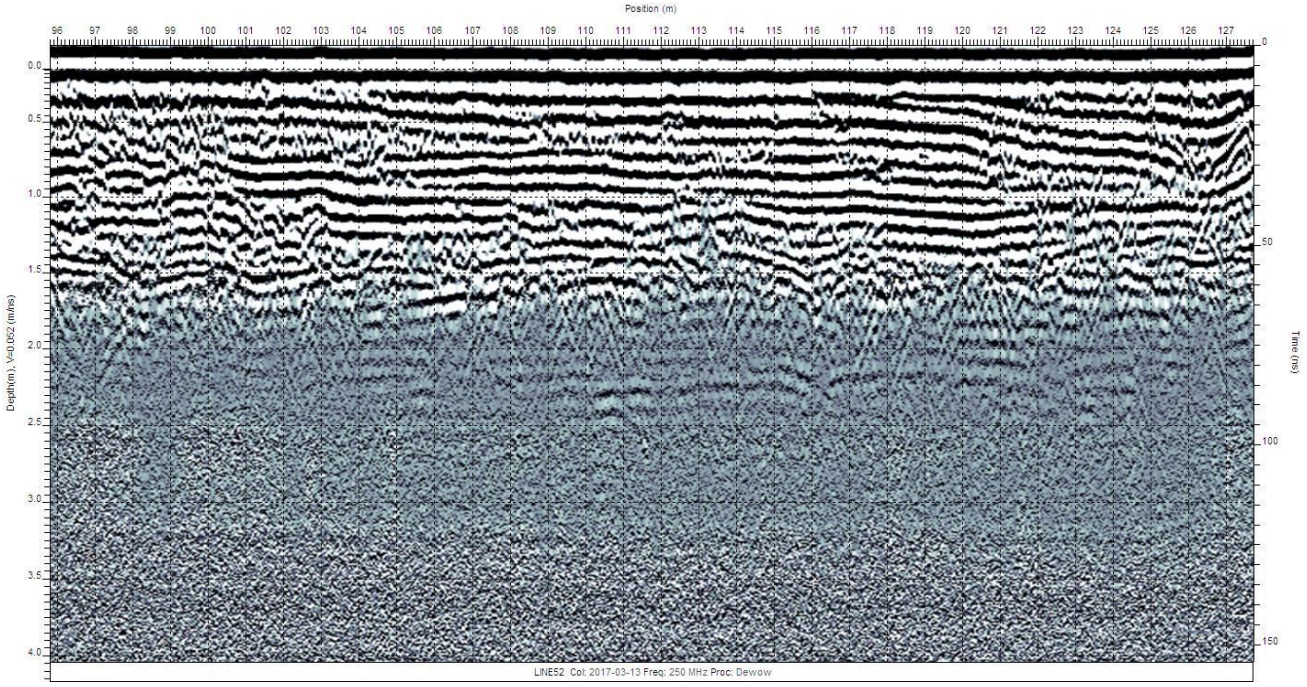

Figure 26 GPR image of the location of Figure 25A. The pattern is characterized by straight lines.

Since most of the transects outside the bends were along the channel, this could explain the lack of inclined surfaces. However even in the major part of the transects outside of the bends, which were perpendicular to the channel, inclined surfaces did not appear (Figure 25). This suggests the absence of lateral migration outside the bends. At two locations, between the eastern and southern meander and south of the southern meander, lateral accretion surfaces occurred outside the bends. However it is hard to determine whether these are point bar or counter point bar deposits.

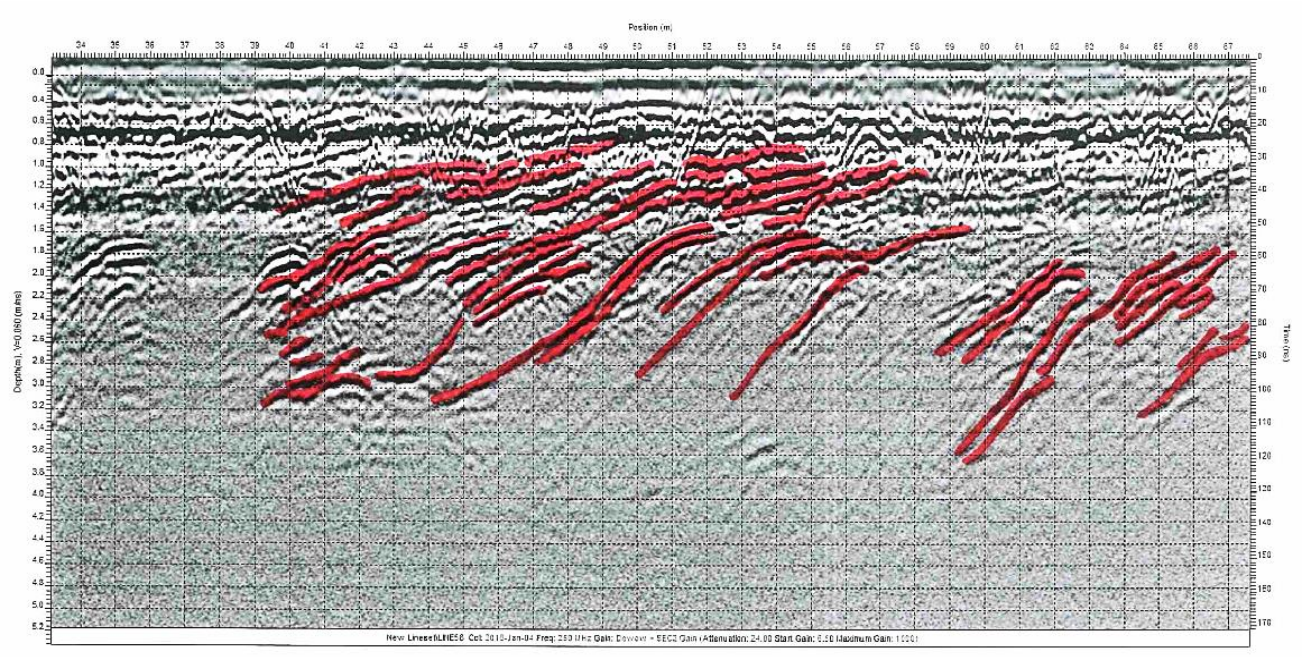

Figure 27 Interpreted GPR image of the location of Figure 25B (northern meander). The pattern is characterized by inclined lines indicating lateral accretion surfaces. The steepness of the surfaces is between 8° and 16°. The original image, without interpretation, is included in Appendix III

[6] See section 4.1 Ground Penetrating Radar

The major part of the GPR images originating from the area within the former meanders represents inclined surfaces (Figure 27 & 28). These surfaces are surprisingly steep, having a steepness between 8° and 15°. Generally the southern meander shows less steep surfaces. The most shallow lines are around 2°, while the most steep lines have a steepness of about 24°. Despite their steepness, the inclined surfaces are interpreted as lateral accretion surfaces. The lateral accretion surfaces are present until a depth of 2 to 4 m below surface. In the transects representing the northern meander, the inclined lines are mostly visible within 1 m, while in the southern, eastern and western meander they often start within 0.5 m below surface.

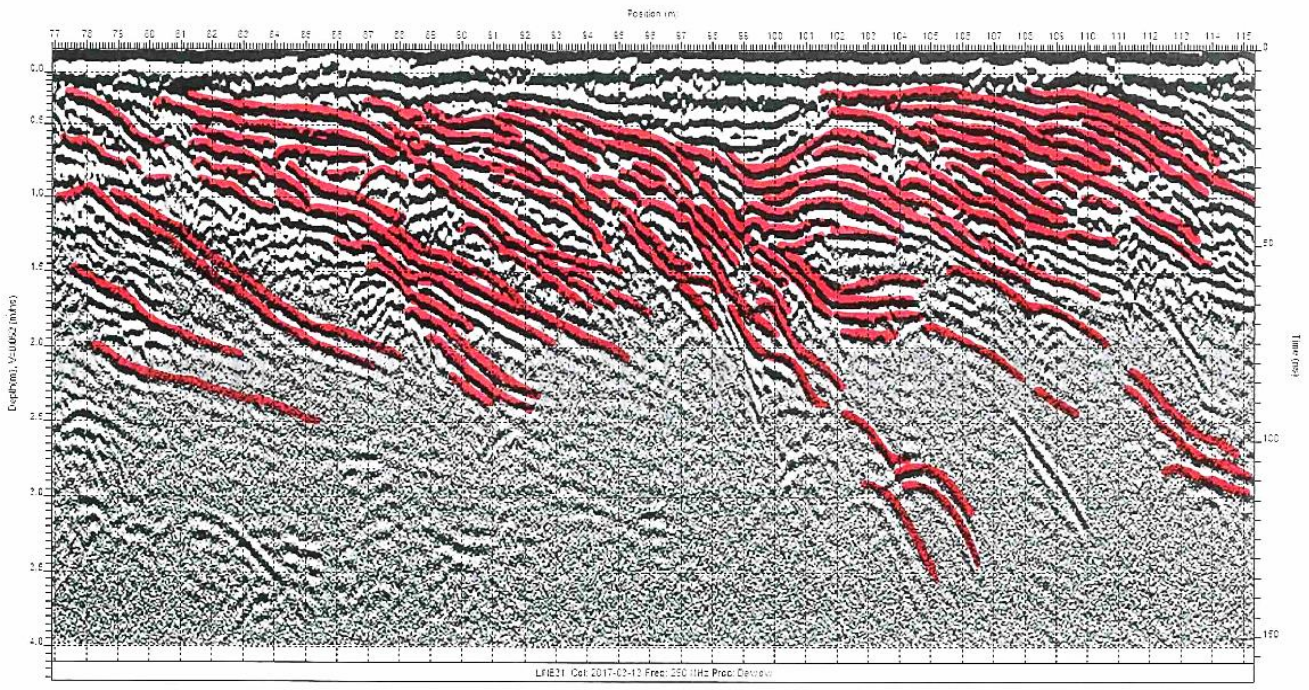

Figure 28 Interpreted GPR image of the location of Figure 25C (southern meander). The pattern is characterized by inclined lines indicating lateral accretion surfaces. The steepness of the surfaces is between 2° and 11°. The original image, without interpretation, is included in Appendix III.

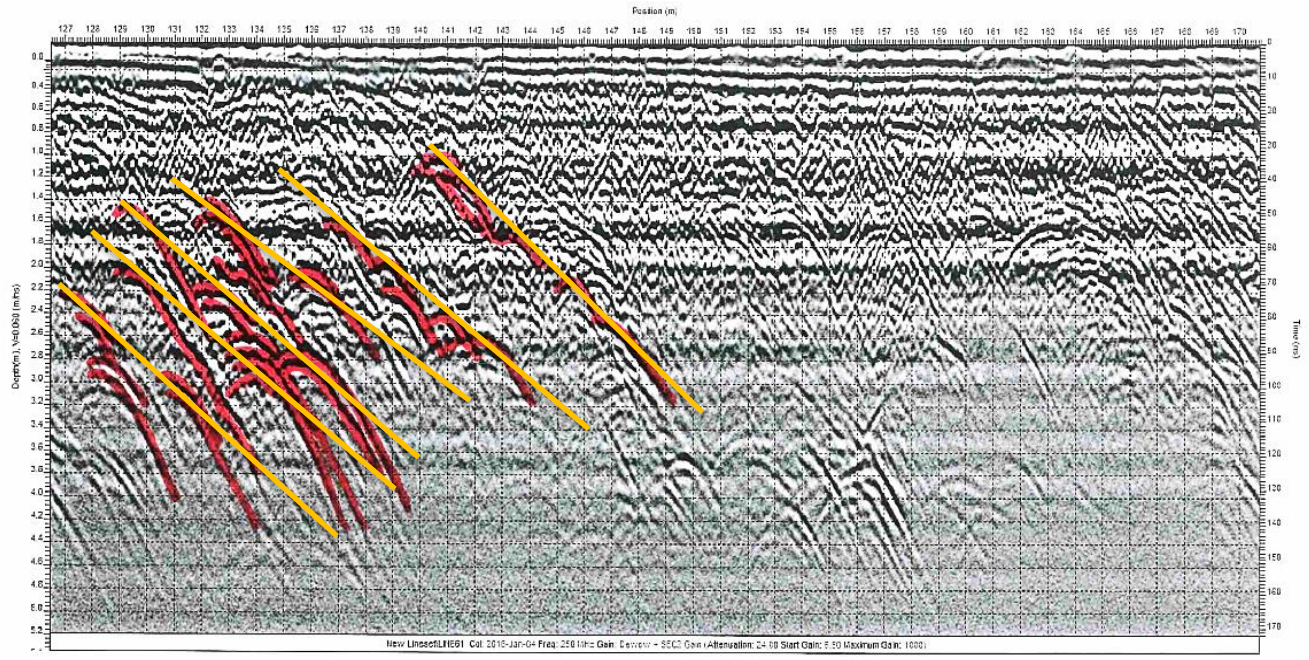

Figure 29 Interpreted GPR image of the location of Figure 25D (southern meander). The pattern is characterized hyperbolic structures. By connecting the tops of the hyperboles, inclined surfaces can be recognized, which likely represent lateral accretion surfaces,. The steepness of the surfaces is approximately 11° and thus comparable to the lateral accretion surfaces recognised in Figure 27 & 28. The original image, without interpretation, is included in Appendix III.

In the southern meander hyperbolic structures were found at several GPR images (Figure 29). The hyperbolic structures might refer to objects laying on an inclined surface, probably layers consisting of wood particles as found in the cores (Figure 16). Connecting the tops of the hyperboles results in inclined surfaces (Figure 29), which have a similar steepness as the lateral accretion surfaces found in the GPR images (Figure 29 & 30).

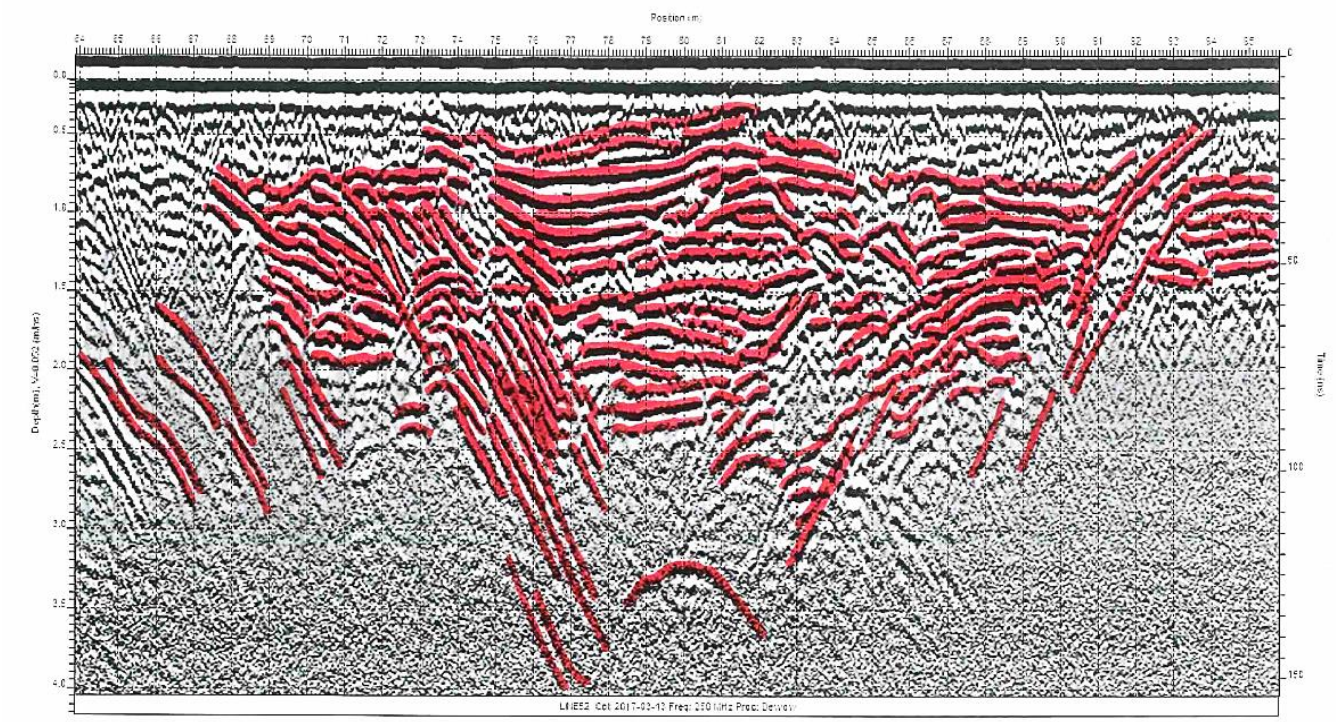

Figure 30 Interpreted GPR image of the location of Figure 25E (northern meander). The pattern is characterized by steep inclined lines (around 22°) indicating the location of a disappeared part the northern meander. The original image, without interpretation, is included in Appendix III.

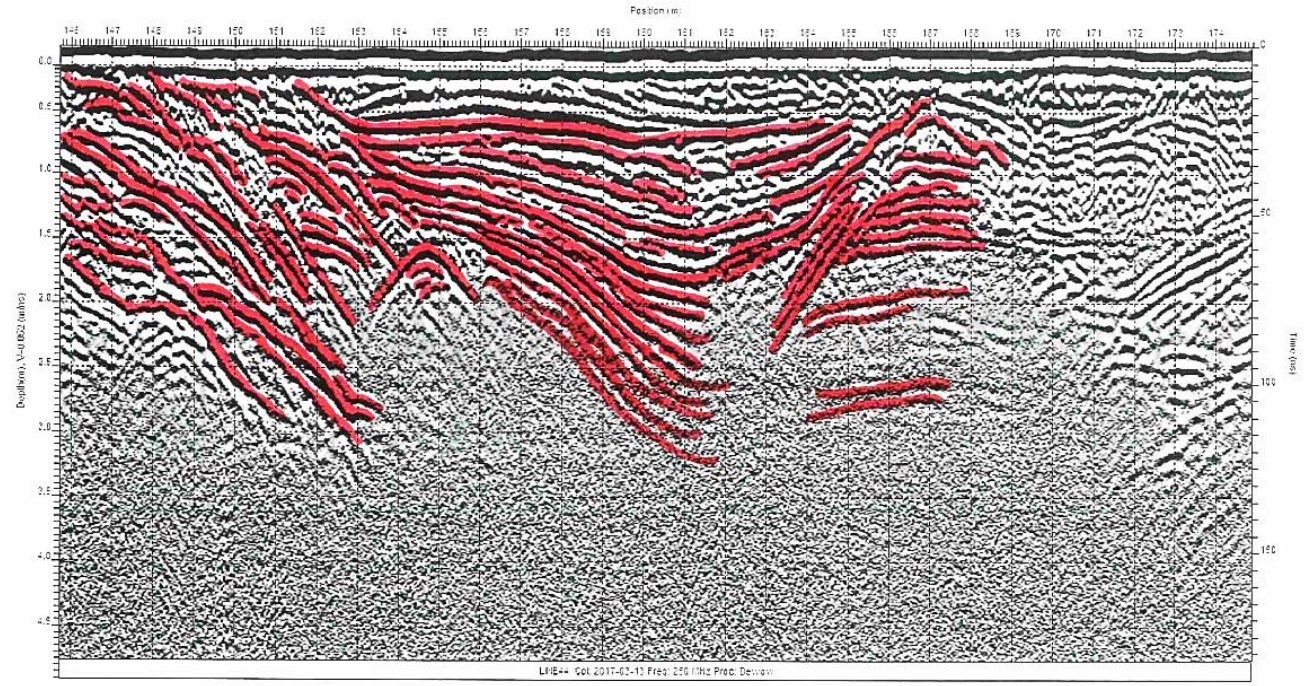

Figure 31 Interpreted GPR image of the location of Figure 25F (eastern meander). The pattern is characterized by steep (right: around 24°) and less steep (left: around 14°) inclined lines indicating the location of a disappeared part of the eastern meander. The original image, without interpretation, is included in Appendix III.

Furthermore at some locations channel-shaped patterns appear (Figure 30 & 31). These patterns, referring to disappeared channels, are often recognisable as steep inclined lines that bow to each other. The inclined lines increase in steepness towards the channel. Considering the relation between bankfull width and depth of a channel and the sinuosity of small rivers (Leeder, 1973) it could be argued that the steepness of lateral accretion surfaces increases with sinuousity and thus increases towards the final (most sharp) stage of meanders. The extent of disappeared channels is estimated based on the channel-shaped patterns. Disappeared parts of the northern meander were found in three transects (Figure 25). Figure 30 represents one of these parts. The depth of the channels was approximately 4 m and the width varies between 10 and 25 m. At the transects towards the current northern meander the steep inclined lines were visible up to a depth of 2 to 3.5 m, indicating a channel depth of approximately 4 m.

In the southern meander inclined surfaces were often lacking. However some images, show steep inclined lines, indicating a channel depth of 4 to 4.5 m. The depth of the Dommel is currently approximately 6 m + NAP, which corresponds to a depth of 4 to 4.5 m below the surface.

The disappeared part of the western meander, visible at two transects, has a depth of 4 m and a width of 20 m. The eastern meander seems to be smaller: 3 to 3.5 m deep, and 10 to 15 m wide, based on several transects. At the location outside the southern meander towards the eastern meander (Figure 25), two GPR images show the remnants of an older deeper (4.5 m) and wider (30 m) channel, below the shallow channel. At the location where the channel appears, the GPR pattern of straight lines abruptly changes into a channel-shaped pattern, indicating the maximum extent of the southern meander. The inclined lines indicating the channels are quite steep: 14° to 24°. Which is more often observed in small rivers (Leeder, 1973). Although at one side in one transect, they were less steep (Figure 31). This could be explained by the direction of this transect, which was in this case probably not exactly in the direction of migration and might therefore be less steep.

5.2 Lithological and lithogenetical cross-sections

5.2.1 Lithology in general

The dominant soil texture in the area is fine sand. A fining upward could be recognised in most of the cores, indicating a fluvial origin of the deposits. At the bottom, coarse or moderately fine sand was found and the texture gradually changed upward into fine and very fine sand. In some cores also extremely fine sand was observed. The southern meander seems to be finer textured, only three of the cores contained coarse sand and there were some patches of extremely fine sand, which were missing in the northern meander.

Figure 32 Different types of deposits found in the cores. **A:** Fine sand with small bands consisting of black material. In this image the bands are several millimetres to centimetres, however often a series of bands of only one millimetre were found. **B:** A mixture of fine and coarse sand containing organic matter particles. **C:** A layer consisting of almost only wood particles surrounded by quite clean sand. **D:** An organic and loamy layer of several centimetres surrounded by smaller dark layers. **E:** A layer of coarse sand and small gravels. **F:** Very clean grey sand, fine to moderately fine-textured.

Figure 32 represents the dominant deposits that were found in the cores. It was remarkable that the major part of the cores contains a large amount of organic matter. Four different types of layering of organic matter could be recognised. These layers varied from small laminae of several millimetres (Figure 32A) with decomposed black material to layers of several decimetres consisting of a mixture of loose wood particles and sand (Figure 32 B & C). The latter clearly differed from in-situ peat, sandy peat or peaty sand, which is much more compacted and at least partly decomposed. At some locations also intervals of loamy and clayey deposits appeared (Figure 32D). The layers consisting of reworked wood particles (Figure 32 B & C) sometimes reach a thickness of 30 cm whereas the loamy layers were merely around 1 to 5 cm (Figure 32D). The sand in between the layers consisting of organic matter sometimes contains small wood particles, however this was not always the case.

The layers of organic matter appear irregularly from 2 to 4.8 meter below surface. This depth matches with the depth of the lateral accretion surfaces of the GPR images, which generally reach a depth of 3.5 to 4.5 m below the surface. In several cores coarse sand and in some cases gravel appeared (Figure 32E) at approximately the same depth, probably indicating the border between a more recent fine textured fluvial system and an older system characterized by more coarse-textured sediment. The cores right (outside) of the northern and southern meander did not contain layers of organic matter and had a clear grey or sometimes whitish colour (Figure 32F). At the inner bend of the northern meander a relatively thick layer of peat is found. In the southern meander at the left border of the floodplain also a layer of peat is found. Below and on top of the peat loamy and clayey deposits occur.

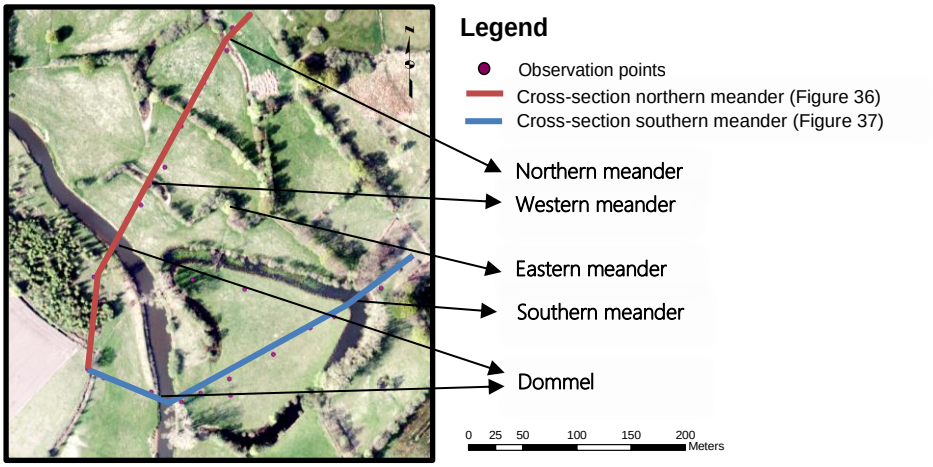

Figure 33 The study area including the locations of the observation points, the cross-sections and the channels. Background: Arial photo of 2010, retrieved from: GeoDesk, Wageningen

Lithological cross-sections, covering the northern, western and southern meander (Figure 33), were constructed (Figures 34 and 35), based on the coring data. The cross-sections represent an interpretation of the continuation of the textures in the subsoil. The profiles are most detailed at the left side of the Dommel, as most cores were taken in that part. In the profiles the results of the OSL dating are presented.

5.2.2 Lithogenetical units

The lithological cross-sections are interpreted using the DEM and the GPR radar profiles. The following lithogenetical units are distinguished: (1) point bar deposits, which originate from different periods, (2) channel-fill deposits, (3) pre-Holocene valley fill deposits and (4) pre-Holocene upland deposits. The lithogenetical profiles are represented in Figure 34B and 35B.

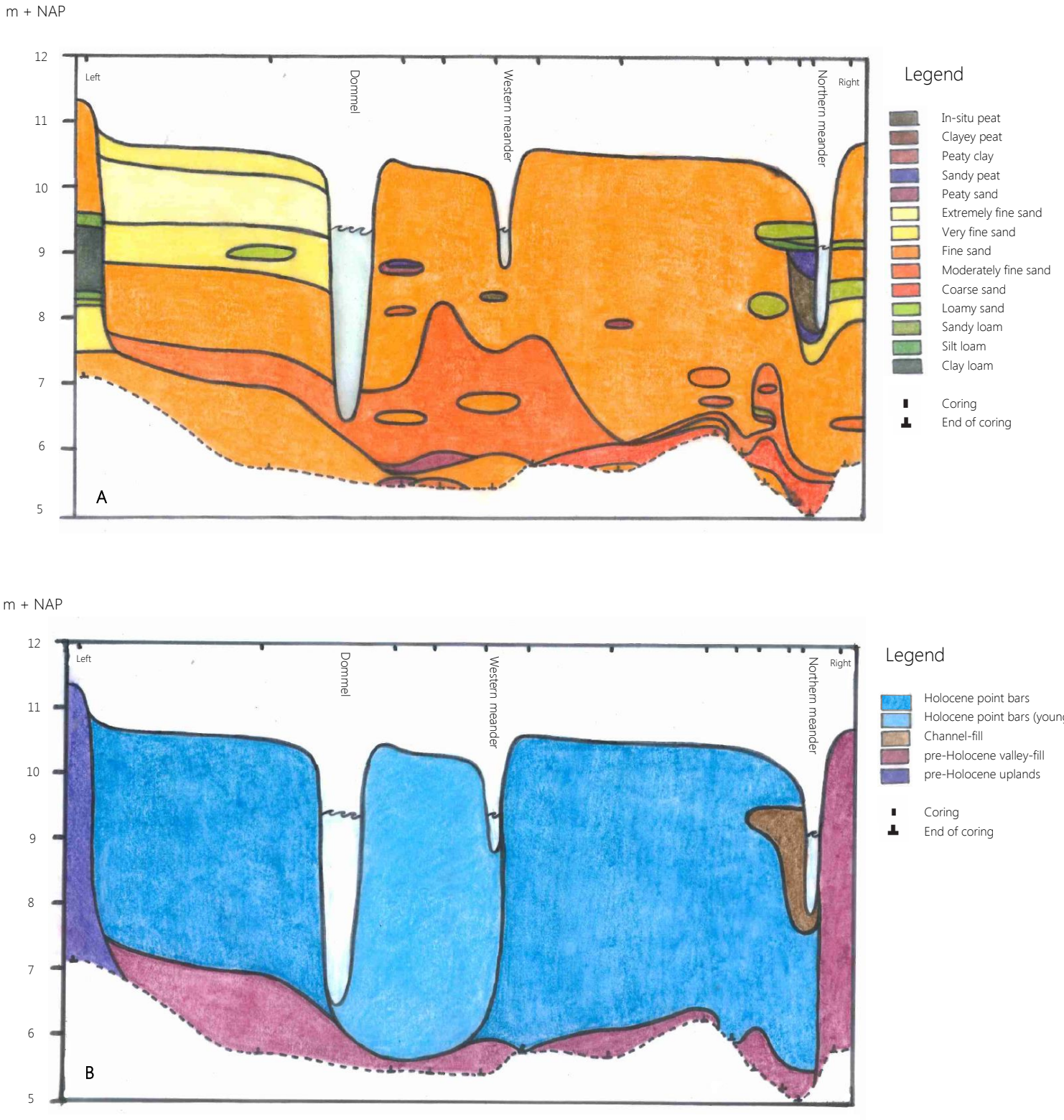

Figure 34 Cross-sections of the northern meander. The length of the profile is about 300 m **A.** The lithological profile indicating the different textures occurring in the subsurface. The interpretation is based on the cores. **B.** The lithogenetical profile indicating the different lithogenetical units as described in the text.

Southern meander

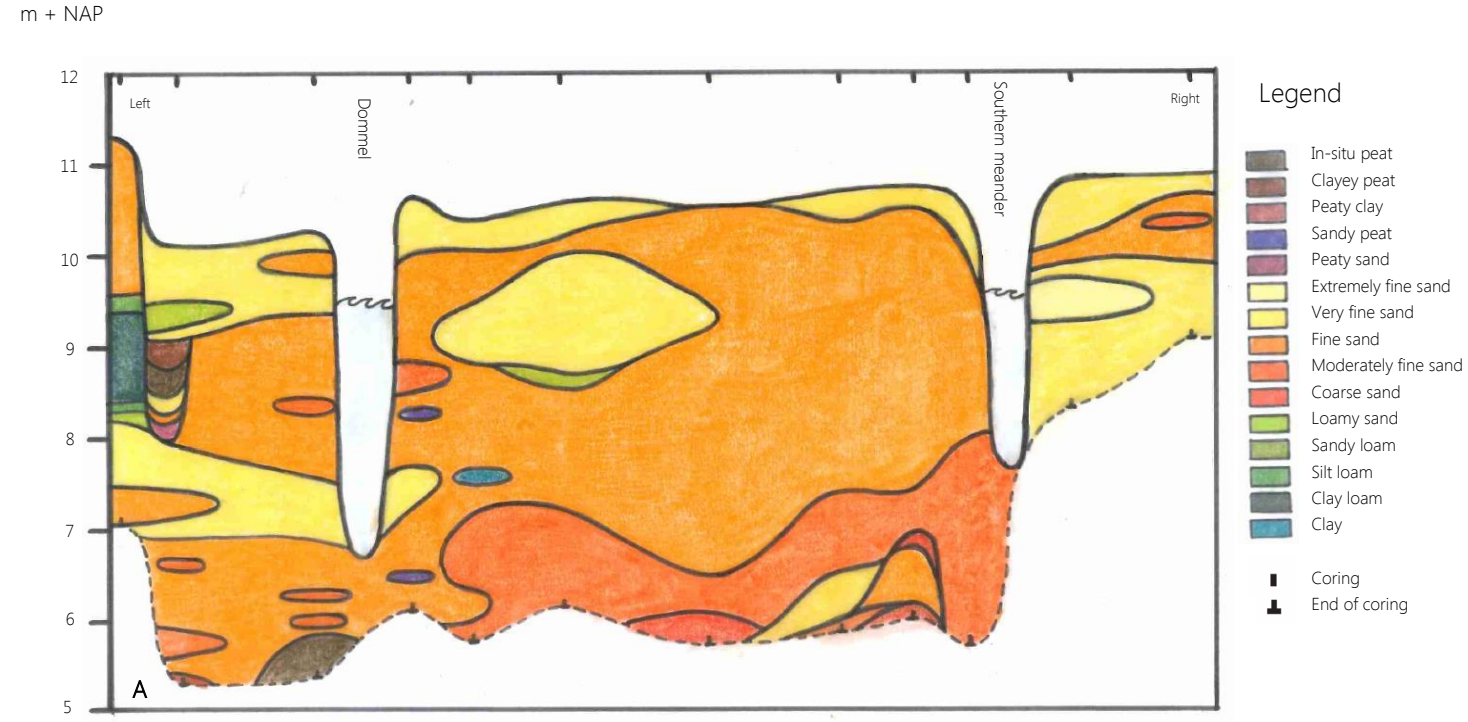

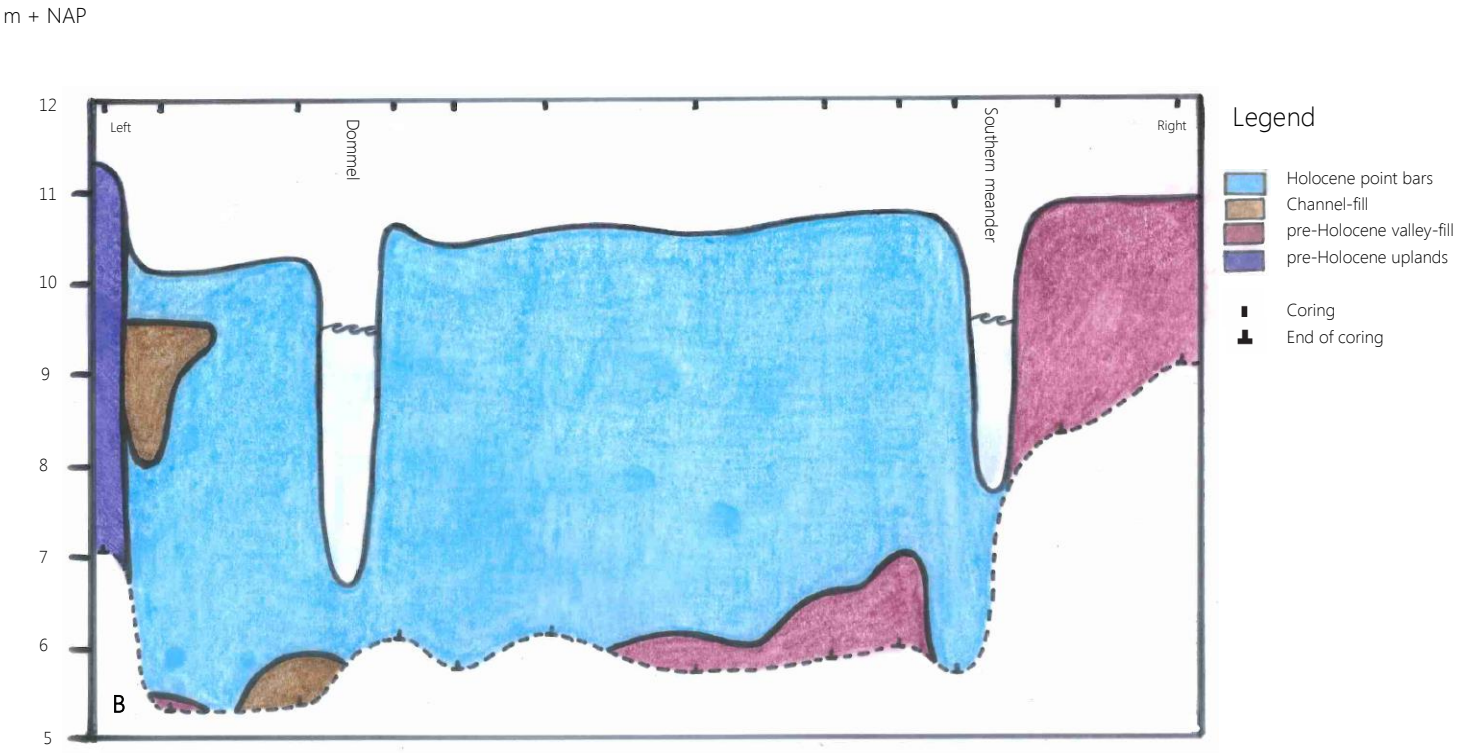

Figure 35 Cross-sections of the southern meander. The length of the profile is about 300 m. **A.** The lithological profile indicates the different textures occurring in the subsurface. The interpretation is based on the cores. **B.** The lithogenetical profile indicates the different lithogenetical units as described in the text.

Holocene point bar deposits

Most deposits in the area are recognised as point bar deposits (Figure 34B & 35B). These point bar deposits meet the following description. They are characterized by a fining upward sequence from coarse or moderately coarse towards fine or extremely fine sand. At a depth of about 2 m below the surface, layers with different types of organic matter could appear until a core-depth of 4 to 4.8 m (Figure 34). The top 20 to 30 cm is of dark colour, indicating the presence of organic matter. This is often followed by a (very) red soil, which marks the occurrence of iron, which could be the result of seepage in the area. Below the red soil the colour changes into light brown, grey brown or grey. At some locations loamy, clayey or peaty layers might occur, however their extent is mostly less than 10 cm. Considering the OSL dates, it is assumed that the point bar deposits date from the Holocene.

The fining upward sequence is a clear indication for the fluvial origin of these deposits. The fluvial origin of the deposits is further specified as being point bar deposits. An important feature that indicates point bar deposits, is the occurrence of lateral accretion surfaces in the subsurface. As described in section 5.1 lateral accretion surfaces were found within the four meanders, right of the Dommel. It is not known if lateral accretion surfaces are present at the left side of the Dommel, however considering the fining upward sequence in these cores and their similar valley position, it is likely that the sediments left of the Dommel could also be interpreted as point bar deposits.

In Figure 34B two different point bar deposits are distinguished, the point bars resulting in the larger northern meander and those of the smaller western meander. This distinction is based on the DEM (Figure 14), that indicates the location of both meanders. Since the eastern meander is located within the northern meander it is assumed that the northern meander must be older. The depth of the western meander is retrieved from the GPR images. This depth is at the same level as the border between moderately coarse and fine sand; which likely indicate the border between two fining upward sequences. Although there were more locations, where fine textured layers were found below layers with a more coarse texture, it was not possible to further distinguish these point bar deposits. This was due to the small extent and irregular occurrence of the different fining upward sequences. The fine or very fine sand patches, below a coarser textured layer, were often very small, which could mean that they were still part of the above fining upward sequence. Furthermore, in both cross-sections the occurrence of these fining upward sequences on top of each other, was not continuous. This discontinuity could indicate variation in depth of the last meandering system, resulting in the local perseverance of former fining upward sequences.

Channel-fill deposits

Channel-fill deposits consists of in-situ peat, which is often surrounded by layers containing peaty sand, sandy peat, sandy loam or loamy sand. The name 'channel –fill deposits' refers to a former channel, which is filled with new deposits, for example when a meander neck cut-off took place. During the process of a meander cut-off, the channel will first be filled with more coarse sandy sediments. When the cut-off is accomplished, the finer loamy particles will be deposited. Subsequently, peat can develop when there are still wet conditions in the former channel. The channel will gradually grow narrow until it is completely filled. During that process, the former channel still has a low position in the landscape, which can explain the occurrence of fine textured (loamy) sediments that were found on top of the peat. In case of flooding, fine particles will be deposited in the lower areas.

The main characteristic of channel-fill deposits in this area, is a layer of in-situ peat with a thickness of at least 30 cm. This was found at one location in Figure 34 and at two locations in Figure 35. Indeed fine textured loamy and clayey deposits were found below the in-situ peat, except for the most deep location (Figure 35A). However at this location the peat continued until the end of the core, it is thus possible that loamy or clayey deposits occur at larger depths below the peat. The peat at this location differs from the peat found at the two other locations since it was very compacted.

The channel-fill deposits at the two other locations were similar. The depth of the peat was between 8 and 9 m + NAP. It is remarkable that in both cases the top part of the peat gradually changed towards sandy peat, fine textured clayey and loamy deposits and finally sand occur. This might indicate that at one time the former channels were (again) influenced by flooding. They received loam, clay and sand, since the cut-off channels were still located low in the landscape. Channel-fill deposits indicated the extend of the northern meander before the neck-cut off (Figure 34). In the southern meander channel fill deposits seems to be the fill of an old bend buried by a layer of sand (Figure 35). However considering the Topographical Military Map of 1850 and the Bonne Projection of 1900 it appears that this peat layer in the southern meander, could also represent an old muted ditch (Figure 14). Further research on the extent of this deposit is needed to confirm its origin.

Pre-Holocene valley-fill deposits

Pre-Holocene valley-fill deposits are extremely fine to coarse textured sandy sediments and also loamy layers can occur. The deposits can contain organic material at larger depth, below 7.5 m + NAP. The sediments had a grey brown, clear grey or whitish colour. Where these deposits occur at the surface they were found to meet the same characteristics as the Holocene point bar deposits, except of the layers containing organic matter, which were not found. In some cases a fining upward sequence could be recognised, indicating the fluvial origin of these deposits. However often the deposits where too thin to recognise a clear pattern in the lithology or merely the coarse sediments remained. The border between Holocene point bar deposits and pre-Holocene valley-fill deposits is indicated by the start of a new fining upward sequence or by the occurrence of coarse material that contains small gravels. The depth of this border matched with the GPR images, which indicated the depth of the Holocene fluvial system at 3 to more than 4 m below surface, which is between 5 and 7.5 m + NAP.

Within the northern and southern meander the pre-Holocene valley-fill deposits were found below the Holocene point bar deposits. In the southern meander these deposits seem to start at a larger depth, compared to the northern meander. During stream migration in the Holocene, the (pre-Holocene) valley-fill deposits were reworked and deposited as point bar deposits. It is therefore difficult to distinguish between those two, since their lithological characteristics are quite similar. In addition to that, the pre-Holocene valley-fill deposits might not be reached in every core, because the Van der Staaij suction-corer had a maximum reach of 4.8 m.

Outside, at the right side of the northern and southern meander, fine and extremely fine sand occur, indicating the top part of a fining upward sequence. It was remarkable that the cores outside the southern meander were very difficult to auger, compared to the other locations. Due to the firm structure of the sediment, these cores merely reached a depth 180 and 250 cm below surface. Since organic matter layers often occur at a depth of 200 to 250 cm below the surface, it could not be established that these locations did not contain comparable layers of organic matter. However it could be assumed that layers of organic matter did not appear in these cores since in the core outside of the northern meander also no layers containing organic matter were found. Except for the firm structure of the sediment, this core had a similar lithology as the cores outside (at the right side of) the southern meander. In addition to that, the radar images of both locations were similar and characterized by straight patterns. No lateral accretion surfaces appear, which were commonly found in the Holocene point bar deposits. This confirms that these deposits differ from the Holocene point bar deposits.

Pre-Holocene upland deposits

Pre-Holocene upland deposits meet the following requirements. The deposit contains extremely fine to coarse textured sand and loamy to clayey layers occur. There are no layers with organic matter particles present and the colour varies from light brown to clear grey. The loamy layers have a more dark brown colour compared to the sand. The pre-Holocene upland deposits are recognised as Brabant loam, which is

part of the Liempde Member of the Boxtel Formation (Schokker, 2003). It is locally found in the central part of the province of Noord-Brabant (Meijer, 2010), where also the study area was located. Brabant Loam consists of (cohesive) fine grained sand, sandy loam and clay and is dated to Weichselian age (Schokker, 2003). Brabant loam is an aeolian deposit but can also be the result of locally washed out cover sand (Schokker, 2003).

Pre-Holocene upland deposits were found in one core that marks the left border of the northern and southern meander (Figure 34 & 35). At a depth of 3 to 3.6 m below surface the fine sand was mixed with small gravels. This poorly sorted part points to a fluvial origin of at least this part of the deposit. The most remarkable of this deposit was the 1 m thick layer of loamy sand, silt loam and clay loam, which was not found in one of the other cores. Furthermore, this deposit differed from the Holocene point bar deposits, since layers containing organic matter particles were lacking. Pre-Holocene upland deposits were also found at the right side of the Moerkuilen. At that location the deposit is dated to 16 550 ± 2070 years ago (Kijm, *in press*), which confirms the Weichselian age.

However the origin of the top part of the pre-Holocene upland deposits remains unsure. Since drift sands occurred in the surrounding area of the Dommel, the top part could also be of Late Holocene age. In addition to that the arable land, were the core was taken, has a very smooth surface and towards the stream valley there was a quite steep edge. This could indicate that this border of the floodplain is incremented. However at this location no clear distinction could be made between Holocene and pre-Holocene sediments.

5.3 Optically Stimulated Luminescence Dating

5.3.1 Context of the samples

In Figure 36 and 37 the location of the OSL samples is indicated in the cross-sections of the floodplain. Sample number 2116074 and ~75 were not located on the transect line of the cross-section (Figure 33).

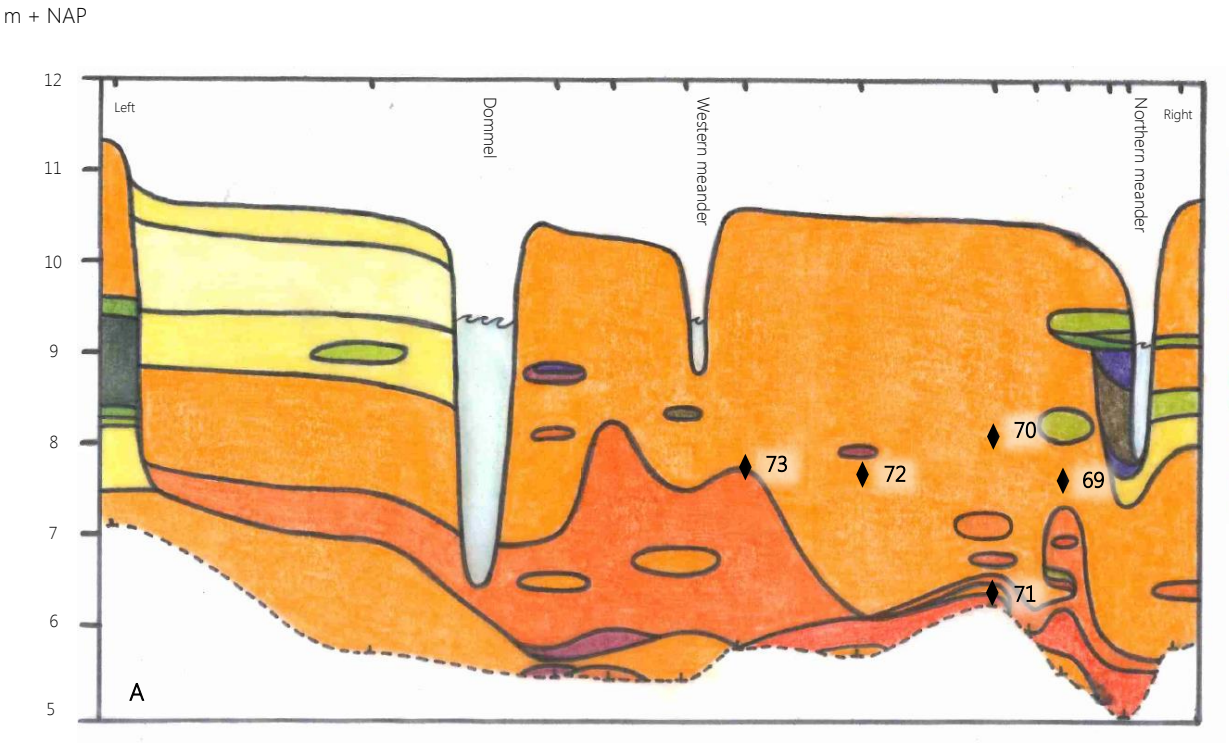

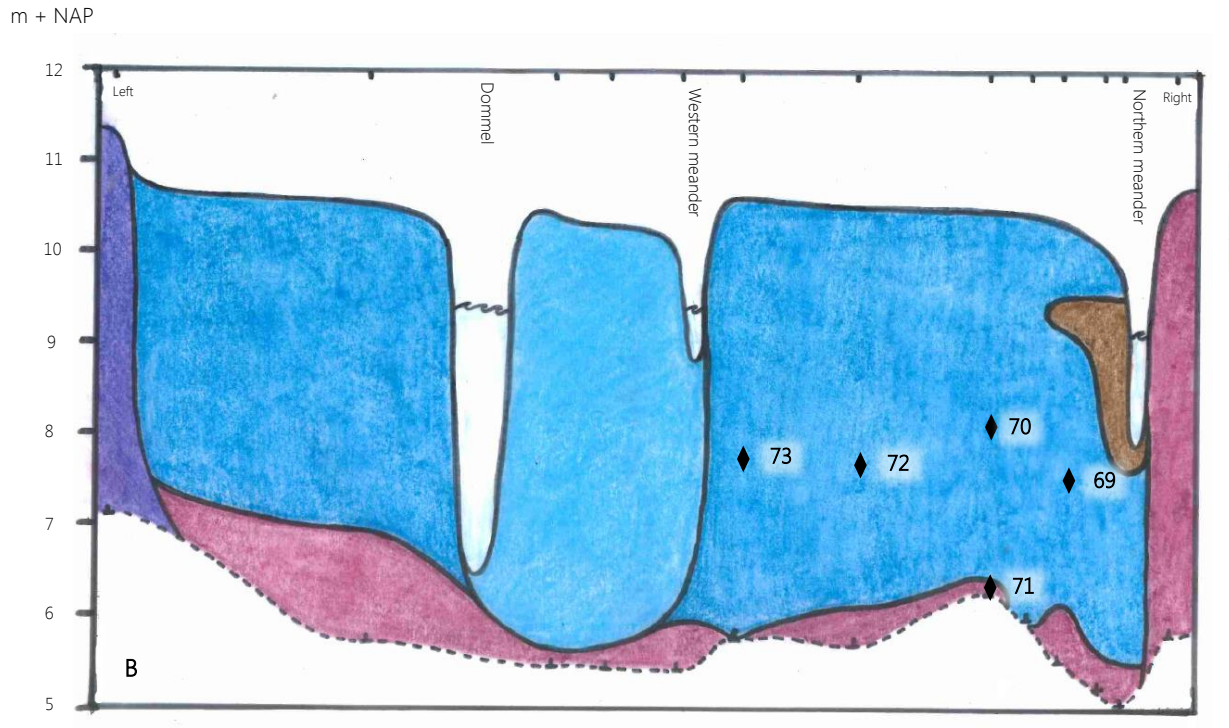

Figure 36 Cross-sections of the northern meander. The length of the profile is about 300 m. The locations of the OSL samples are indicated in the figures. **A.** The lithological profile indicating the different textures occurring in the subsurface. The interpretation is based on the cores. **B.** The lithogenetical profile indicating the different lithogenetical units.

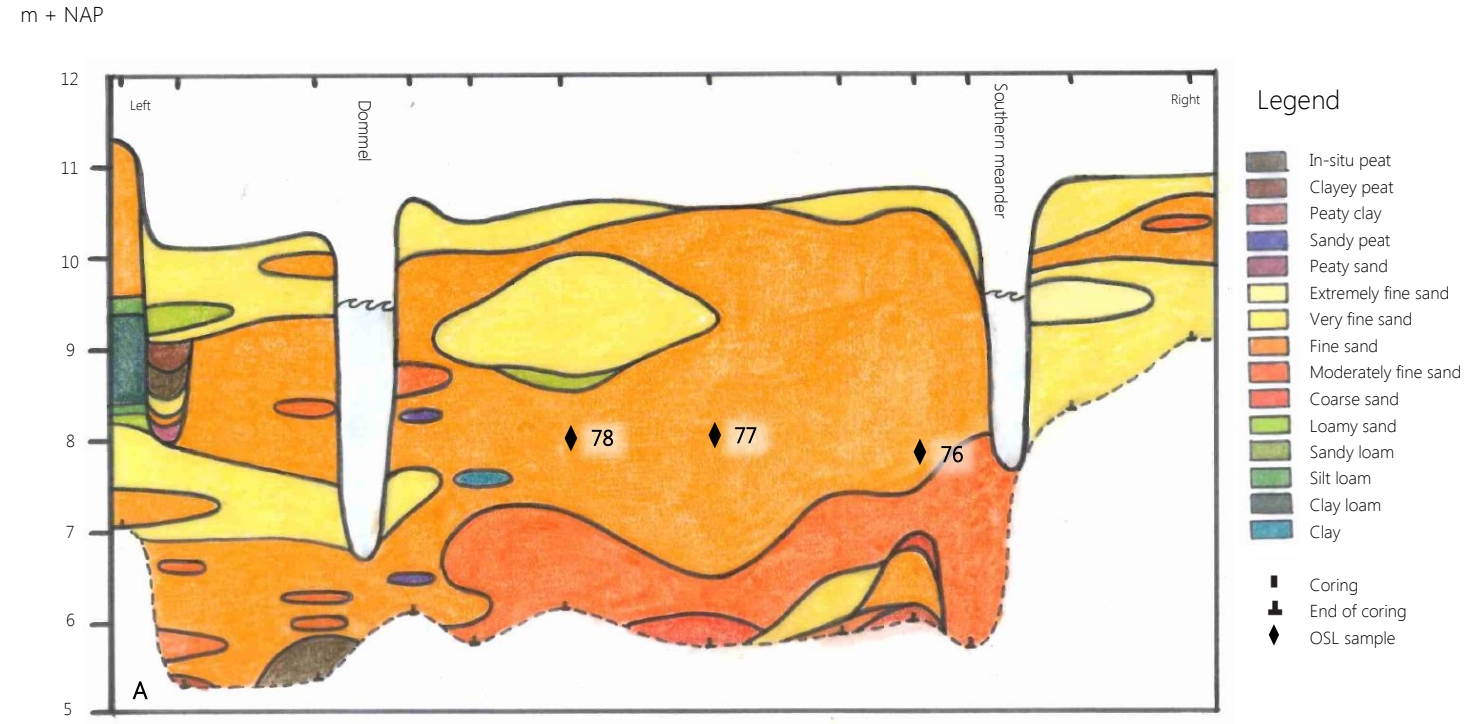

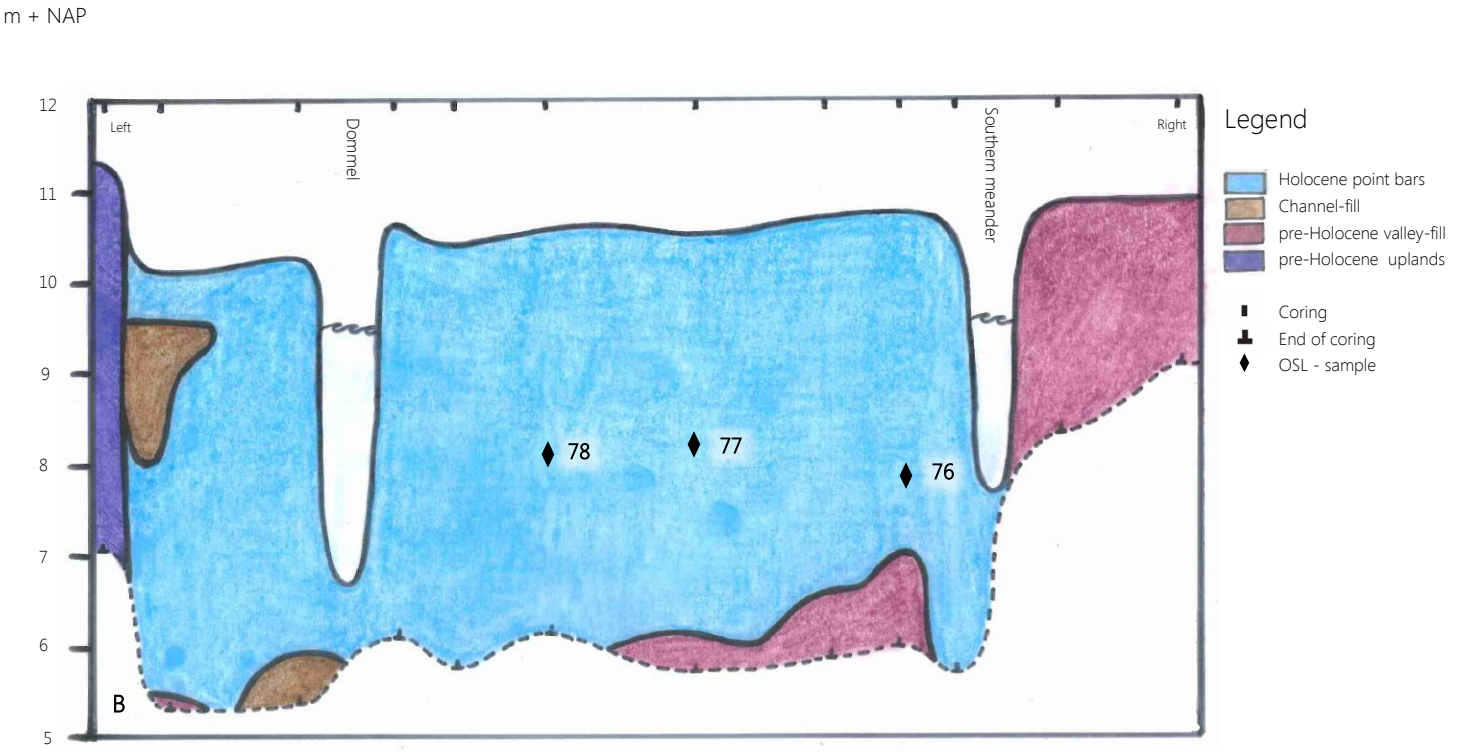

Figure 37 Cross-sections of the southern meander. The length of the profile is about 300 m. The locations of the OSL samples are indicated in the figures. Their ages are included in the table of Figure 36B. **A.** The lithological profile indicates the different textures occurring in the subsurface. The interpretation is based on the cores. **B.** The lithogenetical profile indicates the different lithogenetical units.

5.3.2 First measurement series

The first measurement series contained four different measurements e.g. the quartz signal at 125°C and the feldspar signal at 50°C, 150°C and 225°C. The time of exposure to the beta source that was needed to get the same luminescence signal as the undisturbed sample (natural signal) was multiplied with the dose rate of the Bèta source to obtain the paleo dose values. Figure 38 represents the results of the first measurement series. The IR225 measurements generally showed the largest scatter and greatest values. This is not very surprising because the IR225 measurements represent the signal of the deepest traps. The IR50 had in most samples a larger scatter than the B125, however the latter also showed quite some dispersion. It is notable that in some samples the lowest B125 values were higher than the lowest IR50 values, which was not expected since the IR50 signal is more difficult to bleach. This low IR50 signal could probably be caused by anomalous fading (Auclair *et al.,* 2003).

Figure 38 The results of the first measurement series. The graphs represent the paleo dose values of the B125, IR50 and IR225 measurements of the Northern and Southern meander. The subsamples are ordered per sample and error bars are included. Some IR225 and a single IR50 signals have been rejected as they did not fit in the SAR-requirements (e.g. contain a testdose error larger than 15%).

When the paleo dose values of B125, IR50 and IR225 are close to each other, especially when the IR225 is close to the B125, it can be assumed that a sample is well bleached. This was the case for sample ~70, ~74 and ~76. Considering the IR50 and B125 values, sample ~71, ~75 and ~77 also seemed to be relatively well bleached. Sample ~69, ~72, ~73 and ~78 contained the largest scatter. Although the differences in dispersion between the meanders were not so pronounced, it seemed that the values of the northern meander generally had a larger scatter, and therefore a relatively poorer bleaching. There was no relation found between the depth of the sample and the degree of bleaching.

5.3.3 Second measurement series

Comparison of the first and second measurement series

In the second measurement series the feldspar minerals were removed from the samples so that the measurements represent the quartz luminescence signal. The results were compared with the B125 signal of the first measurement series (Figure 39). The samples ~69 to ~73 represent the northern meander. Sample ~70 and ~71 were from the same core at different depths. Samples ~74 to ~78 represent the southern meander.

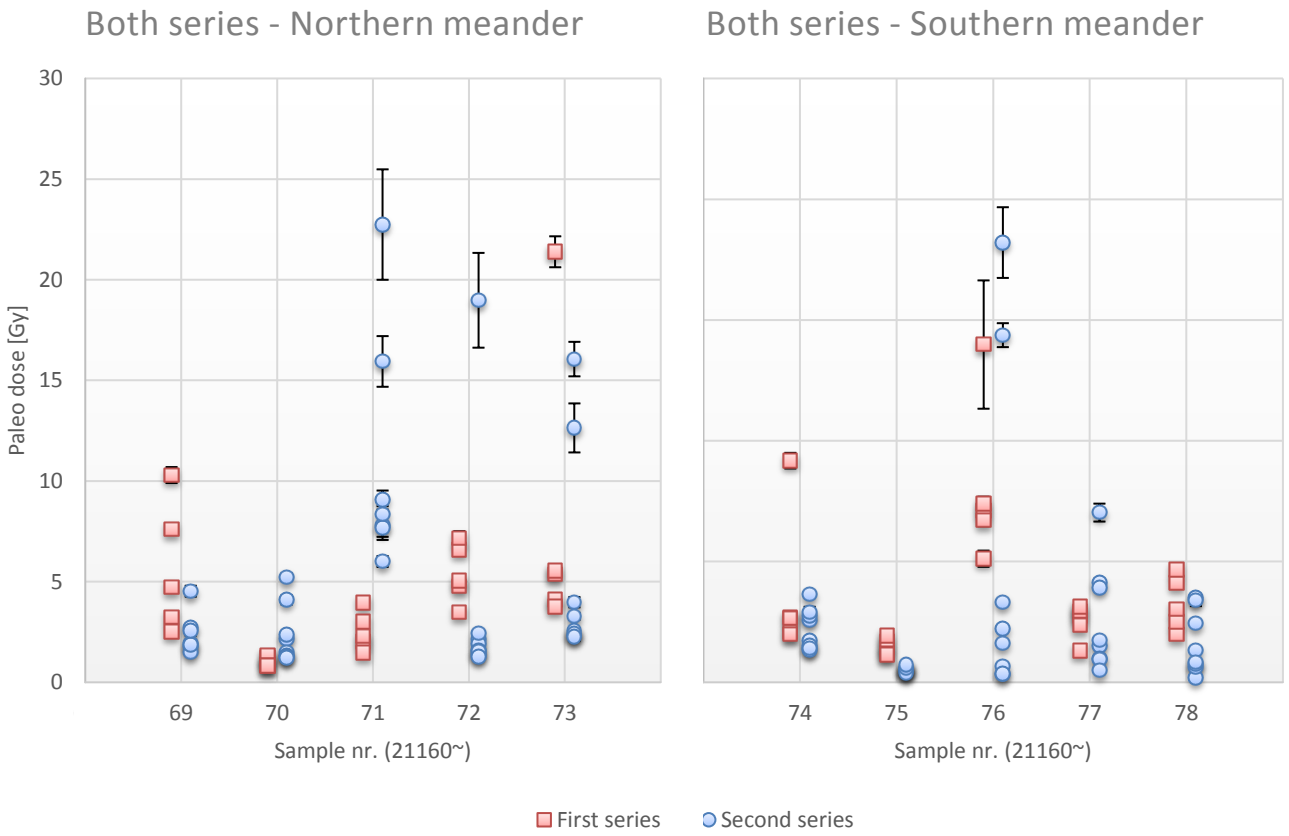

Figure 39 The results of the first and second measurement series. The graphs represent the paleo dose values of the quartz measurements of both series of the Northern and Southern meander. The subsamples are ordered per sample and error bars are included. Further explanation in text.

The first finding that was clear from the graphs was the large spread of the paleo dose values within the samples for both series. However it seemed that the points were concentrated in the lower part of the graph. One exception, that had a very high precision compared to the other samples, was sample ~75. The second finding that could be derived from the graphs was that the subsamples that had high paleo dose values generally showed a larger error, compared to subsamples with lower paleo dose values. This is indicated by the wider error bars. For both series the larger part of the data is in the range of 0 to 4 Gy.

The B125 results of the first series were slightly higher compared to the second series, which might be explained by the difference in preheat of the measurement series (first: 250 °C; second: 180 °C). In all samples, except for ~71 and ~72, the results of the first and the second series overlapped at least partly. The second measurement series contained relatively more outliers, which could probably be explained by the mask size (5 vs 3 mm) and the amount of subsamples (5 vs 8). In young samples generally 1 of the 100 grains will produce a luminescence signal. A mask size of 5 mm contains a few hundred grains and therefore, there is a higher chance that more than one grain will produce a luminescence signal. When several grains produce a luminescence signal, their differences will be averaged out, resulting in smoothening of the final result. It was assumed that the signal produced by the 3 mm discs (≈ 100 grains)

originated from merely one grain, which could lead to the higher amount of outliers in the second series. In addition to that, the chance that outliers appear, increases when more subsamples are measured.

Final age estimations

The analysis of the final age estimations only consider the second measurement series, as this is a more precise measurement (e.g. smaller mask size, larger amount of subsamples), in which only the quartz signal is measured. The dose rate (DR) was determined for two samples representing the northern (~70) and the southern meander (~74). The dose rate values were in the same range: ~70 has a DR value of 0.66 ± 0.3 Gy and ~74 had a DR value of 0.62 ± 0.02. For good comparison of the ages both values were averaged resulting in a DR value of 0.64 ± 0.02. This DR value is corrected per sample for the sample specific characteristics. Combined with the paleo dose values the ages were estimated. For every sample one representative paleo dose is calculated using the Minimum Age Model. This resulted in the final estimations of the ages. The results are presented in Figure 40 and Table 3.

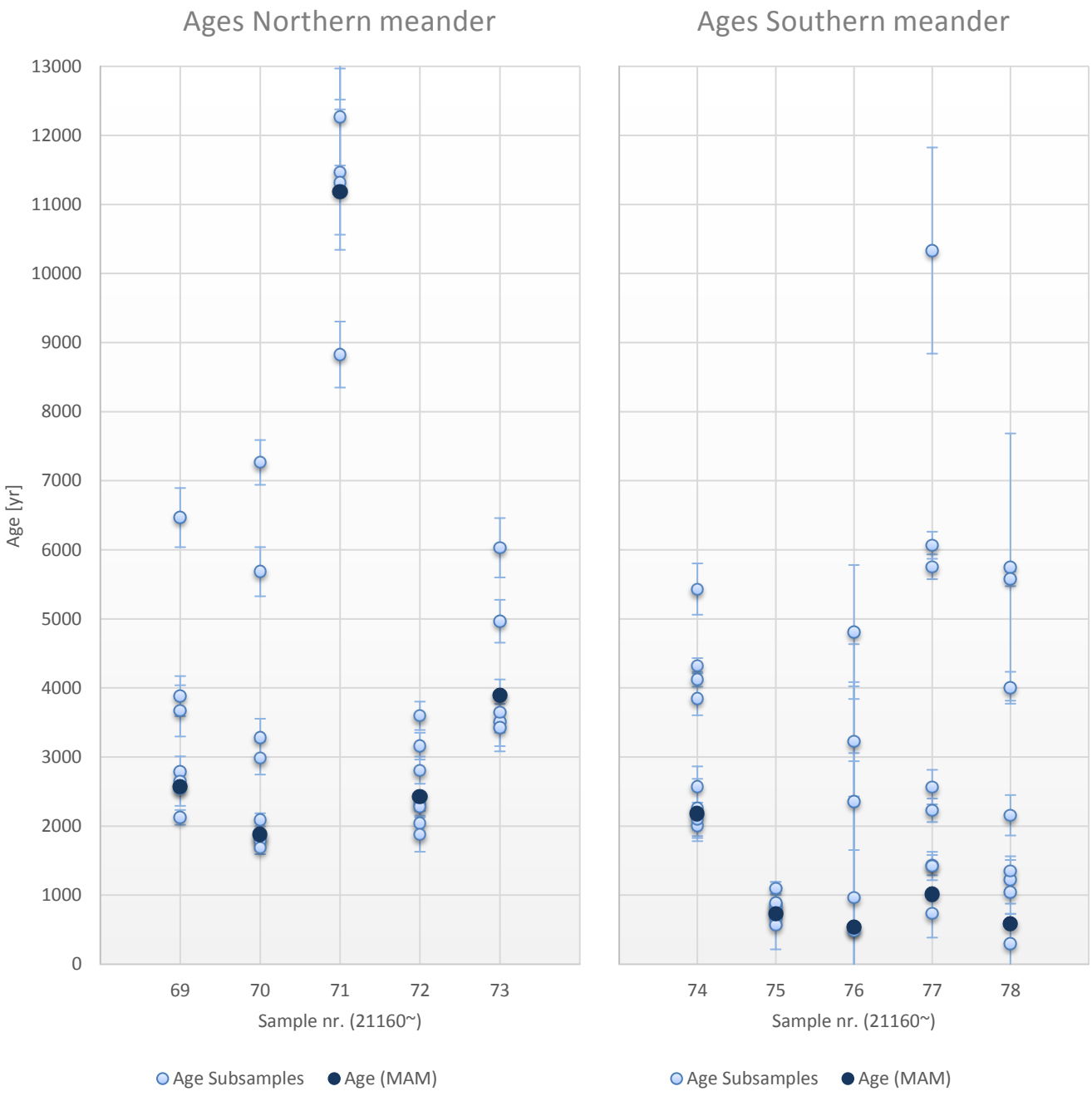

Figure 40 The results of the second measurement series of the northern and southern meander. The graphs represent the ages of the subsamples (light blue), ordered per sample and including error bars. The dark blue points indicate the ages calculated by the Minimum Age Model. The sample numbers are on the x-axis and the y-axis contains the age in years.

The samples of the northern meander were found to origin from ages in the range of 1740 to 12 380 yr including uncertainty, where most ages lay between 1800 and 2800 yr. The southern meander seemed to be younger in accordance to what was expected. Including uncertainty the ages were in the range of 160 to 2370 yr. The subsamples showed a larger spread compared to the data of the northern meander, which could point to an even poorer bleaching.

Note that the errors of the age estimation of the southern meander were relatively high compared to their age. Except for one, all errors were larger than 10%, and some of them were 50 to 60 %. The errors of the northern meander were around 10 %. It seemed that higher ages relatively had a higher precision. This can point to a difference in depositional environment, however it can also indicate that OSL dating yields relatively more precise results for older deposits (>2000 yr).

Table 3 Overview of the results of the second measurement series including information about the sample locations and the final age

Sample		Postion		Depth		Dose		Age estimation	
NCL-code 21160~	Name	Latitude [RD_new]	Longitude	Below surface [cm]	m-NAP	Paleodose [Gy]	Dose rate [Gy]	[yr]	[yr BC or AD]
69	T3-1	162048	397020	250-280	10.32	1.8 ± 0.2	0.70 ± 0.02	2570 ± 290	570 ± 290 BC
70	T3-2A	162038	397000	220-250	10.37	1.4 ± 0.1	0.72 ± 0.02	1880 ± 140	120 ± 140 AD
71	T3-2B	162038	397000	380-410	10.37	7.6 ± 0.8	0.68 ± 0.02	11 180 ± 1200	9 180 ± 1200 BC
72	T3-3	162019	396961	255-280	10.55	1.7 ± 0.2	0.68 ± 0.02	2430 ± 280	430 ± 280 BC
73	T3-4	162004	396924	270-295	10.56	2.6 ± 0.2	0.66 ± 0.02	3880 ± 330	1880 ± 330 BC
74	T4-1	162028	396822	270-300	10.55	1.5 ± 0.2	0.67 ± 0.02	2180 ± 290	180 ± 290 BC
75	T4-2	162075	396814	210-240	10.57	0.5 ± 0.0	0.66 ± 0.02	740 ± 70	1260 ± 70 AD
76	T4-3	162156	396789	260-290	10.74	0.4 ± 0.2	0.69 ± 0.02	540 ± 300	1460 ± 300 AD
77	T4-4	162104	396753	225-250	10.51	0.7 ± 0.3	0.68 ± 0.02	1010 ± 430	990 ± 430 AD
78	T4-5	162062	396718	230-260	10.66	0.4 ± 0.3	0.61 ± 0.03	590 ± 430	1410 ± 430 AD

5.3.4 Interpretation of the results

The question arises how these data could be used to reconstruct the development of the two former meanders. When the bends had been migrated by erosion in the outer bend and sedimentation in the inner bend it is expected that the age increases with distance to the cut-off channel. For the northern meander sample ~69 should represent the latest stage of migration and therefore the youngest age and for the southern meander this was expected to be sample ~74, as hypothesized in section 4.3.2.

The results of the northern meander showed a nearly natural pattern. Sample ~71 had the highest age indicating a pre-Holocene origin. This deposit might belong to an older fluvial system, since the texture was coarser and below the sample also gravel was found (Figure 36). Excluding sample ~70, the following chronological sequence was expected: ~73, ~72, ~70, ~69. The sequence, however, does not follow a chronological order: 3880 yr – 2430 yr – 1880 yr – 2570 yr. Sample ~73 has the highest age, in order to what was expected. Sample ~69 and ~72 are in the same range, bur sample ~70 is younger. This difference in age can probably be explained by the difference in sample depth. As explained for sample ~71, a deeper sample depth could result in a poorer bleaching. The value of sample ~70, though, is still close to the values of ~69 and ~72, in comparison with sample ~71 and ~73. These differences could be explained by the methods that were used. Since merely eight subsamples per sample were measured with large samples spread. Additional measurements are needed to confirm the time sequence of the samples. An aerial photograph of the study area (Figure 41) however enhances the suspect that ~70 fits within the range of sample~69 and ~72 as the subsamples of the three samples are all in the same range.

The results of the southern meander seemed to be more difficult to interpret, due to the complex shape of the meander. The expected chronological sequence was ~78, ~77, ~76, ~75, ~74 however that is not in accordance with the final ages: 590 yr – 1010 yr – 540 yr – 740 yr – 2180 yr. Sample ~74 was expected to be the youngest, but it had a striking high age compared to the other samples. The age of this sample fits within the ages that were found in the northern meander. Therefore, this deposit might be part of the development of the northern meander.

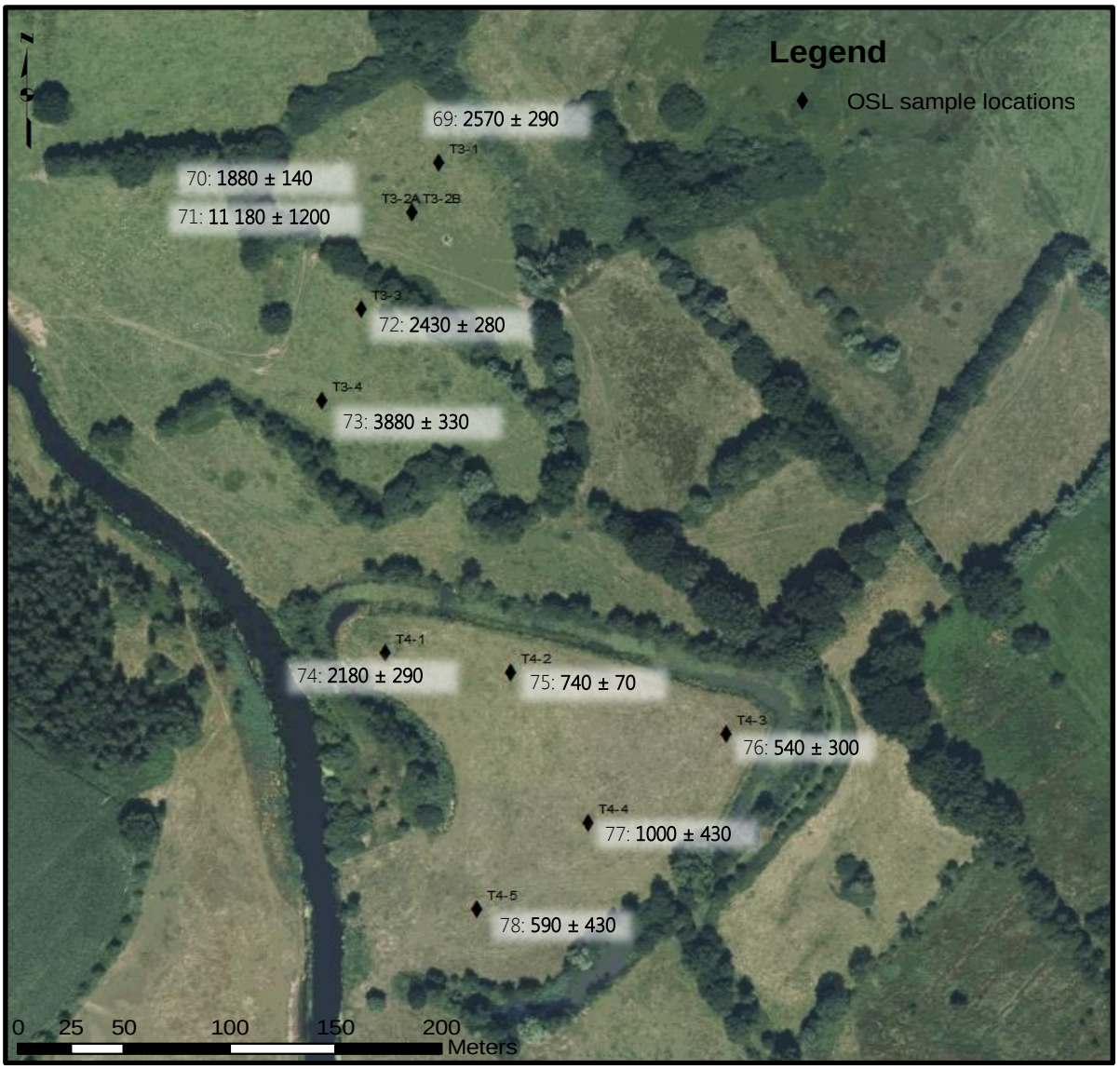

Figure 41 Aerial photograph of the study area indicating the OSL sample locations and the final age estimations. The sample names and OSL codes (without the project code: 21160~) are indicated in the figure. More details of the sample locations and calculations can be found in Table 3. Background: aerial photograph of 2010, retrieved from: GeoDesk Wageningen.

Sample ~75 had a very high precision that indicated an age of 740 ± 70. The four other values were found to be close to this value. Sample ~75 and ~77 were estimated to be older than sample ~76 and ~78. It is possible that the stream first migrated in the direction of ~75 and ~77 and later on created the bends in the direction of sample ~76 and ~78. It is not possible to accurately determine the precise sequence of development due to the large errors of sample ~76, ~77 and ~78.

The results of the northern and southern meander do not result in a clear and precise direction of meander development. The expected chronological sequences are not completely chronological and the data is difficult to interpret. However the data provides global insight in when and how fast de meanders evolved. Roughly four periods can be distinguished (Figure 42). The distinction of periods might indicate alternated phases of active migration and lateral stability.

Period 1 is dated to ~11 000 years ago and represents the pre-Holocene deposits. Period 2 is dated to ~4000 years ago, it probably indicates the initiation of meandering. Period 1 and 2 are both based on merely one sample and encompass a large time span. It is therefore not possible to further specify this periods and relate them to meander migration rates. Period 3 and 4 can, however be related to the development of the northern and respectively southern meander, since the distinction of these periods is based on more than one sample.

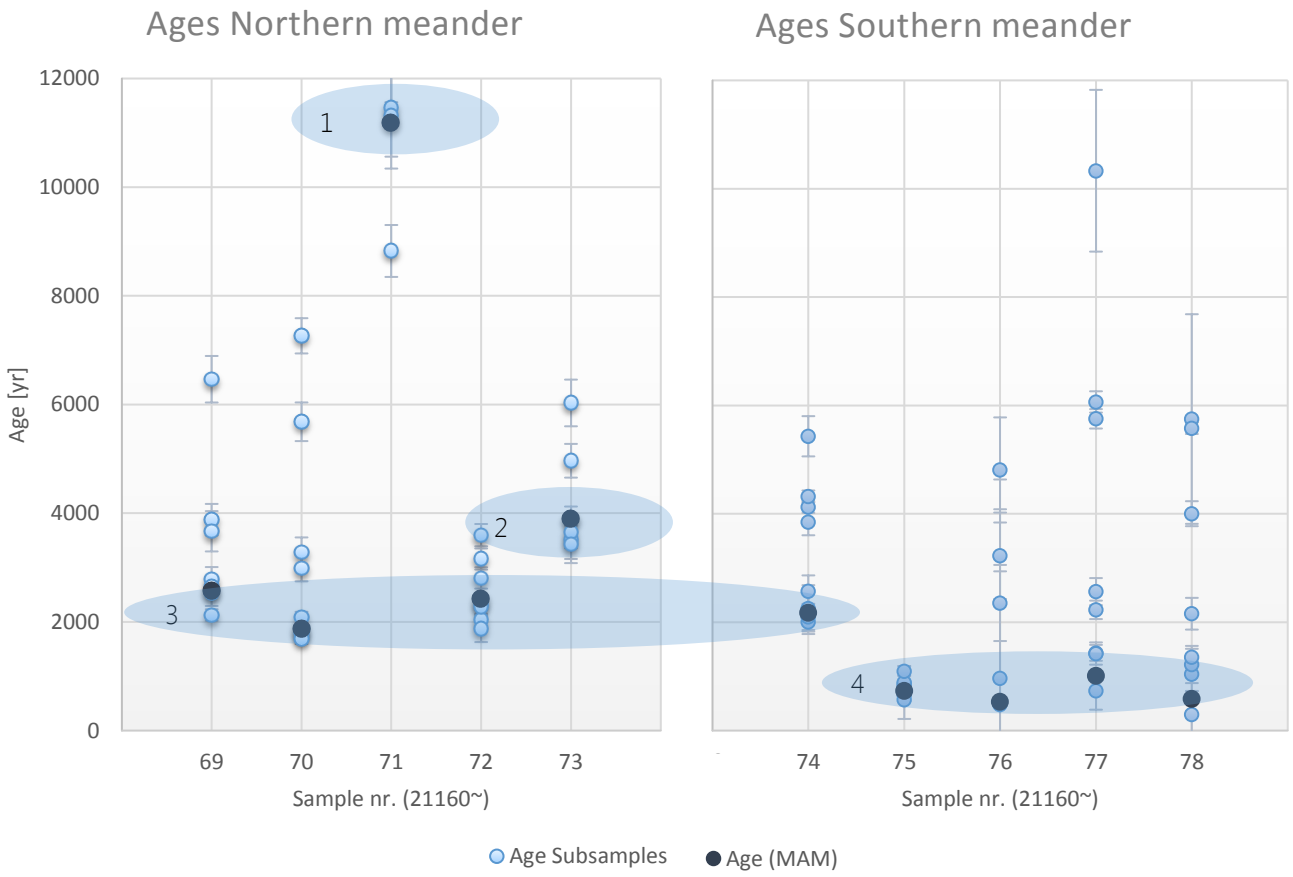

Figure 42 The graph represents the phases that roughly can be distinguished based on the calculated age (MAM) of every sample. The estimated ages of the subsamples are included. Period 1 ≈ 11 000 years ago, period 2≈ 4000 years ago, period 3≈ 3000 to 2000 years ago and period 4 ≈ 1500 to 300 years ago.

Period 3 is represented by four samples and dated to 3000 to 2000 years ago. In this period the northern meander is evolved over a distance of 80 m, and sample ~74 is deposited, which is currently located in the southern meander. In period 3 the cut-off of the northern meander took place as well. Sample ~73 was excluded from this period, based on the relation between the difference in age and distance of meander development. If sample ~73 would have been included, period 3 encompassed the period of 4000 to 2000 years ago. The difference between sample ~73 and ~72, is about 1000 yr. The same as the difference between the oldest and youngest sample within period 3. The distance however between sample ~73 and ~72 is 40 m. This is a short distance for a period of 1000 yr in comparison with the distance of sample ~72 to ~69, which is 80 m and also developed in 1000 yr. It seemed that at least the meander migration rate in

3000 to 2000 years ago was twice as fast as the migration rate 4000 to 3000 years ago. It is therefore decided to consider sample ~73 as a distinct period.

Period 4 is represented by four samples and has a maximum extent of 1500 to 160 years ago. This is period is quite long because of the large errors in the final age estimations. In this period the southern meander is evolved. Since the ages does not follow a clear sequence and the direction of migration can only be roughly estimated, therefore the migration rate could not be further specified.

Although the data might suggest two periods of lateral migration, alternated by periods of lateral stability, continuous migration is still a plausible possibility. The eight samples merely cover the northern and southern meander, there is no information available about the western and eastern meander. In addition there is no data available at other locations in the floodplain of the Dommel.

5.4 Paleo geographic reconstruction

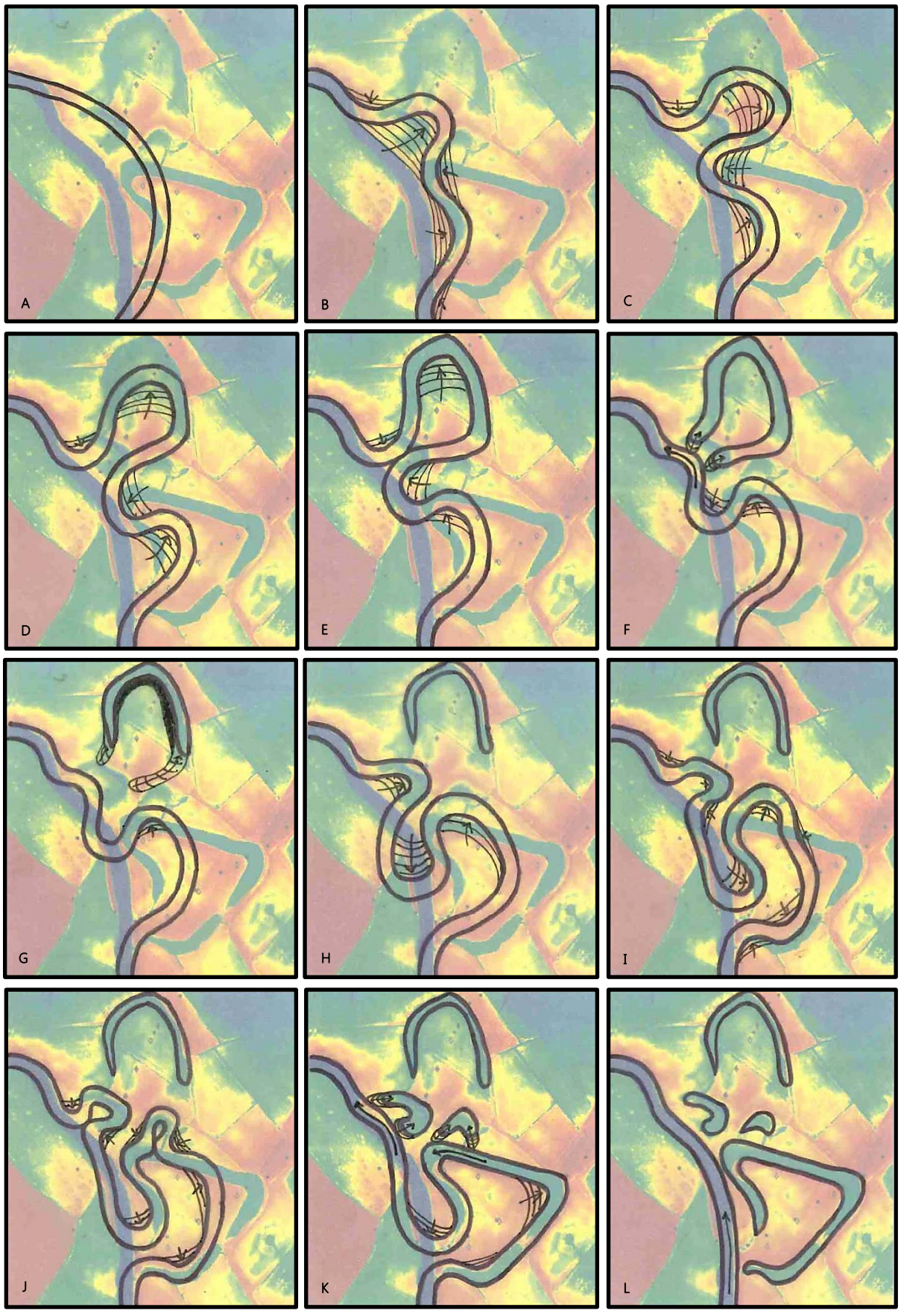

Figure 43 The reconstruction of the development of the Dommel in the last 4000 years represented on the Digital Elevation Model (value 9.5 to 11 m +NAP). The arrows show the direction of migration, the meander neck cut-off and indicate the sedimentation of the disconnected channel. Further explanation is in the text.

The data collected in the previous sections was used to reconstruct the planform evolution of the Dommel prior to channelization (Figure 43). Since the Dommel is a low energetic system it was for this reconstruction assumed that meander neck cut-offs took place instead of chute cut-offs (Figure 5). Figure 43A shows the starting scenario of the planform evolution in this research. The start and end point of the stream coincide with the current stream, however the exact shape and location of the stream at that time are unsure. The location is based on the principle of meandering: the stream will migrate in the direction of the outer bend, therefore the stream should – in case of migration – once have been located at the point where the bend started to form. It is assumed that the bends start to form approximately at the location of te current Dommel, since the floodplain of the Dommel upstream and downstream of the area is quitte small and the potential original locations of the stream are limited. Furthermore, it is assumed that there was one single stream present in this part of the valley at that time.

Figure 43B shows a reconstruction of the situation of ± 4000 years ago. This reconstruction was based on the age of OSL sample ~73 (3880 ± 330 yr). In Figure 43 the start of the migration of the stream is reconstructed. The GPR profiles confirmed that latteral accretion surfaces occur around the location of OSL sample ~73 indicating migration towards the east. In Figure 43C is visualised that the nortern meander continued migrating in eastern direction, where the migration might be blocked by a resistant layer. This might have changed the direction of migration towards the north (Figure 43D). The other bends that appeared in the reconsturction are visualized in Figure 43B. These bends also continued migrating as visualized in Figure 43 C, D and E, and thereby prepared the meander neck cut-off of the northern meander.

The stream could have been an actively migrating system before ± 4000 years ago. However this remains unsure since the deposits that might provide information about the situation before are all reworked by the stream and no abandonned channels dating from that period were found at this location. Based on the OSL dating it can be concluded that the northern meander, is developed earlier than the southern meander. It is possible that during the enlargement of the nortern meander, the stream formed a meander at the location of the southern meander. However it is unlikely that a sinuous meander similar to or large as the current southern meander developed. There were no indications in the field that referred to an older cut-off meander than the southern meander itself and when the stream was located right of the southern meander, it should have been migrated as a whole to the west; thus in the direction of the inner bend, before the development of the southern meander started. Although migration in the direction of the inner bend is observed in lowland stream systems (Kleinhans *et al.,* 2009), it is unlikely that this occurred in this situation. At first inward migration should have occurred over a relatively large distance of ± 100 m, which is not observed in low energetic rivers or streams. Secondly, the connection of the stream to the northern meander would become very sharp, which would induce a meander cut-off, while this did not occur. It is therefore more likely that the northern meander predominantly migrated, as reconstructed in Figure 43 B – E.

The sediment which is dated by the OSL samples ~69, ~70 and ~72 is deposited in Figure 43D and E. These samples were all found to have an age in the range of 1800 to 2800 yr. If sample ~73 is taken into account, it could be argued that the meander migrated in approximately 2000 years (3800 to 1800 yr) from the location of sample ~73 towards its final stage. In Figure 43F the meander neck cut-off of the northern meander and the migration of the southern meander are visualised. During this reconstructed migration sediment dated by OSL sample ~74 is deposited. The age of sample ~74 is in the same range as sample ~69, ~70 and ~72 and therefore these samples were probably deposited in the same period. After the meander is cut-off, a large part of the former channel is sedimented. This continued in Figure 43G, where the cut-off meander is gradually fillled with fine sediments and peat. The peat growth, visualised in Figure 43G by the black area along the northern meander, might indicate a period of decreased fluvial activity. In section 5.3.4 it is argued that the meander migration rates of the northern meander increased over time.

Figure 43 C – F might represent a period of increased meander migration rates, whereas the reconstruction as visualized in Figure 43B might refer to a period of low fluvial activity.

The auguring data could provide information about the period after the meander neck-cutoff. In the cores at the inner bend area of the northern meander peat is found (Figure 34). The cores show a sharp border between sand (below) and peat at ± 2 m below surface. The first ± 10 cm of peat contained some sand and was classified as sandy peat. On top of that, a layer of ± 80 cm consisting of insitu peat occurred, followed by ± 30 cm sandy peat and ± 20 cm loamy sand or sandy loam. This suggested that the period after the meander cut-off was characterized by a low fluvial activity, with less flooding or at least the flooding events did not reach the northern meander. If there would have reached the northern meander, layers of sand or loam should have been found within the layer of peat, however they did not appear. On top of the peat, sandy peat, loamy sand and sandy loam occured. This suggests that after a period of peat development, the northern meander was influenced by flooding, wich resulted in sedimentation along the northern meander.

This period of fluvial activity is reconstructed in Figure 43 H – K, showing the development of the eastern, western and southern meander. First the eastern and western meander developed. At both locations a meander neck cut-off occurred, leaving the remnants of the bends in the landscape. As there is no dating information available yet, it is unknown when these neck cut-offs took place. It is assumed that they took place in approximately the same period. The western meander is located almost in the northern meander, this leads to the assumption that the western meander developed later than the northern meander. The GPR data suggested that northern and western meander had a similar extent: a depth of about 4 m and a width of about 20 m. The eastern meander seemed to have been smaller with a depth of 3 to 3.5 m and a width of 10 to 15 m, which could refer to another period of origin.

After the small meander neck cut-offs, the the southern meander was reconstructed to have continued developing, thereby depositing the sediment at the locations that were dated by OSL samples ~75, ~76, ~77 and ~78. The meander started with a smooth rounded shape as visualised in Figure 43J but developed towards a shape with straight parts and sharp bends as displayed in Figure 43K. Except for sample ~74, the estimations of the ages including errors were in the range of 1500 to 160 yr. This period might refer to another phase of increased meander migration rates, however it is unsure how the southern meander exactly was evolved. Considering the small differences in ages between the samples, it could be argued that the stream first migrated in the direction of ~75 and ~77 and finally created the small bends of ~76 and ~78, instead of what was hypothesised in Figure 22.

In the period of 1850 to 1965 large-scale channelization projects were constructed. In this period the southern meander is artificially cut off, which is visualise in Figure 43L. The arrow indicates where the meander cut-off took place. North of the neck cut-off the stream was straightened. The left bank of the current channel was enhanced with a small dike to prevent erosion. At the right bank and a part of the southern meander is muffled. The channelization of the Dommel resulted in the current morphology of the study area.

6. Discussion

In this chapter the results of this study are discussed and compared to other studies executed in lowland stream areas. Firstly it is discussed whether there are indications for active migration or lateral stability in the floodplain of the Dommel. This is followed by a discussion about the occurrence of distinct periods of active migration. Subsequently the rectangular planform of the Dommel is compared to the planform evolution of other lowland streams. The chapter ends with a connection between past and recent morphodynamic functioning of the Dommel.

6.1 Active migration or lateral stability

Lowland streams are often classified as laterally stable systems (Kleinhans *et al.*, 2009; Eekhout *et al.*, 2014) although they generally show a highly sinuous planform, especially prior to channelization. There are several theories that might explain the cause of lateral stability in lowland streams. In the stable-bed-aggrading-banks model, described by Brown & Keough, (1992), it is argued that the sinuous planform was inherited from pre- or early Holocene fluvial regimes. They found that low-energy rivers in the United Kingdom (UK) underwent a metamorphosis from braided to laterally stable systems during the Holocene. This metamorphosis was indicated by the sediment sequence, that consisted of coarse Pleistocene deposits which contained scars of lateral migration, covered by unstructured fine-textured silty material. It seemed that the sediment calibre in lowland streams changed around the mid-Holocene: from lateral accretion of moderately coarse deposits towards vertical accretion of fine-textured deposits. This led to a decrease in floodplain relief and a relative incising channel, which resulted in a decrease of the width/depth ratio of the channel. The absence of lateral migration after the mid-Holocene was confirmed by the lack of scroll bars and neck cut-offs in the major part of the floodplains. The silty banks had a higher resistance which fostered stabilisation of the beds. The change in river style from braided to meandering had been documented for many lowland rivers throughout Europe during the first half of the Holocene (e.g. Huisink, 2000; Mol *et al.,* 2000; Antoine *et al.,* 2003; Kostic & Aigner, 2007). The change in sediment calibre was probably related to land use changes (Brown & Keough, 1992).

In Walter & Merritts, (2008) it is argued that lowland streams became laterally stable as a consequence of the introduction of watermills, which were commonly used in the 17th to 19th century. Their research was based on mapping and dating of deposits along mid-Atlantic streams in the United States (US). Prior to the introduction of watermills these streams were found to be small anabranching systems in extensive vegetated wetlands (Walter & Merritts, 2008). For efficient use of the water the anabranching systems were reduced to one single channel. The occurrence of streams consisting of merely one single channel might thus be related to artificial channel engineering (Brown, 2002). Milldams caused a rise in base level and a decrease in stream flow velocity. This was noticeable several kilometres upstream of the milldam, especially in floodplains with a low valley gradient. The reduced flow velocity resulted in a decrease in erosion and meander migration rates (Marren *et al.,* 2014). Since milldams are efficient sediment traps (Marren *et al.,* 2014), the floodplains behind the watermills might gradually be filled with fine textured sediments (Walter & Merritts, 2008), which enhanced floodplain aggradation and led to stabilisation of the channel.

Brown & Keuogh (1992) and Walter & Merritts (2008) both argue that lowland streams transform from more channel systems into single channel systems and that these channels became laterally stable as a consequence of a change in sediment calibre, which resulted in floodplain aggradation. The period in which the lowland stream metamorphosis started is different in both studies (Mid-Holocene vs 17th – 19th centuries), however this difference might be explained by the land use history of both countries. In the US intensive cultivation started in 16th century with the first European settlements, whereas in the UK this already started centuries before. In both countries the introduction of watermills might have enhanced the floodplain aggradation which was initiated by land use changes that started decades (US) or centuries (UK) before.

In the floodplain of the Dommel coarse deposits were found at 3.5 m below surface (Figure 34 & 35) which were dated to pre-Holocene age (Figure 41) and covered by fine textured sand (90 to 210 μm) dated to an age of 4000 yr and younger (Figure 41). If the stable-bed-aggrading-banks model is applied to the Dommel, the coarse deposits could be remnants of a braided system and the fine textured sediments would represent the vertical aggradation, which might be caused by land use changes and further increased by the introduction of watermills. Human impact on land use in the area gradually increases since the Bronze Age (Janssen, 1972). Important intensification of agricultural practices occured from 1000 AD ownwards, when large-scale exploitation of the uplands took place (Jansen, 1972). In the same period the first watermills were constructed along the Dommel. In 1790 fifteen watermills were present[7], although it is likely that there have been many more in the centuries before (Theuws, 1976). Most water mills were used until the middle of the 19th century (Van Halder, 2010; Merritts *et al.,* 2011). Nearby the study area two watermills were present, which were at least used from 1381 to 1947 (Mill of Wolfswinkel, 4 km upstream) or 1312 to 1945 (Borch Mill, 2 km downstream). Due to the small valley gradient of the floodplain of the Dommel, the rise in base level and decrease in stream velocity should have been noticeable in the study area.

In contrast to the above described models, In the floodplain of the Dommel indications for floodplain aggradation were less pronounced. The floodplain of the Dommel is characterized by structured fluvial deposits. A clear fining upward sequence was found in most of the cores (Figure 34 & 35). The texture gradually changed from coarse sediments at 4 m depth to extremely fine to fine sand at the surface. In contrast to the floodplains described in Brown & Keough, (1992), remnants of former meander bends and neck cut-offs are present in the floodplain of the Dommel. In addition to that GPR images indicated the presence of lateral accretion surfaces, referring to point bar development and lateral migration. The lateral accretion surfaces started within 1 m below surface and continued until a depth of 3 to more than 4 m, thus encompassing the major part of the fine textured deposits. The major part of the fine textured deposits are thus evidently not the result of vertical aggradation but rather the result of lateral migration. The absence of lateral stability might be explained by the still relatively coarse sediment load of the Dommel. The banks of the Dommel consist of fine to extremely fine sand whereas in areas studied in Brown & Keough, (1992) and Walter & Merritts, (2008) silty clays were found, which have a much higher resistance and are more difficult to erode.

In the floodplain of the Dommel two locations were found, which might indicate floodplain aggradation. At both locations sand and silty deposits occurred on top of peat. This sequence of deposits was found in the cross-section of the northern as well as the southern meander (Figure 34 & 35). It was assumed that the peat in the northern meander was developed after the meander neck-cut off (Figure 34). The floodplain aggradation could thus not have resulted in stabilization of the northern meander, since it was already cut-off and narrowed by peat growth before the sandy sediments were deposited. The peat in the cross-section of the southern meander might also indicate the fill of a former channel however it could also refer to an old muted ditch (Figure 14 & 35). In that case the origin of the sandy deposits might be anthropogenic.

Floodplain aggradation could also be recognised in the GPR images by the depth that lateral accretion surfaces appear. The lateral accretion surfaces of the northern meander generally started between 0.5 and 1 m below surface, which is in accordance with thickness of the sandy deposits that buried the peat. In the eastern, western and southern meander lateral accretion surfaces appeared within 0.5 m. The extent of aggradation was might thus have been varied throughout the floodplain and was probably the largest at the lowest locations (Brown & Keough, 1992). It is unsure whether floodplain aggradation fostered or induced lateral stability of the channels of the eastern, western and southern meander. Since it is unknown in which period the meanders were exactly formed and under which circumstances floodplain aggradation occurred.

[7] For an overview of the watermills along the Dommel, see Appendix I

Furthermore the thickness of the floodplain aggradation was relatively small, about 0.5 m compared to a thickness of several metres, which was found in Brown & Keough (1992) and Walter & Merritts (2008).

The Dommel has a small width/depth ratio and is characterised by steep banks. Steep banks might be the result of floodplain aggradation, however the extent of floodplain aggradation seemed to be small (0.5 – 1 m). Steep banks could also be the result of the incision of streams after dam breaching (Merritts *et al.,* 2011). In the past 100 years many watermills have been expired and the mill dams have been breached (Walter & Merritts, 2008). Dam breaching generally resulted in channel incision into the milldam reservoir sediments and increased erosion of the steep stream banks (Walter & Merritts, 2008; Pizzuto & O'Neal, 2009). However the GPR images indicated that the depth of the ancient Dommel, represented by the meander remnants in the floodplain, is comparable to the current Dommel. The former meanders were dated to 3000 to 2000 yr (northern meander) and 1500 to 300 yr (southern meander) and had a depth of 4 to 4.5 m. When accounting for floodplain aggradation, the depths reduce to 3 to 3.5 m for the northern meander and 3.5 to 4 m for the southern meander. This still results in a small width-depth ratio (5 to 7) and thus steep banks. The depth of the southern meander might be the result of channel incision after dam breaching, since it is disconnected relatively recent, however the northern meander represents a fluvial regime that encountered minor human influence. This might indicate that the Dommel is originally characterised by steep banks.

The lateral accretion surfaces found in the floodplain of the Dommel, were also surprisingly steep. Generally lateral accretion surfaces have a steepness of 1° to 4° (Kostic & Aigner, 2007), while in the study area the major part of the lateral accretion surfaces had a steepness between 8° and 15° and the most steep surfaces had a steepness of up to 24°. In Smith *et al.* (2009) inclined surfaces with a steepness of 16° and 22° were found at one location in counter point bar deposits of a river. In other counter point bar deposits upstream of the same river the surfaces were less steep (3° to 4°). The steepness of the lateral accretion surfaces was thus not directly related to the occurrence of counter point bars. The steepness was might be related to the more downstream position, however more research is required to confirm that (Smith *et al.,* 2009). In the floodplain of the Dommel the steepness of the lateral accretion surfaces can probably be related to the steep banks of the Dommel: migration of a channel with steep banks might result in more steep lateral accretion surfaces.

The morphodynamic functioning of the Dommel during the last century might increase insight in the morphodynamic functioning of the Dommel prior to channelization. Comparison of historical maps dating from 1850 (Topographic Militairy Map) and 1989 (Bonne Bladen) suggested minor differences in planform evolution. However the exact differences were difficult to determine, due to the questionable accuracy and the difference in scale of the maps.

Figure 44 Current erosion and sedimentation in the Dommel, 15 km upstream of the Moerkuilen. **A**: Collapsing or erosion of the outer bank. **B**: Sedimentation at the inner bank. Photos were taken in February 2015.

In the period of 1850 to 1965 large normalization projects were constructed resulting in the channelization of many rivers and streams (Heezik, 2007; Buskens *et al.*, 2011). Channelization changes the natural morphological equilibrium of a channel. When a channel planform is artificially adjusted, a new morphological equilibrium will develop (Eekhout *et al.,* 2014; Eekhout & Hoitink, 2015), which might result in increased migration rates. The Dommel is channelized at several locations, although the major part of the stream still has a sinuous pattern. By comparing aerial photographs, it was observed that in the period after channelization migration rates increased at locations where meanders were cut-off (Kamstra, 2015). Comparison of aerial photgraphs of 1996 and 2010 suggested that there was still some lateral migration and also inward migration was observed (Kamstra, 2015). Fieldobservations of the current situation of the Dommel might also suggest active erosion and sedimentation (Figure 44). It was observed that the banks of the Dommel at some locations were collapsing. In addition to that at some locations upstream of the study area sedimentation in the inner bend took place (Figure 44B), however this was rarely observed (Kamstra, 2015).

To determine whether the current stream has the power to migrate the Dommel can be plotted in the stability diagram. The following characteristics were used to calculate the position of the Dommel in the diagram: a bank-full discharge of ($Q_{2.3}$) is 22.3 m^3/s (Waterschap de Dommel, 2016), a median grain size (D_{50}) of 200 μm = $2.0 \cdot 10^{-4}$ m (fine sand) and a longitudinal slope of 0.00032, measured over a distance of 11 km. The Dommel is plotted in the lowest part of the meandering area (Figure 45). This implies that the stream has enough power for active migration, however there is also a reasonable chance that it is laterally stable.

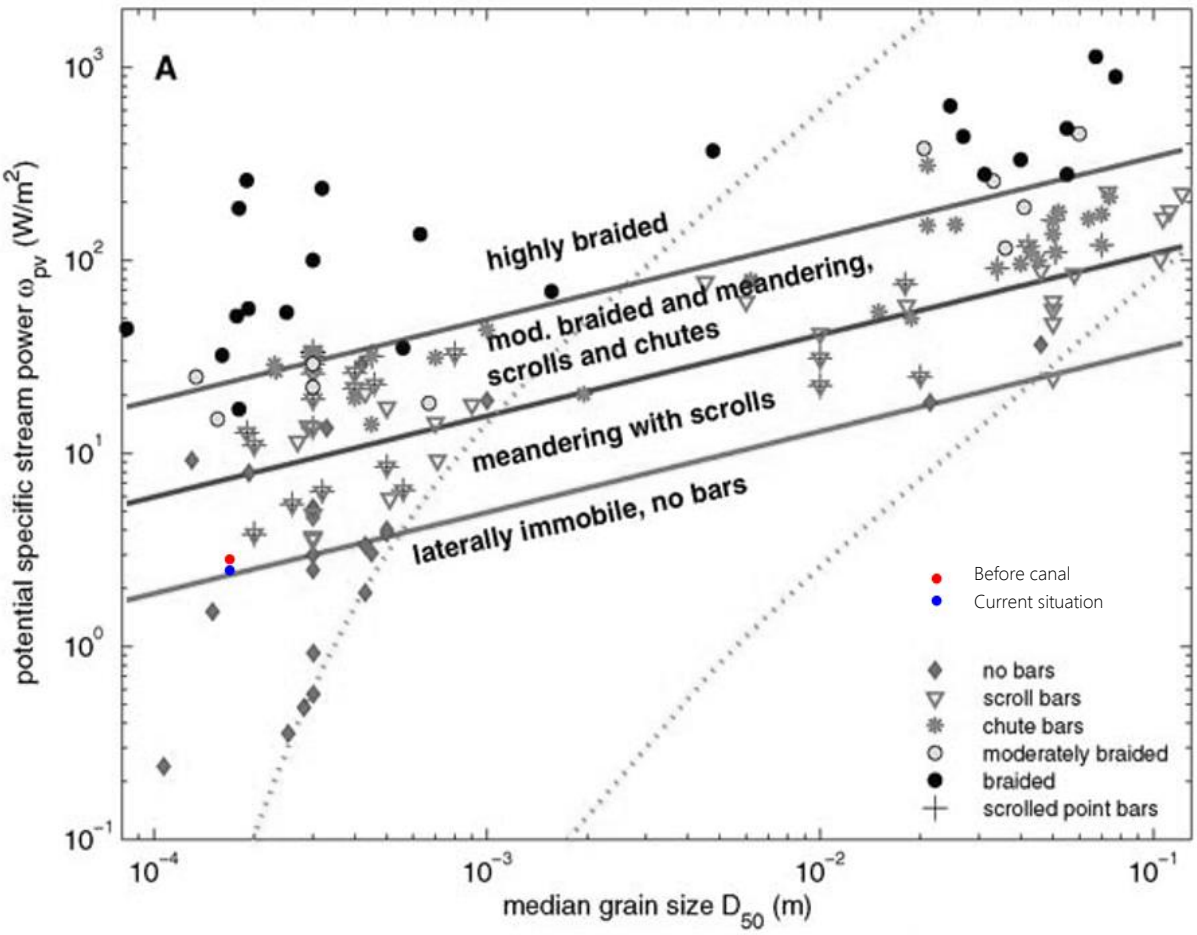

Figure 45 Stability diagram that represents the patterns of alluvial rivers in morphologic equilibrium. The current situation of the Dommel and the situation before the construction of the canal are plotted in this diagram. Retrieved from: Kleinhans & Van den Berg (2011).

In the period of 1910 to 1923 a canal was constructed upstream of the study area, which is used to lower the peak discharges of the Dommel to avoid high water levels in the citycentre of Eindhoven. This has led to reduced peakdischarges and consequently a reduced stream power. The $Q_{2.3}$ before the construction of the canal was 25.4 m^3/s (Waterschap de Dommel, 2016), the corresponding value, is plotted higher in the area 'meandering with scrolls' (Figure 45). The position prior to the canal could still indicate a laterally stable system however the chance that the stream was migrating is higher. It is possible that the construction of the canal led to or fostered, a transition from a meandering to a laterally stable stream. Because especially peakdischarges enhance meander migration rates (Meade, 1982; Kleinhans *et al.*, 2009).), and just these discharges were buffered by the canal.

However in both cases the Dommel is plotted low in the area 'meandering with scrolls', close to the threshold of active migration. This implies that when active migration might occur, the development of meanders can be very slow (Makaske *et al.,* 2016). To determine wheter the Dommel is migrating nowadays detailed planform evolution should be considered over a longer period.

6.2 Periods of meander migration

In this study it is argued that the planform evolution of the Dommel could be distinguished in at least four periods (Figure 42). Based on the collected OSL data the following periods were identified: period 1 ≈ 11 000 years ago, period 2 ≈ 4000 years ago, period 3 ≈ 3000 to 2000 years ago and period 4 ≈ 1500 to 160 years ago. Period 3 and 4 might refer to phases of active migration probably alternated by stable periods. Period 3 indicates the formation of the major part of the northern meander and period 4 the formation of the southern meander. For a rough confirmation of the age of the northern and southern meander a complete OSL analysis was executed for two samples (no. ~70 and ~77) representing the northern and southern meander. Sample ~70 is dated to 2350 ± 250 years ago and ~77 is dated to 650 ± 130 years ago (Candel *et al.,* 2018). Since a complete OSL analysis, results in a more reliable age, amongst others due to the larger amount of subsamples per sample (30 instead of 7), these new ages will be used to discuss the possibility of the existence of separate periods of migration. The new values of these samples differ from their original estimations, resulting in slightly different periods. Including errors, period 3 is estimated at 2860 to 1890 years ago and period 4 is estimated at 1020 to 160 years ago. However since the new estimation of sample ~70 is even outside the range of its original estimation (1880 ± 140 yr) the reliability of all age estimations in this study seems to be low and the periods should merely be considered as a rough estimation of the time of meander development. However the data might still indicate the occurrence of multiple periods of increases meander migration rates.

When phases of active migration occurred, there should be a process that triggered the increase of meander migration rates. Important factors on planform evolution are bank stability, discharge and sediment supply, which are all closely related to climate and human intervention on land use. Therefore general developments in climate and land use from the mid-Holocene, could provide insight in potential periods of increased fluvial activity. Climate deterioration especially associated with extreme events is closely related to fluvial activity phases (Starkel *et al.,* 2007) and the occurrence of high discharges could result in meander migration (Kleinhans *et al*., 2009). Land use changes and intensification of agricultural practices are generally associated with increased sediment supply. When the suspended load in low-energetic systems increases, this could result in an increase in overbank sedimentation, aggradation of the floodplain and siltation of secondary channels (Brown, 2002; Marren *et al.,* 2014). In the context of floodplain impacts, reductions in suspended load are less important, except where they enhance bank erosion and migration rates (Marren *et al.,* 2014). Increased sediment supply could result in channel stability and relative incision (Brown & Keough, 1992), however in combination with increased discharges it could also be associated with increased meander migration rates (Quick, 2016).

There are indications for a period of climate deterioration around 2700 years ago (e.g. Van Geel *et al*., 1996; Van Geel 1998a; Dergachev *et al.,* 2004; Tipping *et al.,* 2008; Wang *et al.,* 2012) which can be related to increased fluvial activity of rivers and streams (Dark, 2006; McDonald & Sangster, 2017). The change in climate is probably related to migration of the earth magnetic field, the so called Sterno-Etrussia excursion, which led to an increase in cosmic ray flux, mainly in the northern hemisphere (Dergachev *et al.,* 2004). In combination with a lower solar activity this triggered an abrupt shift to a colder and wetter climate (Van Geel *et al*, 1996; Dergachev *et al,* 2004; Wang *et al.,* 2012). Besides a change in solar activity, the climate deterioration is probably also influenced by an increased amount of atmospheric ^{14}C (Van Geel *et al*., 1996; Mauquoy *et al.,* 2004). The period of (abrupt) climate deterioration is known as the Subboreal/Subatlantic transition (Wang *et al.,* 2012) and coincides with the Late Bronze Age/Early Iron Age (1200 to 500 BC) (Zolitschka *et al.,* 2003).

Other remarkable periods in the past climatological record were recognized in the period from the High Middle Ages (1000 to 1300 AD) to the Modern Time (1500 to 1850 AD). In northern Europe the 10th to 13th century is recognized as a relatively warm period, known as the Medieval Warm Period (Lamb, 1977; Brown,

2002). This warm period is followed by a time of climate deterioration, which again coincided with low solar activity (Dergachev *et al.*, 2004) and increased atmospheric ^{14}C (Van Geel *et al.*, 1996; Mauquoy *et al.,* 2004). The Little Ice Age, which encompasses the 15th to 19th centuries, represents a large climatic signal, although recent, more complete climatological records suggest that only a few decades, showed very cold conditions (Brown, 2002). The Little Ice Age is also associated with increased fluvial activity (Notebaert & Verstraeten, 2010).

Fluvial systems reflect both human impacts and climate changes (Zolitschka *et al.,* 2003). It is possible that land use changes fostered the sensitivity of rivers and streams to climate change (Tipping *et al.,* 2008), resulting in a higher fluvial activity. Human influce might even prevail the influence of climate change, especially at short time-scales (Zolitschka *et al.,* 2003). Human impact, in terms of woodland clearance and farming, increased since the Bronze Age (2000 – 800 BC) (Bebermeier *et al.,* 2017). It further increased during the Iron Age (800 to 12 BC), when the iron tools were introduced (Zolitscka *et al.,* 2003) and during the Roman time (12 to 500 AD), which is associated with intensification of deforestation and farming (Renes, 1988; Notebaert & Verstraeten, 2010). There is less information availabe about land use developments during the Early Middle Ages (500 to 1000 AD) (Brown, 2009). Important intensification occured from 1000 AD ownwards, when large-scale exploitation of the uplands took place (Jansen, 1972). Because of overexploitation of the poor sandy soils, heathlands expanded and later on drift sands started to occur (Janssen, 1972) which continued until the Late Middle Ages (De Bont, 1993). Sand dunes originating from drift sands occur in the surroundings of the Dommel. These drift sands might have influenced the sediment calibre of the Dommel.

The developments of climate and land use, could be related to the planform evolution of the Dommel. The evolution of the northern meander (Period 3: 2860 to 1890 years ago) coincides with the Early Bronze Age and the Iron Age. The presence of human occupation in the Iron Age in the neighbourhood of the study area is confirmed by Paleobotancal research (Janssen, 1972). The evolution of the southern meander (Period 4: 1020 to 160 years ago) coincides with the High and Late Middle Ages and the Modern time. This was a period where agricultural practices were intensified (e.g. Jansen, 1972). Period 3 and period 4 thus both coincide with important changes in climate and land use. The combination of climate deterioration and land uses changes might have triggered active migration of the Dommel.

There were also some indications for a period characterized by lower fluvial activity and less flooding in between phases of active migration (0 to 1000 AD). At two locations, in former channels, an 1 m thick layer consisting of loamy and sandy deposits occurred on top of peat, whereas the peat itself contained almost no sand. This might indicate that after a period of peat development with marginal fluvial activity or flooding, the periods of flooding increased resulting in deposition of sandy sediments on top of the peat. However since merely two bends were dated, more research is required to confirm whether distinct phases of active migration or periods of increased migration rates might have occurred or that continuous migration took place.

There might have been two phases of increased meander migration rates, although it is also possible that the Dommel had been migrating continuously. Since in this research ten OSL samples were taken, that merely cover the northern and southern meander. There is no information available about the western and eastern meander or any other locations in the younger part of the floodplain of the Dommel, which might indicate other periods of migration.

6.3 Planform evolution and floodplain resistance

The planform of the Dommel has a remarkable shape, characterized by sharp bends and straight parts. Such rectangular planforms are more often observed in lowland streams, however they are rarely observed in rivers. Figure 46 represents the difference between a smoothly rounded and a rectangular planform. The evolution of rectangular planforms can probably be explained by the composition of the floodplain. Due to the smaller size and lower stream power of lowland streams, in comparison to large rivers, lowland streams seem to be much more restricted by for example, resistance-bearing layers in floodplains and banks (Kleinhans *et al.*, 2009; Makaske *et al.*, 2016). A high complexity in the floodplain sediments can be an explanation for the complexity of a channel planform (Güneralp & Rhoads, 2011).

Figure 46 The comparison of the planform and morphology of a meandering river and a lowland stream. **A**: The Chinchaga River Canada is characterized by a smoothly rounded planform and abandoned bend structures are common. **B**: The Schipborgse Diep, part of the catchment of the Drentsche Aa. Retrieved from: **A**: maps.google.nl ; **B**: www.cultuurlandschap.com

The effect of highly cohesive floodplain sediments on planform evolution was investigated by Kleinhans *et al.* (2009). In this research an intertidal mudflat in the Westerschelde estuary in the Netherlands was studied. In spite of the contrasting setting, this floodplain demonstrates noticeable similarities with the setting of the Dommel. The channel was smaller (~1 m vs ~20 m), but had a similar width/depth ratio (~4 vs ~5) and was also characterized by sharp bends and straight parts. At the mudflat, two important processes were identified, which weakened the cohesive banks and initiated meandering (Kleinhans *et al.,* 2009). The first process was the occurrence of backward migrating steps, which can take place when stream power strongly increases over distance. This was the case at the downstream edge of the mudflat, towards the falling tide. In the bends, the backward migrating steps led to excavation of the bed and undercutting of the banks. Especially in the bends, the initial cohesive banks became less stable. The second process that was observed, is called flow separation. Instead of following the thalweg, the stream flow separated from the inner bend towards the opposite side of the channel, weakening this bank. In most bends, the separation point was identified at a sharp and pointed mud ridge (Kleinhans *et al.,* 2009). At both sides of the separated flow, at the outer bank and inner bank, directly after the bend, circular flows (vortexes) occur, which led to erosion of the banks (Figure 47A). Lateral migration of the channel was merely observed in periods with high rainfall and mainly took place in the bends. Over time this resulted in a rectangular channel planform with sharp bends (Figure 47B) and also inward migration was observed (Kleinhans *et al.,* 2009). Other studies confirm

the relation between the process of flow separation and meander migration in low-energetic systems (Blanckaert, 2010; Blanckaert, 2011). According to Blanckaert, (2011), it seems that inner-bank flow separation enhances meander migration and that the process is most relevant in narrow relative deep

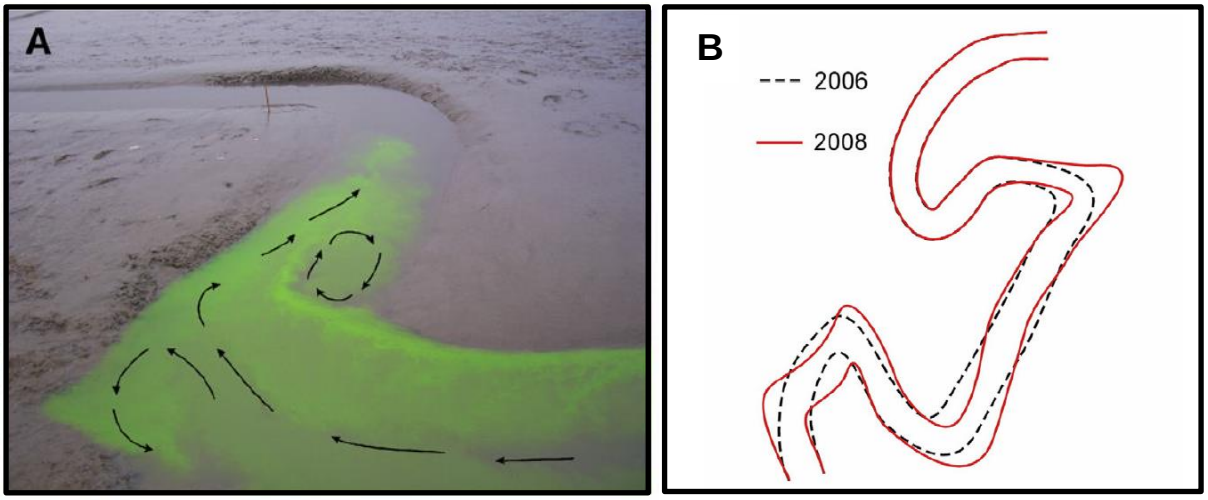

Figure 47 Planform evolution of the Westerschelde Estuary, Netherlands. The channel is approximately 1 m wide. **A:** The direction and separation of the flow. At both sides of the separated flow, circular flows (vortexes) develop, enhancing bank erosion. **B:** A sketch of the observed changes in the period 2006 to 2008 (not to scale). Both retrieved from: Kleinhans *et al.,* (2009).

streams.

Considering the similarities in planform between the Westerschelde estuary and the Dommel and the assumption that the process of flow separation is most relevant in narrow deep streems, flow separation might have been an important proces in the planform evolution of the Dommel as well. However flow separation can not be observed in the former meanders of the Dommel, since they are not connected to the channel anymore and the set up of such an experiment (Figure 47A) in the current Dommel was beyond the scope of this research. Although, there are indirect indications that flow separation could have occurred.

The floodplain of the Westerschelde Estuary consists of highly cohesive sediments, therefore meander migration, mainly took place in the bends which were weakened as a consequence of backward migrating steps and flow separation. The floodplain of the Dommel mainly consists of sand, which is much less resistant and should enable stream migration. However additional field research and coring demonstrated that at several places at the outer banks of the former meanders resistant layers occur (Candel *et al.,* 2018), preventing the stream from further migration. At the east side of the northern meander and at the south-east of the southern meander resistant layers consisting of cohesive sandy sediments were found. In the paleo-geographic reconstruction (Figure 43) it was assumed that a resistant layer occurred north east of the northern meander, however this was not confirmed by additional field research. The evolution of the norhtern meander might thus be directed more to the north, instead of to the nort-east, which is drawn in the reconstruction (Figure 43).

Furthermore, in Makaske *et al.,* (2005), flow separation is related to the occurrence of mud beds in counterpoint bars of a paleo-river. The mud beds were up to 20 cm thick and somethimes contained fine reworked organic matter (Makaske *et al.,* 2005). There were three principles that could explain the occurrence of these mud beds. One of them described that deposits with a high silt and clay content and also organic matter, could be captured by the inner-bank circular flow in sharp bends (Carey, 1969). The occurrence the organic deposits found in the floodplain of the Dommel might thus be explained by the process of flow separation. The organic deposits varied from small laminae of several mm (Figure 32A) with decomposed black material to layers of several decimetres consisting of a mixture of loose wood particles and sand (Figure 32 B & C). The organic deposits found in the cores were also found at the streambed of

the current Dommel. Comparable deposits are found in counterpointbar deposits, without a clear reference to the occurrence of flow separation (Smith *et al.*, 2009). The organic deposits found in the floodplain of the Dommel, however, seemed to be coarser and thicker. In agreement with the process of flow separation, the development of counterpoint bars is also related to the occurrence of resistant banks (Smtih *et al.,* 2009). Considering the prescence of resistant banks, the sharp bends and the reworked organic deposits, both flow separation and counterpointbar development could have played an important role in the planform evolution of the Dommel.

Another lowland stream characterized by such an irregular planform is the Drentsche Aa in the north of the Netherlands (Figure 46B). In Candel *et al.*, (2017) the evolution of this rectangular planform is described as being the result of oblique aggradation. Lowland stream the Drentsche Aa had evolved by eroding the relatively low-resistant sandy borders of the floodplain, while highly resistant peat was accumulating in the floodplain, preventing migration of the channel within the floodplain. This results in a rectangular planform characterized by sharp bends at the sandy borders and a straight path throughout the floodplain. During the period of peat accumulation the channel migrated obliquely towards the sandy sides (Candel *et al.*, 2017). Although resistance in the floodplain seems to play an important role in the planform evolution of the Dommel, the setting of the Drentsche Aa is different at various points. In the floodplain of the Dommel the difference between resistant and less resistant parts is less clear. Resistant layers occur more local and are less homogeneous, since they consists of peat or different types of cohesive sediments. Furthermore the channel is not migrating obliquely, since there is no peat accumulation in this part of the floodplain.

Whereas high resistant layers could determine the opportunities for meander migration, the opposite is also true: the occurrence of low resistant layers can enhance meander migration. A local higher erodibility of the banks can result in small perturbations in the channel planform, that could initiate and foster meandering (Ikeda *et al.,* 1981; Van Balen *et al.,* 2008). An increase in the erodibility of banks can be the result of seepage flow. This is observed in the Nierskanaal in the Netherlands (Eekhout *et al.*, 2013). The banks of this channel consisted of sand and along the sides iron oxide was found locally, indicating seepage. The locations were iron oxide was found correspond to the parts where meandering had been initiated and the occurrence of seepage seems to be the most plausible explanation (Eekhout *et al.*, 2013). On the other hand long-term seepage flow can result in the development of 'Ijzer-oer' which is highly resistant sediment, containing consolidated iron (Baaijens *et al.,* 2011). The occurrence of 'IJzer-oer will impede erosion. In the floodplain of the Dommel also seepage occurs, which might have influenced its planform evolution. In several cores, mainly in the cross-section of the southern meander, a very red soil appeared, indicating the presence of iron oxide as a result of seepage. The occurrence of seepage at the outside of the sharpest bend of the southern meander might be an explanation for the sharpness of this bend. At one single location in the bank of the current Dommel also 'IJzer-oer' was observed.

The occurrence of seepage is observed in many lowland stream floodplains and this is probably not by accident, but might have an artificial cause (Baaijens *et al.,* 2011). Based on field observations and historical research it is argued that lowland streams lack a natural origin and that their existence is related to an inundation system that made use of natural sources of seepage water (Baaijens *et al.,* 2011). Probably already in the Early Middle Ages the fertile seepage water was used as natural fertilizer for the meadows to increase the hay production. Locations that contain the highest seepage flow were connected by a channel resulting in a channel with an irregular planform. The nutrient rich seepage water was led through a designed complex of ditches towards the meadows. Low gradients were sufficient for a small current and small differences in heights further divided and directed the flow. Remnants of this inundation system are observed in the major part of lowland stream floodplains in the Netherlands (Baaijens *et al,* 2011). This does not directly imply that all lowland streams lack a natural origin but there could be a correlation between the location of lowland streams, their irregular planform and the occurrence of seepage. Considering the major artificial channel works in Medieval times it is not impossible that channels where cut from scratch, however

it seems more likely that only parts of a channel were dug, to bridge the distance between a natural stream and a location where seepage occurs. In that case there was a natural channel, which is artificially adapted to obtain more fertile water. Prior to the introduction of artificial fertilizer, this natural fertilizer was very important for farmers and worth the effort. The (partly) artificial origin of channels could explain the sharp bends and straight parts, since the planform should represent the most efficient way to connect locations where seepage flow occurs. It is possible that the (artificial) bends became more sharp over time, due to the relatively low resistance of banks when seepage takes place.

The hypothesis of an artificial channel is however, not applicable to the Dommel. In the floodplain of the Dommel lateral accretion surfaces were found, starting from the surface, referring to a migrating channel and the coring data represents a fining upward sequence indicating the fluvial origin of the deposits. However the inundation system itself is applied in the area by using the water of the Dommel, since the remnants of the patterns of ditches can still be found in the landscape (Figure 12 & 14).

7. Conclusion

Prior to channelization, lowland streams were characterised by a highly sinuous planform. It is unknown when and how these planforms were evolved, since there is scarcely information about the natural morphodynamic functioning of lowland streams in the past. However understanding of the origin and evolution of lowland streams is of great importance for stream restoration projects. This research investigated the morphodynamic functioning of lowland stream the Dommel prior to channelization, by a paleo-geographic reconstruction. To increase insight in its planform evolution the following research questions were formalized:

What was the morphodynamic functioning of the Dommel before channelization?

- How did the Dommel develop and gain its sinuous pattern?
- How fast did the bends form and could the formation of the bends be related to specific periods?
- How could the morphodynamic functioning before channelization be related to the current morphodynamic functioning of the Dommel and what does this mean for stream restoration projects?

In the study area, which is located south of St. Oedenrode in the southern Netherlands, remnants of four meanders of the Dommel were present. The evolution of these bends is investigated by GPR transects, coring data and OSL dating. Based on GPR images and coring it seemed that these bends had been evolved by meandering before they were naturally or artificially cut-off. At the GPR images inclined surfaces appeared, which were interpreted as lateral accretion surfaces, although they were surprisingly steep. The steepness of the lateral accretion surfaces increased towards the former channels and might be related to the steep banks of the channels. The lateral accretion surfaces started within one meter below surface and continued until a depth of 3 to 4.5 m. Over the same depth a fining upward sequence was identified in most of the cores. The occurrence of lateral accretion surfaces and the fining upward sequences refer to a fluvial origin of the floodplain deposits and active migration of the channels.

The GPR images and coring data suggest that the top 50 to 100 cm of the floodplain might origin from floodplain aggradation. Floodplain aggradation could be induced by land use changes and also the introduction of water mills along the Dommel in the Middle Ages might have played an important role. The latter could also cause a decrease in stream power by a rise in base level. The combination of increased sediment supply and a decrease in stream power are recognised as important causes for lateral stability in lowland streams. However the extent of the floodplain aggradation in the study area is relatively small, the sediment is quite coarse (90 to 210 µm) and it is unknown how much the stream power was affected by the introduction of watermills. It is therefore unsure whether floodplain aggradation and the practice of water mills fostered or induced lateral stability of the Dommel.

It seemed that the depth and width of the ancient Dommel, represented by the meander remnants in the floodplain, is comparable to the current Dommel. The GPR images indicated steep lateral accretion surfaces and steep banks of a channel that originated from the Late Bronze or Iron Age. This might suggest that the Dommel is originally characterised by a small width/depth ratio and steep banks. The occurrence of steep banks could not be explained by floodplain aggradation or channel incision after dam breaching. Accounting for floodplain aggradation, the point bar deposits, still encompassed a depth of 3 to 4 m in all former meanders.

The similarities between the ancient Dommel and the current Dommel increase the importance of the understanding of the current morphodynamic functioning. The current stream power and the sediment load of the Dommel might result in lateral movement of the channel, although the values are close to the threshold of active migration. Comparison of aerial photographs of the last century and fieldobservations suggested minor lateral migration. Meander migration rates might have been decreased since the start of the 20th century due to the construction of a canal which reduces the peak discharges of the Dommel.

Based on OSL dating it could be argued that there might have been distinct phases of increased meander migration rates alternated by periods of lower fluvial activity or even lateral stability. One period is dated at 3000 to 2000 years ago and coincides with the Late Bronze Age and the Iron age (1200 – 500 BC). This period is associated with climate deterioration and is also recognised as a time in which human impact on land use became noticeable. Another period is dated 1000 to 160 years ago and covers the period of the High Middle Ages to the Modern times (1000 to 1850 AD). This period encompasses the Medieval Warm Period and the Little Ice Age and is also known of increased land use agricultural practices. Changes in climate and human impact are closely related to discharge, sediment supply and vegetation growth and might therefore be considered as important external controls on planform evolution. Thus, the described changes in climate and land use might have triggered increased meander migration rates of the Dommel.

In the floodplain of the Dommel, there were also some indications for a period characterized by lower fluvial activity and less flooding in between the phases of active migration (0 to 1000 AD). The occurrence of loamy and sandy deposits on top of in-situ peat, might indicate that after a period of peat development with marginal fluvial activity or flooding, the periods of flooding increased, resulting in deposition of sandy sediments on top of the peat. However, since merely two bends were dated, more research is required to confirm whether distinct phases of active migration or periods of increased migration rates might have occurred or that continuous migration took place.

The planform of the Dommel has a remarkable shape, characterized by sharp bends and straight parts. In the planform evolution of the Dommel it seemed that resistance-bearing layers played an important role. The local occurrence of layers with a high resistance, for example loam or peat, might prevent the stream from migration, resulting in a complex rectangular planform. At several locations along the former meanders resistance-bearing layers were found. The occurrence of resistant floodplain deposits might result in the development of counter point bars. The combination of floodplain resistance and the sharp bends in the planform of the Dommel might also refer to the process of flow separation, whereby the stream flow separated from the inner bend towards the opposite side of the channel and weakened this bank. Since migration as a consequence of flow separation mainly occurs in the bends, this results in a planform characterized by sharp bends and straight parts. Furthermore the process is most relevant in narrow, relative deep streams, which is also typical for the Dommel. Both, counter point bar development and the process of flow separation could result in the deposition of layers containing reworked organic material, which were commonly found in the floodplain of the Dommel. It might be concluded that flow separation and counterpointbar development could both have played an important role in the planform evolution of the Dommel.

Whereas high resistant layers could determine the opportunities for meander migration, the opposite can also occur: the presence of low resistant layers can enhance meander migration. A local higher erodibility of the banks can result in small perturbations in the channel planform, that could initiate and foster meandering. An increase in the erodibility of banks can be the result of seepage flow. Indications for seepage flow were observed in the floodplain. The occurrence of seepage might be an explanation for the evolution of one of the most sharp bends in the study area.

It could be concluded that the morphodynamic functioning of the Dommel prior to channelization is characterized by at least several periods of active migration. These periods of lateral migration might be

related to changes in climate and human intervention. In seemed that the ancient Dommel had a similar width and depth as the current Dommel, which might indicate that the Dommel is originally characterised by steep banks. Floodplain aggradation that occurred in the area, might have played a minor role in the planform evolution of the lowland stream. There were some indications for periods of less fluvial activity, however active meandering might have occurred continuously, since the Dommel still has the power to migrate. The heterogeneity in the floodplain of the Dommel in combination with the processes of counter point bar development and flow separation might have resulted in the complex sinuous planform of the Dommel.

Application and recommendations

In restoration projects it is often aimed to construct a near-natural geomorphology and to advance free morphological behaviour (Eekhout *et al.,* 2013). To achieve this, detailed knowledge about the natural morphodynamic functioning of the system is required, however many restoration projects are conducted with minimal scientific context (Wohl *et al.,* 2005). In Makaske & Maas (2015) a method is developed which provides information on the current potential of active migration and the consequences for stream restoration. Potential specific stream power and the median grain size of the bedload seems to be important determining factors in the final shape of the stream. However in this research it is argued that in lowland streams heterogeneity of the floodplain might also play a major role in planform evolution. The local occurrence of resistant deposits could prevent the stream from migration. At the other hand, the occurrence of seepage might initiate meandering. When stream restoration projects are aimed at advancing free morphological behaviour, it is very important to investigate lithology of the floodplain and the occurrence of seepage, since both seemed to be important determining factors for bank stability. In a very cohesive floodplain it is presumably not possible for a low-energetic stream to actively form meanders. When resistant layers occur occasionally in the floodplain, these layers should be avoided in the design of stream restoration. However it will still also depend on the stream power and the bed load of the restored stream whether a stream has the potential for lateral migration. To further investigate the impact of floodplain composition on planform evolution it might be interesting to compare the lithology of the floodplains of lowland streams with a smooth rounded and a rectangular planform. The examination of the origin and distribution of resistant layers would also be an interesting subject for further research.

Furthermore additional research is required to confirm the existence of phases of increased migration rates. Phases of increased migration rates might explain the sinuous planform of lowland streams that currently seem to be laterally stable. When phases of increased migration occurred, indications of these phases should be found in other parts of the floodplain of the Dommel. It might be interesting to date the eastern and western meander of the study area or other former meanders in the floodplain of the Dommel.

Investigation of the current fluvial dynamics of the Dommel indicated that there still might be minor active migration. Lateral migration might be (partly) caused by the process of flow separation. For a better understanding of planform evolution of lowland streams, especially those that are characterised by a small width/depth ratio, it is important to increase insight in the origin and effect of flow separation and its relation to meander migration rates.

Throughout this study, the planform evolution of lowland streams seems to be a very broad and complex subject of research. Although many questions remain unanswered and new questions came up, this research provided a small contribution to a better understanding of the origin of the beautiful sinuosity of lowland streams.

8. References

Aitken, M.J., (1998). An Introduction to Optical Dating. Oxford University Press, 267 pp.

Allen, J.R.L., (1964). Studies in fluviatile sedimentation: six cyclothems from the lower old red sandstone, Anglo-Welsh Basin. *Sedimentology,* Vol. 3, p. 163 – 198.

Antoine, P., Munaut, A.V., Limondin-Lozouet, N., Ponel, P., Duperon, J. & Duperon, M. (2003). Response of the Selle River to climatic modifications during the Lateglacial and Early Holocene (Somme Basin-Northern France). Quaternary Science Review, Vol. 22, p. 2061–2076.

Arnoldussen, S., (2013). Zoektocht in het zuiden: Celtic fields op ongestuwde afzettingen in Zuid-Nederland. *Paleo-aktueel*, Vol. 24, p. 59 – 66.

Asprion, U. & Aigner, T., (1997). Aquifer architecture analysis using ground penetrating radar: Triassic and Quaternary examples (S-Germany). Environmental Geology, Vol. 28, p. 1–10.

Aurclair, M., Lamothe, M. & Huot, S., (2003). Measurement of anomalous fading for feldspar IRSL using SAR. *Radiation Measurements*, Vol. 37, Is. 4-5, p. 487 – 492.

Baaijens, G.J.E., Brinckmann, P. Dauvellier & P. van der Molen, (2011). Stromend landschap; vloeiweidenstelsels in Nederland. KNNV Uitgeverij, Zeist

Barends, S., Baas, H.G., De Harde, M.J., Renes, J., Rutte, R., Stol, T., Van Triest, van, J. C., Vries, de, R. J. & Van Woudenberg, F. J., (2010). Het Nederlandse landschap; Een historisch-geografische benadering. Uitgeverij Matrijs, Utrecht.

Bebermeier, W., Hoelzmann, P., Meyer, M., Schimpf, S. & Schütt, B., (2017). Lateglacial to Late Holocene landscape history derived from floodplain sediments in context to prehistoric settlement sites of the southern foreland of the Harz Mountains, Germany. *Quaternary International*, Vol. 463, p. 74 – 90.

Beekx, G., (1970). Bronzen hielbijl uit St. Oedenrode. *Brabants Heem*, tweemaandelijks tijdschrift voor Brabants heem en oudheidkunde, Vol. 22, Is 3, p. 21.

Berendsen, H.J. & Stouthamer, E., (2001). Paleogeographic development of the Rhine-Meuse Delta, the Netherlands. Koninklijke van Gorcum, Assen.

Berendsen, H.J.A., (2004). De vorming van het land: Inleiding in de geologie en de geomorfologie. Fysische geografie van Nederland, Van Gorcum & Comp. B.V., Assen.

Bersezio, R., Giudici, M. & Mele, M., (2007). Combining sedimentological and geophysical data for high-resolution 3-D mapping of fluvial architectural elements in the Quaternary Po plain (Italy). Sedimentary Geology, Vol. 202, p. 230–248.

Blanckaert, K., (2010). Topographic steering, flow recirculation, verlocity redistribution and bed topography in sharp meander bends. Water Resources Research, Vol. 46., W09506, (doi:10.1029/2009WR008303).

Blanckaert, K. (2011). Hydrodynamic processes in sharp meander bends and their morphological implications. *Journal of Geophysical Research*, Vol. 116, F01003. (doi:10.1029/2010JF001806)

Bøtter-Jensen, L., Andersen, C.E., Duller, G.A.T. & Murray, A.S., (2003). Developments in radiation, stimulation and observation facilities in luminescence measurement. *Radiation Measurements*, Vol. 37, p. 535 – 541.

Bøtter-Jensen, L., Bulur, E., Duller, G.A.T. & Murray, A.S., (2000). Advances in luminescence instrument systems. *Radiation Measurements*, Vol. 32, p. 523 – 528.

Braillard, L. & Guelat, M., (2008). An upper Pleistocene alluvial sheet in Delemont Valley (Swiss Jura): Lithostratigraphy and dating. *Quaternaire*, Vol. 19, Is. 3, p. 217 – 228.

Brock, A.C., (~1825). De sand en meierij van 's Hertogenbosch of derzelver beschrijving – Tweede afdeeling bevattende een Geographische, Historische en Chronologische Beschouwing van de steden, dorpen, vlekken, heerlijckheden, gehuchten en voornaamste buurtschappen der Meierij. Streekarchivaat 'Langs Aa en Dommel, Veghel.

Brookes, A. & Gregory, K.J., (1983). An assessment of river channelization in England and Wales. *The Science of the Total Environment*, Vol. 27, Is. 2 – 3, p. 97 – 111.

Broothaerts, N., Verstraeten, G., Kasse, C., Bohncke, S., Notebaert, B. & Vandenberghe, J., (2014). From natural to human-dominated floodplain geoecology – a Holocene perspective for the Dijle catchment, Belgium. *Anthropocene,* Vol. 8, p. 46 – 58.

Brown, A.G., (1998). Fluvial evidence of the medieval warm period and the late medieval climatic deterioration in Europe. *Palaeohydrology and Environmental Change*, p. 43–52.

Brown, A.G., (2002). Learning from the past: paleohydrology and paleoecology. *Freshwater Biology*, Vol. 47, p. 817 – 829.

Brown, A.G., (2009). Colluvial and alluvial response to land use change in Midland England: An intergrated geoarchaological approach. *Geomorphology,* Vol. 108, p. 92 – 106.

Brown, A. & Keough, M., (1992). Holocene floodplain metamorphosis in the Midlands, United Kingdom. *Geomorphology*, Vol 4, p. 433–445.

Brown, A., Keough, M. & Rice, R., (1994). Floodplain evolution in the East Midlands, United Kingdom: the Late glacial and Flandrian alluvial record from the Soar and Nene valleys. *Philosophical Transactions of the Royal Society of London A*; Mathematical, Physical and Engineering Sciences, Vol. 348, p. 261–293.

Buskens, R., Van der Straaten, J., Braam, A., Oonk, M., Poelmans, W., & Voorn, P., (2011). De Dommel - Stroom door tijd, natuur en landschap. Brabants Landschap, Haren.

Candel, H. J., Makaske, B., Storms, J. E. A. & Wallinga, J. (2017). Oblique aggradation: a novel explanation for sinuosity of lowland streams in peat-filled valley systems. *Earth Surface Processes and Landforms*. Vol. 42, Is. 15, p. 2679 – 2696.

Candel, J.H.J., Makaske, B., Kijm, N., Storms, J.E.A. & Wallinga, J. (2018). Decreasing lateral migration and increasing planform complexity of the Dommel River during the Holocene. NCR Days 2018 Proceedings, Vol. 42, p. 32 – 33.

Carey, W.C. (1969). Formation of flood plain lands. *Journal of Hydraulics Division*, Vol. 95, p. 981 – 994.

Carr, A.S., Armitage, S.J., Berrio, J.C., Bilbao, B.A., & Boom, A., (2016). An optical luminescence chronology for late Pleistocene aeolian activity in the Colombian and Venezuelan Lianos. *Quaternary Research*, Vol. 85, Is. 2, p. 299 – 312.

Clark, J.G.D., (1952). Prehistoric Europe: The Economic Basis. Methuen, London.

Cunningham, A.C., (2011). Luminescence dating of storm-surge sediment – Introduction. Proefschrift ter verkrijging van de graad van Doctor aan de Technische Universiteit Delft, p. 1 – 7.

Cunningham, A.C. & Wallinga, J., (2010). Selection of integration time intervals for quartz OSL decay curves. *Quaternary Geochronology*, Vol. 5, p. 657 – 666.

Cunningham, A.C. & Wallinga, J., (2012). Realizing the potential of fluvial archives using robust OSL chronologies. *Quaternary Geochronology*, Vol. 12, p. 98-106.

Dark, P., (2006). Climate deterioration and land-use change in the first millennium BC: perspectives from the British palynological record. *Journal of Archaeological Science*, Vol. 33, Is. 10, p. 1381 – 1395.

De Bont, C., (1993) 'Al het merkwaardige in bonte afwisseling…' Een historische geografie van Midden- en Oost-Brabant. Stichting Brabants Heem, Waalre.

Dergachev, V.A., Raspopov, O.M., Van Geel, B., Zaitseva, G.I., (2004). The Sterno-Etrussia' geomagnetic excursion around 2700 BP and changes of solar activity, cosmic ray intensity and climate. *Radiocarbon*, Vol. 46, Is. 2, p. 661 – 681.

Didderen, K., Verdonschot, P.F.M., Knegtel, B.P.F.J.M. & Besse-Lototskaya, A.A., (2009). Enquete beek(dal) herstelprojecten 2004-2008. Evaluatie van beekherstel over de periode 1960-2008 en analyse van effecten van 9 voorbeeldprojecten. Alterra. Rapport 1858.

Duller, G.A.T., (2004). Luminescence dating of Quaternary sediments: recent advances. *Journal of Quaternary Science*, Vol. 19, Is. 2, p. 183 – 192.

Duller, G.A.T., (2016). Analyst v4.31.9 User manual – february 2016. Aberyswyth Luminescence Reasearch, Aberyswyth University.

Eekhout, J.P.C. & Hoitink, A.J.F., (2015). Chute cut-off as a morphological response to stream reconstruction: The possible role of backwater. *Water Resources Research*. (doi.org/10.1002/2014WR016539).

Eekhout, J.P.C., Fraaije, R., & Hoitink, A., (2014). Morphodynamic regime change in a reconstructed lowland stream. *Earth Surface Dynamics*, Vol. 2, p. 279.

Eekhout, J.P.C., (2014). Morphological processes in lowland streams; implications for stream restoration. Wageningen University Reasearch, Wageningen.

Eekhout, J.P.C., Hoitink, A. J. F., & Makaske, B. (2013). Historical analysis indicates seepage control on initiation of meandering. *Earth Surface Processes and Landforms*. (doi.org/10.1002/esp.3376)

Fałkiewicz-Kozieł, B., Kołaczek, P., Michczynski, A. & Piotrowska, N., (2015). The construction of a reliable absolute chronology for the last two millennia in an anthropogenically disturbed peat bog: Limitations and advantages of using a radio-isotopic proxy and age depth modelling. *Quaternary Geochronology,* Vol. 25, p. 83 – 95.

Galbraith, R., Roberts, R., Laslett, G., Yoshida, H. & Olley, J., (1999). Optical dating of single and multiplegrains of quartz from Jinmium rock shelter, Northern Australia: Part I, Experimental design and statistical models. *Archaeometry*, Vol. 41, Is 2, p. 339 – 364.

Gao, H., Li, Z., Pan, B., Liu, F., Liu, X., (2016). Fluvial responses to late Quaternary climate change in the Shiyang River drainage system, western China. *Geomorphology*, Vol. 258, p. 82 – 94.

Grabowski, R.C., Surian, N. & Gurnell, A.M., (2014). Characterizing geomorphological change to support sustainable river restoration and management. *WIRE's Water*, Vol. 1, p. 483 – 512.

Grove, J.R., Webb, J.A., Marren, P.M., Stewardson, M.J. & Wealands, S.R., (2012). High and dry: comparing literature review approaches to reveal the data that informs the geomorphic management of regulated river floodplains. *Wetlands*, Vol. 32, p. 215 – 224.

Güneralp I. & Rhoads, B.L., (2011). Influence of floodplain erosional heterogeneity on planform complexity of meandering rivers. *Geophysical Research Letters* 38: L14401.

Heesters, W., & Prinssen, A.J.H.M., (1984). Schijndel – Historische verkenningen. Stichting Brabants Heem in collaboration with municipality Schijndel, Waalre.

Heezik, A.A.S., (2007). Strijd om de rivieren; 200 jaar rivierenbeleid in Nederland. HNT Historische producties Den Haag, in collaboration with Rijkswaterstaat.

Hesse, P.P., (2016). How do longitudinal dunes respond to climate forcing? Insights from 5 years of luminescence dating of the Australian desert dune fields. *Quaternary International*, Vol. 410, part B, p. 11 – 29.

Hoffmann, T., Lang, A. & Dikau., R., (2008). Holocene river activity: analysing ^{14}C-dated fluvial and colluvial sediments from Germany. Quaternary Science, Vol. 27, p. 2031-2040.

Huisink, M. (2000) Changing river styles in response to Weichselian climate changes in the Vecht valley, eastern Netherlands. Sedimentary Geology, Vol. 133, Is. 1 – 2, p. 115–134.

Ikeda, S., Parker, G., & Sawai, K., (1981). Bend theory of river meanders. Part 1. Linear development. *Journal of Fluid Mechanics*, Vol. 112, p. 363 – 377.

Iversen, T.M., Kronvang, B., Madsen, B.L., Markmann, P. & Nielsen, M.B., (1993). Re-establishment of Danish streams: restoration and maintenance measures. *Aquatic Conservation*: Marine and Freshwater ecosystems, Vol. 3, p. 73-92.

Janssen, C.R., (1972). The Palaeoecology of plant communities in the Dommel. *Journal of Ecology*, Vol. 60, Is. 2, p. 411 – 437.

Jia, F., Lu, R., Gao, S., Li, J. & Liu, X., (2015). Holocene aeolian activities in the southeastern Mu Us Desert China. *Aeolian research*, Vol. 19, p. 267-274.

Kamstra, B.R.W., (2015). De interactie tussen beek en omliggend landschap. Bsc. Thesis, Wageningen University & Research.

Kleinhans, M., Schuurman, F., Bakx, W. & Markies, H., (2009). Meandering channel dynamics in highly cohesive sediment on an intertidal mud flat in th Westerschelde estuary, the Netherlands. *Geomorphology*, Vol. 105, p. 261 – 276.

Kleinhans M.G. & van den Berg, J.H., (2011). River channel and bar patterns explained and predicted by an empirical and a physics-based method. Earth Surface Processes and Landforms, Vol. 36, Is. 6, p. 721 – 738.

KNMI. Klimaatatlas, langjarig gemiddelde 1981 – 2010; gemiddelde jaarlijkse neerslag. Retrieved from: http://www.klimaatatlas.nl/klimaatatlas.php; accessed at 24-1-2016.

Kostic, B., & Aigner, T., (2007). Sedimentary architecture and 3D ground penetrating radar analysis of gravelly meandering river deposits (Neckar Valley, SW Germany). Sedimentology, Vol. 54, p. 789 – 808.

Kroes, D.E. & Hupp, C.R., (2010). The effect of channelization on floodplain sediment deposition and subsidence along the pocomoke river, Maryland. *Journal of the American water resources association*, Vol. 46, Is. 4, p 686 – 699.

Lamb, H.H., (1977). Climate: past, present and future. Volume 2: climate, history and the future. London, Methuen.

Leeder, M.R., (1973). Fluviatile fining-upward cycles and the magnitude of paleochannels. *Geological Magazine*, Vol. 110, Is. 3, p. 265 – 276.

Leeuwarden, W. van & Janssen, C.R., (1986). Differences between valley and upland vegetation development in eastern Noord-Brabant, The Netherlands, during the late glacial and early Holocene. Review of Paleobotany and Palynology, Vol. 52, p. 179 - 264. University of Utrecht, Utrecht.

Leopold, L.B., (1994). *A View of the River*, Harvard University Press, Cambridge

Lespez, L., Viel, V., Rollet, A.J. & Delahye, D., (2015). The anthropogenic nature of present-day low energy rivers in western France and implications for current restoration projects. *Geomorphology,* Vol. 251, p. 64 – 76.

MacDonald, N. & Sangster, H., (2017). High-magnitude flooding across Britain since AD 1750. Hydrological Earth System Science, Vol. 21, p. 1631 – 1650.

Madsen, A.T. & Murray, A.S., (2009). Optically stimulated luminescence dating of young sediments: A review. *Geomorphology*, Vol. 119, p. 3 – 16.

Makaske, B. & Maas, G. (2015). Handboek Geomorfologisch beekherstel. Alterra, Wageningen in opdracht van stichting toegepast onderzoek waterbeheer (STOWA), Amersfoort.

Makaske, B. & Weerts, H.J.T., (2005). Muddy lateral accretion and low stream power in a sub-recent confined channel belt, Rhine-Meuse delta, central Netherlands. *Sedimentology*, Vol. 52, p. 651 – 668.

Makaske, B., Deijl, E.C. & Kleinhans, M.G., (2016). Het natuurlijke patroon van beken. *Landschap*, Vol. 4, p. 184 – 193.

Malcom, K.H. & Diaz, H.F., (1994). Was there a Medieval Warm Period? So where and when? Climate Change, Vol. 26, p. 109 – 142 .

Marren, P.M., Grove, J.R., Webb, J.A. & Stewardson, M.J., (2014). The potential for dams to impact lowland meandering river floodplain geomorphology. *Scientific World Journal,* Article: 309673.

Mauquoy, D., Van Geel, B., Blaauw, M., Speranza, A. & Van der Plicht, J., (2004). Changes in solar activity and Holocene climatic shifts derived from C-14 wiggle-match dated peat deposits. *Holocene*, Vol. 14, Is. 1, p. 45 – 52.

Meade., R.H., (1982). Sources, sinks and storage of river sediments in the Atlantic drainage of the United States. *Journal of Geology*, Vol. 90, Is. 3, p. 235–252.

Meijer, T., (2010). Palaeomalacology of the Brabant Loam (the Netherlands). Of plants and snails, Netherlands Centre for Biodiversity, Leiden, p. 179 – 192.

Merritts, D.J., Walter, R., Rahnis, M., Hartranft, J., Cox, S., Gellis, A., Potter, N., Hilgartner, W., Langland, M., Manion, L., Lippincott, C., Siddiqui, S., Rehman, Z., Scheid, C., Kratz, L., Shilling, A., Jenschke, M., Datin, K., Cranmer, E., Reed, A., Matuszewski, D., Voli, M., Ohlson, E., Neugebauer, A., Ahamed, A., Neal, C., Winter, A. & Becker, S., (2011). Anthropocene streams and base-level controls from historic dams in the unglaciated mid-Atlantic region, USA. *Philosophical transactions of the Royal Society,* Vol. 369, Is. 1938, p. 976–1009. Miall, A.D., (1977). A Review of the Braided-River Depositional Environment. *Earth-Science Reviews*, Vol. 13, p. 1 – 62.

Mol, J., Vandenberghe, J. & Kasse, C. (2000). River response to variations of periglacial climate in mid-latitude Europe. *Geomorphology*, Vol. 33, p. 131–148.

Molen, D.T. van der, Pot, R., Evers, C.H.M. & Nieuwerburg, L.L.J. van, (2012). Referenties en maatlatten voor natuurlijke watertypen voor de kaderrichtlijn water 2015 – 2021. Stichting Toegepast Wateronderzoek (STOWA), Amersfoort.

Moor, J.W.W., Kasse, C., Van Balen, R., Vandenberghe, J. & Wallinga, J., (2006). Human and climate impact on catchment development during the Holocene – Geul River, the Netherlands. *Geomorphology,* Vol. 98, p. 316 – 339.

Murray, A.S., Thomsen, K.J., Masuda, M., Buylaert, J.P. & Jain, M., (2012). Identifying well-bleached quartz using the different bleaching rates of quartz and feldspar luminescence signals. *Radiation Measurements*, Vol. 47, p. 688 – 695.

Murray, A.S. & Wintle, A.G., (2000). Luminescence dating of quartz using an improved single-aliquot regenerative-dose protocol. Radiation Measurements, Vol. 32, p. 57 – 73.

Nanson, G.C. & Croke, J.C., (1992). A genetic classification of floodplains. *Geomorphology*, Vol. 4, p. 459-486.

Neal, A. (2004). Ground-penetrating radar and its use in sedimentology: Principles, problems and progress. *Earth-Science Reviews*, Vol. 66, Is. 3-4, p. 261–330.

Notebaert, B. & Verstraeten, G., (2010). Sensitivity of West and Central European river systems to environmental changes during the Holocene: A review. *Earth-Science Reviews*, Vol. 103, p. 163 – 182.

Nouwen, L., (1982). Kijk op Eindhoven. Elsevier, Amsterdam.

Oele, E., Apon, W., Fischer, M.M., Hoogendoorn, R., Mesdag, C.S., De Mulder, E.F.J., Overzee, B., Sesören, A., Westerhoff, W.E., (1983). Surveying The Netherlands: sampling techniques, maps and their applications. Geologie en Mijnbouw Vol. 62, p. 355–372.

Pizzuto, J. & O'Neal, M., (2009). Increased mid-twentieth century riverbank erosion rates related to the demise of mill dams, South River, Virginia. Geology, Vol. 27, Is. 1, p. 19 – 22.

Preusser, F., Degering, D., Fuchs, M., Hilgers, A., Kadareit, A., Klasen, N., Krbetschek, M., Richte, D.r & Spencer, J.Q.G., (2008). Luminescence dating: basics, methods and applications. *Quaternary Science Journal*, Vol. 57, Is. 1-2, p. 95-149.

Quick, C. (2016). Historical morphodynamics of the Overijsselse Vecht: Extreme lateral migration of meander bends cause by drift-sand activity? Msc Thesis, Wageningen University & Research.

Reimann, T., Notenboom, P.D., Schipper, M.A. de & Wallinga, J., (2015). Testing for sufficient signal resetting

during sediment transport using a polymineral multiple-signal luminescence approach. *Quaternary Geochronology,* Vol. 25, p. 26 – 36.

Renes, J., (1988). De geschiedenis van het Zuid-Limburgse cultuurlandschap. Van Gorkum, Maastricht.

Rey, J., Martínez, J. & Hidalgo, M.C., (2013). Investigating fluvial features with electrical resistivity imaging and ground-penetrating radar: The Guadalquivir River terrace (Jaen, Southern Spain). Sedimentary Geology, Vol. 295, p. 27 – 37.

Robert, A. (2003). River processes: an introduction to fluvial dynamics. Arnold Publishers, London, UK, p. 126 – 167

Rodnight, H., Duller, G.A. Smith, D.G., Hubbard, S.M., Leckie, D.A. & Fustic, M., (2009). Counter point bar deposits: lithofacies and reservoir significance in the meandering modern Peace River and ancient McMurray Formation, Alberta, Canada. *Sedimentology*, Vol. 56, p. 1655 – 1669.

Rodnight, H., Duller, G.A.T., Tooth, S. & Wintle, A.G., (2005). Optical dating of a scroll-bar sequence on the Klip River, South Africa, to derive the lateral migration rate of a meander bend. *The Holocene*, Vol. 15, p. 802 – 811.

Schokker, J., (2003). Patterns and processes in a Pleistocene fluvio-aeolian environment. Roer Valley Graben, south-eastern Netherlands. *Netherlands Geographical Studies,* Vol. 314, p. 1 – 142.

Smith, D.G., Hubbard, S.M., Leckie, D.A. & Fustic, M., (2009). Counter point bar deposits: lithofacies and reservoir significance in the meandering modern Peace River and ancient McMurray Formation, Alberta, Canada. *Sedimentology,* Vol. 56, p. 1655 – 1669.

Starkel, L., Gebica, P. & Superson, J., (2007). Last Glacial–Interglacial cycle in the evolution of river valleys in southern and central Poland. *Quaternary Science Reviews* Vol. 26, Is, 22 – 24, p. 2924 – 2936.

Stouthamer, E. & Middelkoop, H., (2003). Morfologische potenties van de Rijtakken, Benedenrivieren en Maas; Historisch referentie (situatie rond 1850). Departement Fysische Geografie, Faculteit Ruimtelijke Wetenschappen, University of Utrecht.

Stuurman, R.J., Peeters, J.E.M. & Reckman, J.W.T.M., (1997). Watermolen-afhankelijke standplaatsen in Noord-Brabant. *Stromingen*, Vol. 3, Is. 3, p. 11 – 30.

Spek, T., Groeneman-van Waateringe, W., Kooistra, M. & Bakker, L. (2003). Formation and land-use history of Celtic fields in North-West Europe - An interdisciplinary case study at Zeijen, The Netherlands. *European Journal of Archaeology*, Vol. 6, Is. 2, p. 141 – 173.

Theuws, F. (1976). Een laat-middeleeuwse watermolen te Bergeijk. *Brabants Heem*: tijdschrift voor archeologie, geschiedenis en volkskunde, Vol 28, Is. 2, p. 56 – 63.

Tipping, R., Davies, A., McCulloch, R. & Tisdall, E. (2008). Response to late Bronze Age climate change of farming communities in north east Scotland. *Journal of Archaeological Science*, Vol. 35, Is. 8, p. 2379 – 2386.

Van Balen, R.T., Kasse, C. & De Moor, J., (2008). Impact of groundwater flow on meandering: example from the Geul River, The Netherlands. *Earth Surface Processes and Landforms*, Vol. 33, p. 2010 – 2028.

Van de Meene, E.A., Staay, J. van der, & Hock, T.L., (1979). The van der Staay suction-corer – a simple apparatus for drilling in sand below the groundwater table. Rijks Geologische Dienst.

Van Halder, P.H., (2010). Watermolens in Noord-Brabant, vroeger en nu. Boedrukdeal Utrecht. 's Hertogenbosch.

Van Geel, B., Buurman, J &, Waterbolk H.T., (1996). Archaeological and paleoecological indications of an abrupt climate change in the Netherlands, and evidence for climatological teleconnections around 2650 BP. *Journal of Quaternary Science*, Vol. 11, Is. 6, p. 451 – 460.

Waterbolk, H.T., (1998a). The sharp rise of Δ14C ca. 800 cal BC: possible causes, related climatic teleconnections and the impact on human environments. *Radiocarbon, Vol.* 40, Is. 1, p. 535 – 550.

Verdonschot, P.M.F., & Nijboer, R.C., (2002). Towards a decision support system for stream restoration in the Netherlands: an overview of restoration projects and future needs. *Hydrobiologica*, Vol. 487, p. 131 –

Wallinga, J., (2002). Optically stimulated luminescence dating of fluvial deposits: a review. *Boreas,* Vol 31, p. 303-322.

Walter, R.C. & Merritts, D.J., (2008). Natural streams and the legacy of water powered mills. *Science*, Vol. 319, p. 299 – 304.

Wang, T., Surge, D. & Mithen, S., (2012). Seasonal temperature variability of the Neoglacial (3300-2500 BP) and Roman Warm Period (2500-1600 BP) reconstructed from oxygen isotope ratios of limpet shells (Patella vulgata), Northwest Scotland. *Paleogeography, Paleoclimatology & Paleoecology*, Vol. 317, p. 104 – 113.

Waterschap de Dommel (2016). Afvoermetingingen, meetpunt St. Oedenrode en Wilhelmina kanaal. Retrieved from: Waterschap de Dommel, 's Hertogenbosch.

Waterschap de Dommel (n.d.). Werkgebied. Retrieved: March 17, 2016, from http://www.dommel.nl/algemeen/bestuur-en-organisatie/werkgebied/werkgebied.html

Wohl, E., Angermeier, P.L., Bledsoe, B., Kondolf, G.M., MacDonnell, L., Merritt, D.M., Palmer, M.A., Poff, N.L., & Tarboton, D. (2005). River restoration. *Water Resources Research*, Vol. 41, Is. 10, p. 1-12.

Wolman M.G. & Leopold L.B., (1953). River flood plains: some observations on their formation. U.S. *Geological Survey Professional Paper*, 282-C, p. 87–107.

Zolitschka, B., Behre, K.E. & Schneider, J., (2003). Human and climatic impact on the environment as derived from colluvial, fluvial and lacustrine archives – examples from the Bronze Age to the Migration period, Germany. *Quarternary Science Reviews*, Vol. 22, p. 81 – 100.

9. Appendices

Appendix I – Overview of the watermills of the Dommel

Appendix II – Requirements of the SAR-procedure

Appendix III – Ground Penetrating Radar Images

- Overview of the GPR transects
- GPR image of location B in Figure 27 & 48
- GPR image of location C in Figure 28 & 48
- GPR image of location D in Figure 29 & 48
- GPR image of location E in Figure 30 & 48
- GPR image of location F in Figure 31 & 48

Appendix I — Overview of the watermills of the Dommel

Name	Municipality	Coordinaten RD	Presence	First mentioned	Minimum period of activity
Dommelse Mill	Valkenswaard	X: 158548, Y: 373512	Existing	1312	1312 - 1938
Hooydonkse watermill	Nuenen, Gerwen en Nederwetten	X: 163715, Y: 389983	Existing	1150	1150 - present
Opwettense watermill	Nuenen, Gerwen en Nederwetten	X: 164893, Y: 385622	Existing	1335	1335 - 1968
Genneper mill	Eindhoven	X: 160772, Y: 381560	Existing	1249	1249 - 1957
Venbergse watermill	Valkenswaard	X: 159052, Y: 371965	Existing	1227	1227 - begin 20th century
Collse watermill	Eindhoven	X: 165475, Y: 384042	Existing	1337	1337 - 1925
Geldropse watermill	Geldrop-Mierlo	X: 167254, Y: 381473	Existing	1403	1403 - 1920
Waalrese Volmolen	Waalre	X: 157498, Y: 376924	Existing	1347	1347 - 1940
Loonder mill	Waalre	X: 158347, Y: 375445	Disappeared	1384	1384 - 1940
Boxtelse watermill	Boxtel	X: 150410, Y: 400340	Ruin	1393	1393 - 1973
Boxtelse watermill of smallwater	Boxtel	X: 150354, Y: 400402	Disappeared	1232	1232 - 1912
Schimmelse or Woenselse watermill	Eindhoven	X: 161818, Y: 384458	Disappeared	1379	1397 - 1956
Watermill of forge Verberne	Eindhoven	X: 161568, Y: 383190	Disappeared	1740	1740 - 1762
Stratumse watermill	Eindhoven	X: 161610, Y: 382895	Disappeared	1442	1442 - 1896
Three watermills of Halder	Halder, Sint-Michielsgestel	X: 150800, Y: 406800	Disappeared	1340	1324 - 1732
Kasterense watermill	Liempde, Boxtel	X: 153554, Y: 399234	Disappeared	1294	1312 - 1936
Het Meulke/Antelse watermill	Liempde, Boxtel	X: 155656, Y: 398267	Disappeared	1371	1371 - 1500
Mill of Wolfswinkel	St. Oedenrode	X: 162565, Y: 393692	Disappeared	1381	1381 - 1947
Borch mill	Sint-Oedenrode	X: 160221, Y: 397543	Disappeared	1381	1312 - 1945
Sonse watermill	Son en Breugel	X: 162580, Y: 391258	Disappeared	1257	1257 - 1740
Watermill of Schaft	Borkel en Schaft	Unknown	Disappeared	1644	Unknown

Source: Van Halder, (2010)

Appendix II - Requirements of the SAR-procedure

Requirements of the SAR-procedure of the first (A) and second (B) measurement series using Risø TL/OSL software®. IR indicates the analysis of the feldspar signal and OSL indicates the analysis of the quartz sign

A. IR

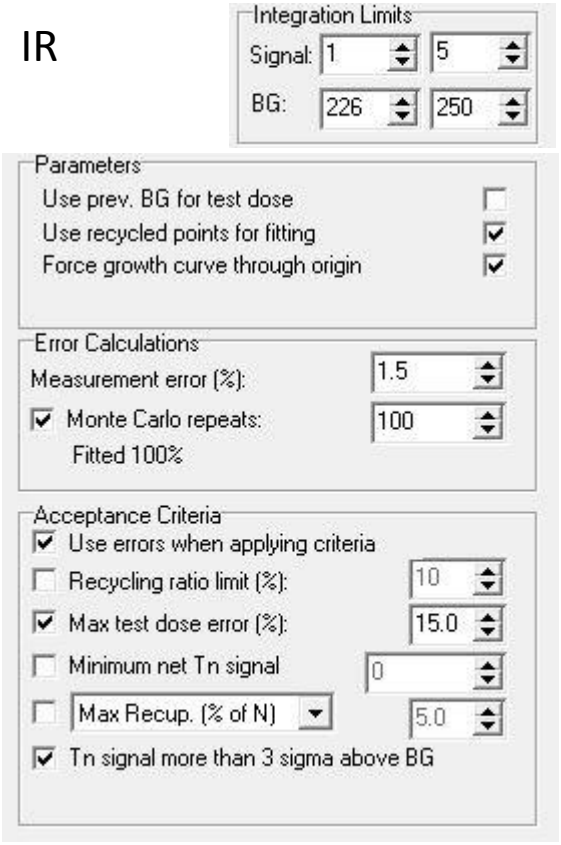

OSL

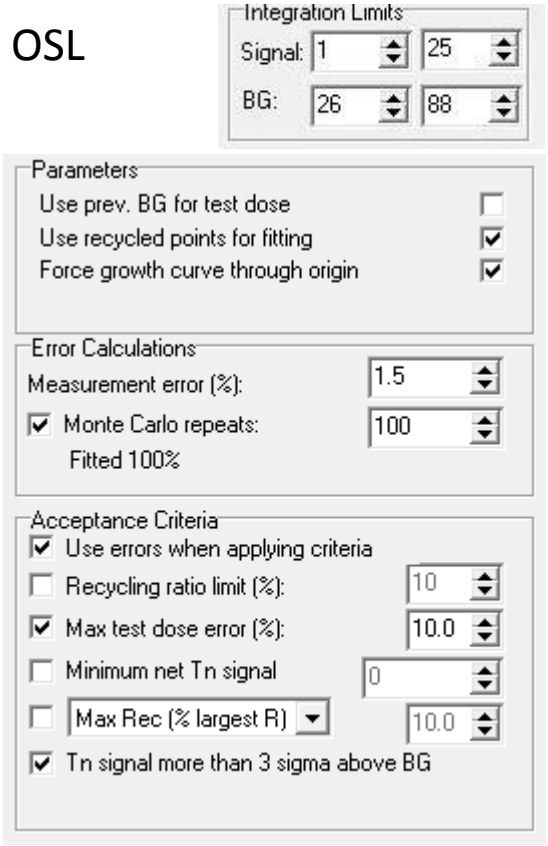

B. OSL

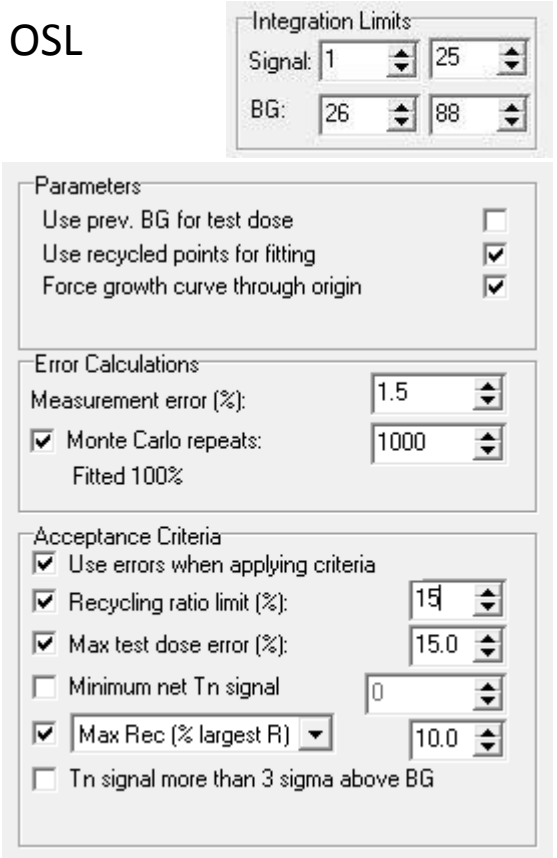

Appendix III — Ground Penetrating Radar Images

An overview of the GPR radar transects

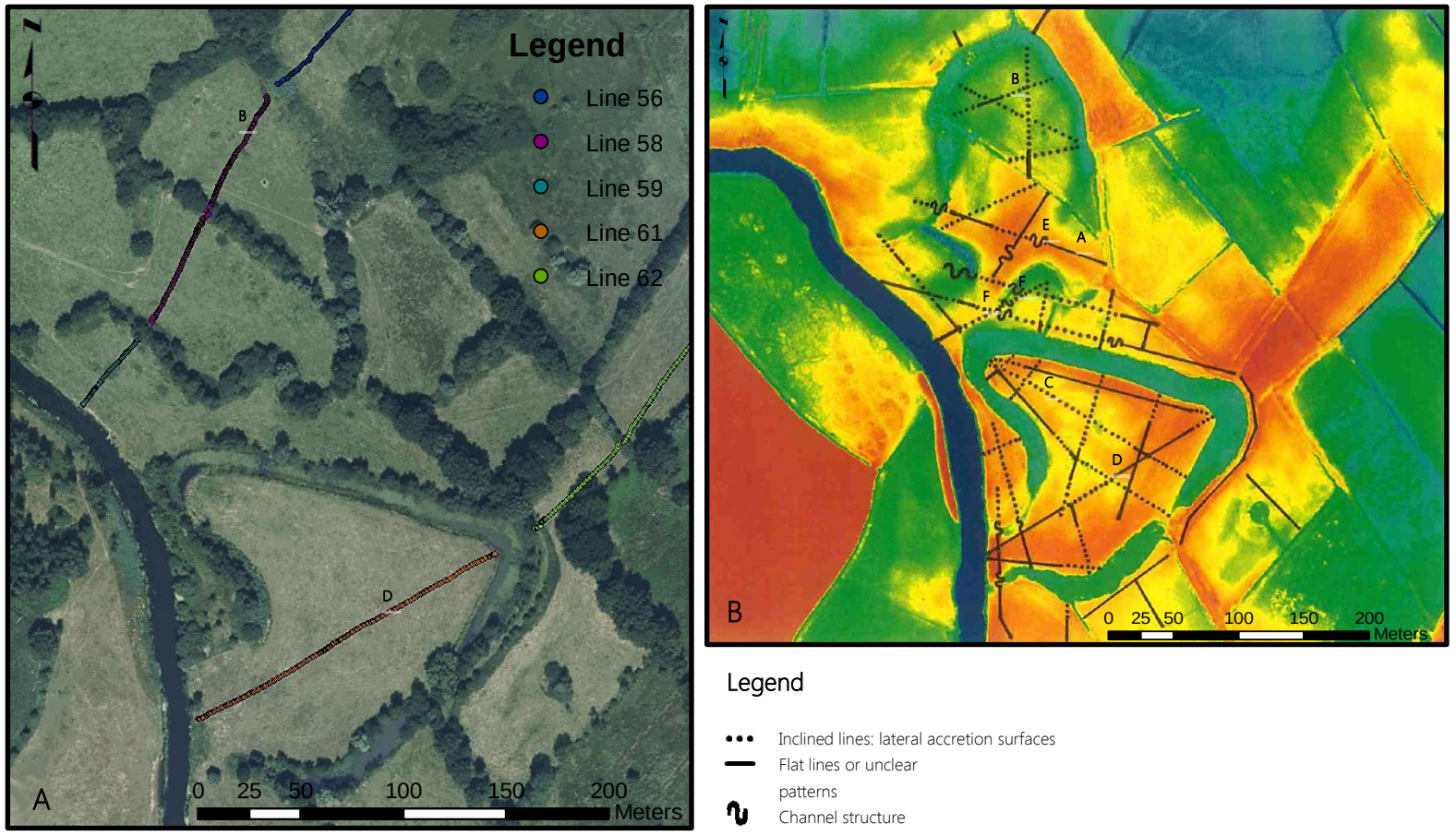

Figure 48 An overview of the locations of the GPR transects **A**: The first exploratory GPR cross section lines of the northern and southern meander. Background: aerial photograph of 2014 **B**: An overview of the (additional) radar transects where the shape of the lines represent the occurrence of lateral accretion surfaces, channel patterns and straight lines or unclear (parabolic) structures, based on the interpretation of the GPR images. The letters B t/m F indicate the locations of the images of Figure 49 to 53.Background: DEM with an elevation value of: 9.5 to 11 m-NAP. Retrieved from: GeoDesk, Wageningen

GPR image of location B in Figure 27 & 48

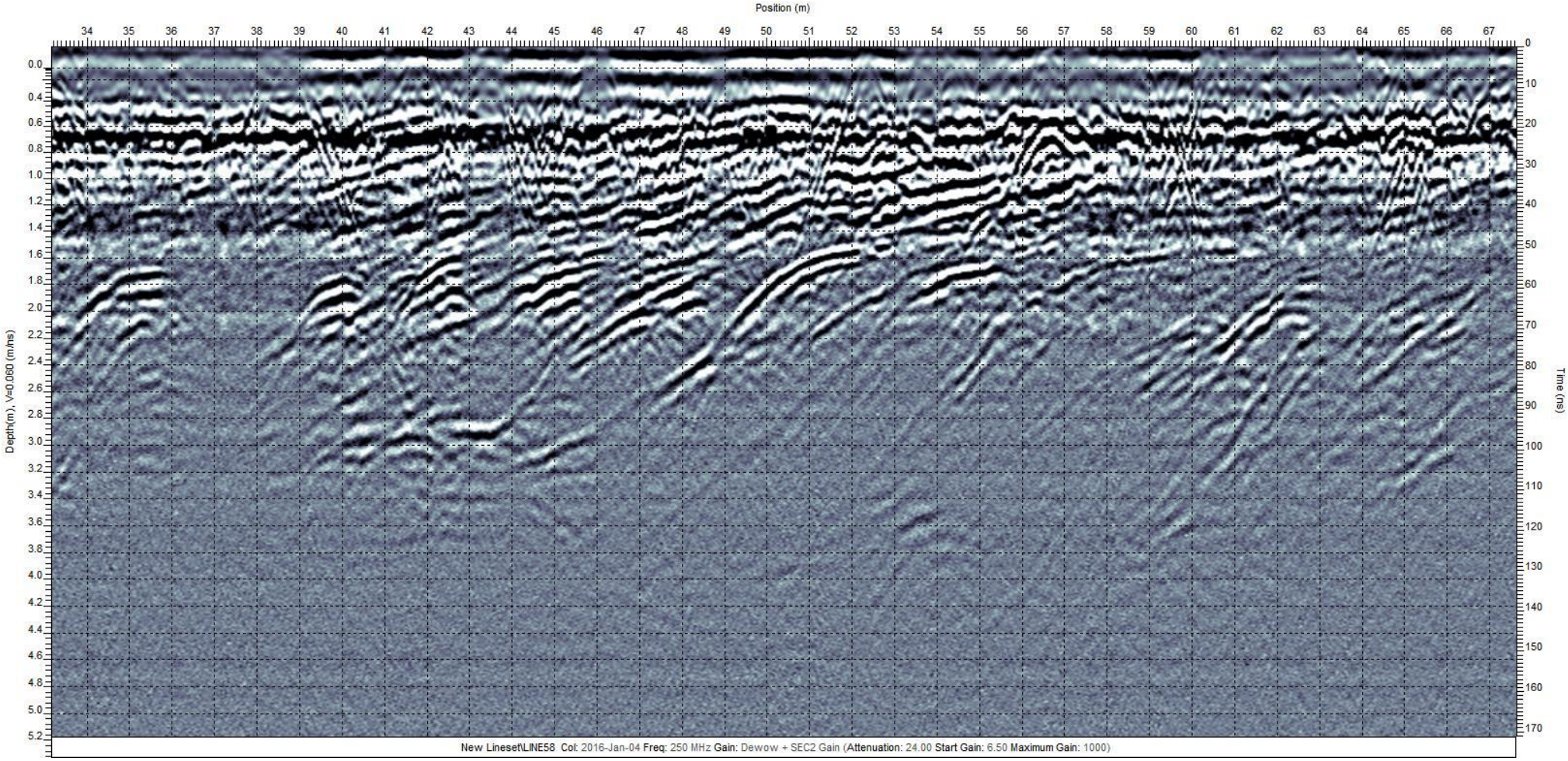

Figure 49 The original GPR image of location B (Figure 27) representing the inclined lines, which are interpreted as lateral accretion surfaces, that occur in the northern meander.

GPR image of location C in Figure 28 & 48

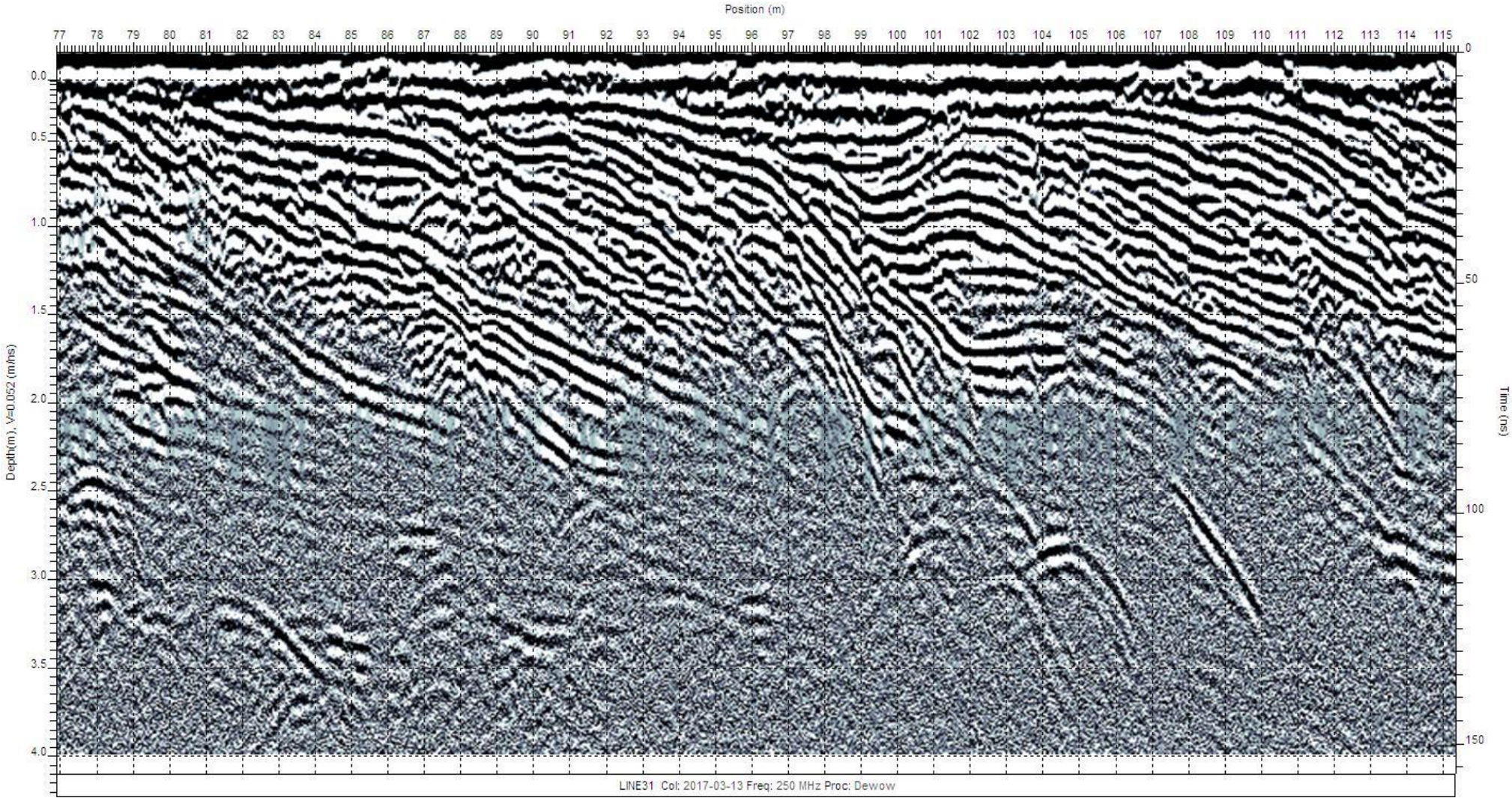

Figure 50 The original GPR image of location C (Figure 28) representing the inclined lines, which are interpreted as lateral accretion surfaces, that occur in the southern meander.

GPR image of location D in Figure 29 & 48

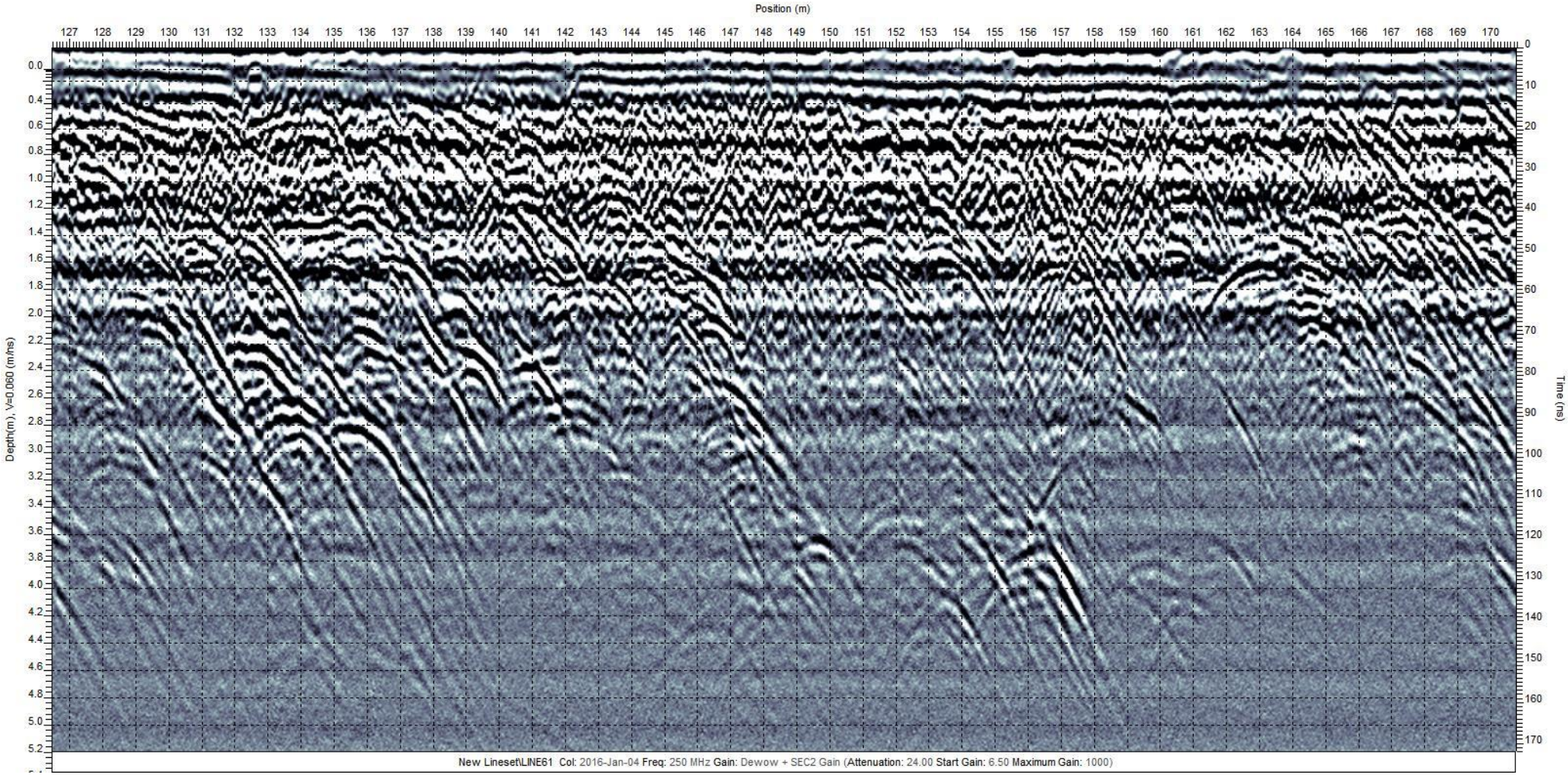

Figure 51 The original GPR image of location D (Figure 29) representing parabolic structures. By connecting the tops of the hyperboles, inclined lines, can be recognized, which can be interpreted as lateral accretion surfaces. The steepness of the lines is similar to the lateral accretion surfaces recognised in other GPR images.

GPR image of location E in Figure 30 & 48

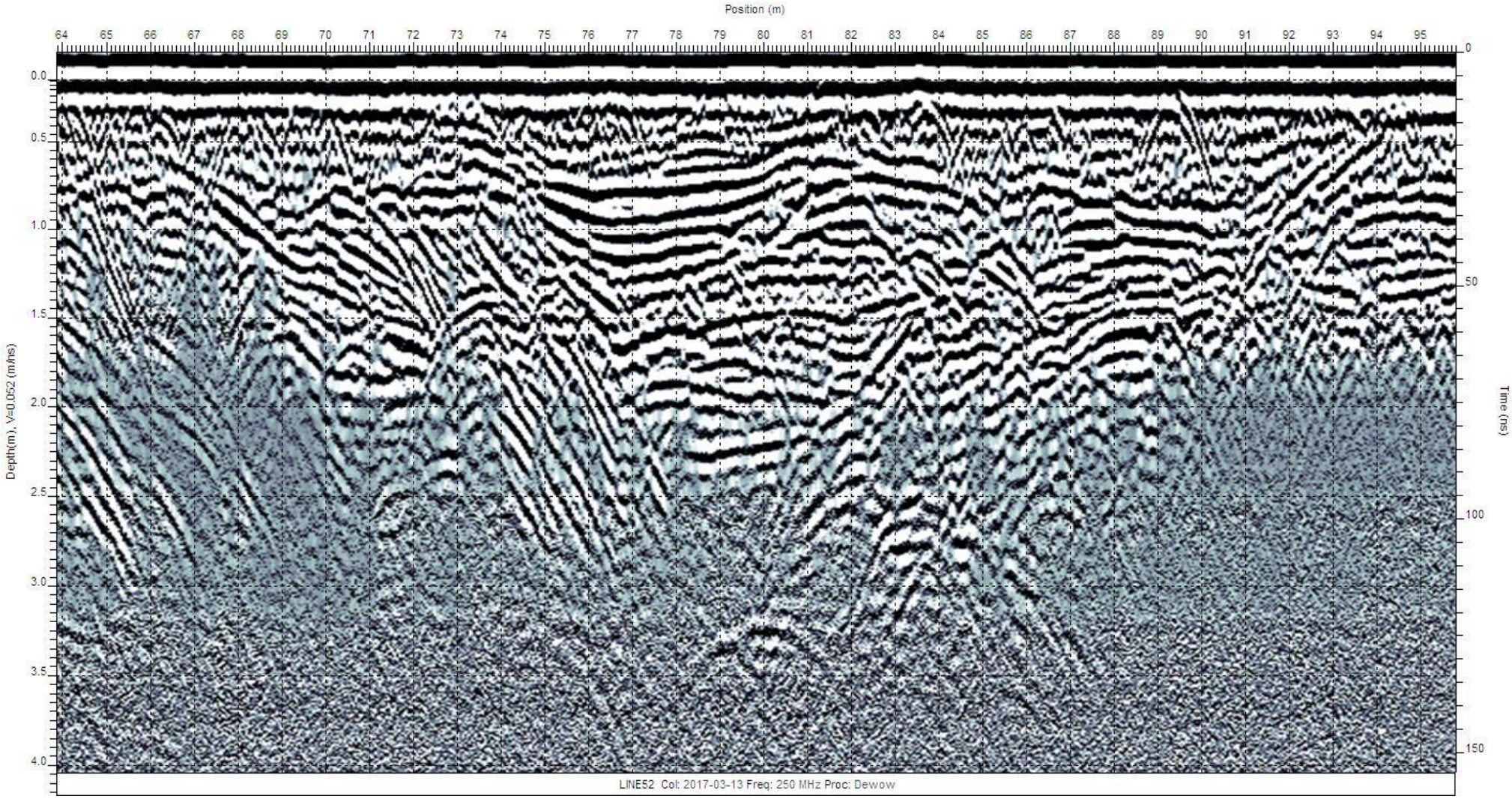

Figure 52 The original GPR image of location E (Figure 30) representing steep inclined lines that can be interpreted as a channel structure; a part of the disappeared northern meander.

GPR image of location F in Figure 31 & 48

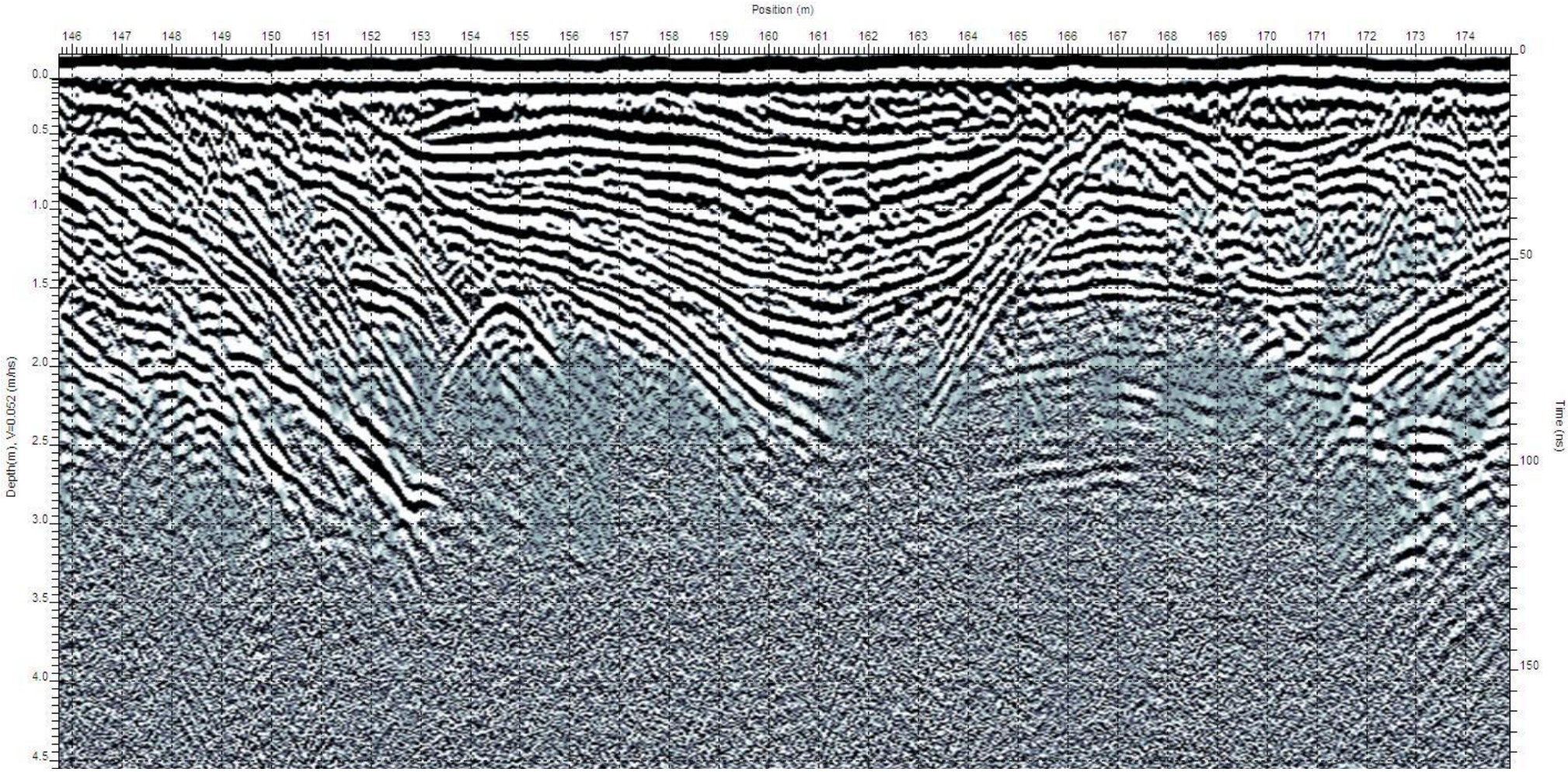

Figure 53 The original GPR image of location F (Figure 31) representing steep and less steep inclined lines that can be interpreted as a channel structure; a part of the disappeared eastern meander.

WAGENINGEN
UNIVERSITY & RESEARCH